Estudios Geológicos
julio-diciembre 2021, 77(2), e141
ISSN-L: 0367-0449
https://doi.org/10.3989/egeol.44385.604

Coupling of trace elements in brachiopod shells and biotic signals from the Lower Jurassic South-Iberian Palaeomargin (SE Spain): Implications for the environmental perturbations around the early Toarcian Mass Extinction Event

Análisis de elementos traza en braquiópodos del Jurásico Inferior del Paleomargen Sud-Ibérico (SE de España). Correlación con las señales bióticas e implicaciones ambientales en torno al Evento de Extinción Masiva del Toarciense inferior

José Francisco Baeza-Carratalá[1], Matías Reolid[2*], Alice Giannetti[1], David Benavente[1], Jaime Cuevas-González[1]

[1] Departamento de Ciencias de la Tierra y Medio Ambiente, Universidad de Alicante, Apdo. 99, San Vicente del Raspeig, 03080 Alicante, Spain. ORCID ID: https://orcid.org/000-0002-3366-6090, https://orcid.org/0000-0001-9030-8604, https://orcid.org/0000-0001-7325-4042, https://orcid.org/0000-0001-7747-0818

[2] Departamento de Geología, Universidad de Jaén, Campus Las Lagunillas sn, 23071, Jaén, Spain. ORCID ID: 0000-0003-4211-3946
*Corresponding author: mreolid@ujaen.es

ABSTRACT

In the westernmost Tethys, the Early Jurassic involved critical environmental changes affecting marine ecosystems. Brachiopods were particularly affected in the South-Iberian Palaeomargin. A late Sinemurian-early Pliensbachian tectonic event led to the collapse of shallow platforms related to the Atlantic Ocean opening. Subsequently, the early Toarcian Extinction Event occurred during a carbon cycle perturbation and the development of oxygen-depleted conditions, mainly affecting benthic communities. In the Subbetic Domain, brachiopod dynamics concur with these major environmental perturbation events. Geochemical imprint of brachiopod shells from this area has been analyzed revealing a clear synchrony between oscillations of trace elements content, global trends in the C and O cycling, and faunal diversity dynamics around critical bioevents, allowing to validate global and regional models related to the platform collapse and the early Toarcian biotic crisis. In the Sinemurian-Pliensbachian turnover and the Toarcian crisis, the redox-sensitive trace metals, REEs, and Fe content in the brachiopod shells show positive excursions. Nevertheless, their trend together with brachiopod diversity patterns, the lower TOC values, and the sedimentary data, support that oxygen depletion must have played a secondary role as environmental stress factor for the benthic fauna. Instead, an increasing temperature gradient is invoked to have played a decisive role, as demonstrated by the main faunal turnover and replacement events correlating with the palaeotemperatures from the peri-Iberian platforms. Shifts on palaeoproductivity, continental influx, and hydrothermal input are also deduced by the increasing concentrations of several trace elements, interpreted as complementary triggering factors of these Early Jurassic bioevents in the westernmost Tethys Ocean.

Recibido el 6 de julio de 2021; Aceptado el 5 de octubre de 2021; Publicado online el 15 de diciembre de 2021

Citation / Cómo citar este artículo: Baeza-Carratalá, J.F. et al. (2021). Coupling of trace elements in brachiopod shells and biotic signals from the Lower Jurassic South-Iberian Palaeomargin (SE Spain): Implications for the environmental perturbations around the early Toarcian Mass Extinction Event. Estudios Geológicos 77(2): e141. https://doi.org/10.3989/egeol.44385.604

Keywords: Brachiopoda; Palaeoecological proxies; Trace elements; Western Tethys; Pliensbachian-Toarcian extinction.

RESUMEN

En el Jurásico Inferior se registran diversos eventos críticos que influyeron significativamente en los ecosistemas marinos del Tethys occidental. Entre las comunidades bentónicas, en el Paleomargen Sudibérico, los braquiópodos se vieron particularmente afectados por dichos eventos. El episodio tectono-sedimentario distensivo asociado a la apertura del proto-Atlántico conllevó el colapso de las amplias plataformas someras imperantes en el Tethys hasta el Sinemuriense superior-Pliensbaquiense basal, con la consiguiente reorganización de los ecoespacios faunísticos. Posteriormente, el evento de extinción registrado en el Toarciense inferior, trajo consigo importantes alteraciones en el ciclo del carbono así como el desarrollo de condiciones anóxicas que afectaron principalmente a las comunidades bentónicas. En el dominio Subbético, la dinámica poblacional de los braquiópodos coincidió con estos importantes eventos de perturbación ambiental. Se ha analizado la impronta geoquímica registrada en conchas de braquiópodos del Subbético oriental, revelando una clara sincronía entre las oscilaciones del contenido en elementos traza, las tendencias globales en el ciclo del C y del O y la diversidad de la braquiofauna en torno a dichos eventos críticos, lo que permite validar modelos globales y regionales relacionados tanto con el evento de rifting incipiente de las plataformas someras en el Sinemuriense-Pliensbachiense, como con la crisis biótica global en torno al Toarciense inferior. En la renovación faunística verificada para el tránsito Sinemuriense-Pliensbachiense y para el evento de extinción del Toarciense, los metales traza sensibles a las condiciones redox, la concentración de REE y el contenido en Fe en las conchas de braquiópodos muestran excursiones positivas. Esta tendencia, junto a los patrones de diversidad de los braquiópodos, los bajos valores de TOC y las evidencias sedimentarias, sugieren que, en esta región, la anoxia debió representar un factor secundario como causa de estrés ambiental para la fauna bentónica. En cambio, se postula que el progresivo aumento de la temperatura jugó un papel determinante en las cuencas marginales del Tethys occidental, como se demuestra al correlacionar los principales eventos de renovación y sustitución faunística con las paleotemperaturas de las plataformas peri-ibéricas. Los cambios en la paleoproductividad, los aportes continentales y posibles contribuciones hidrotermales se relacionan asimismo con las oscilaciones de determinados elementos traza y se interpretan, por tanto, como factores coadyuvantes desencadenantes de estos bioeventos del Jurásico Inferior en el Tethys occidental.

Palabras clave: Braquiópodos; Análisis paleoecológico; Elementos traza; Tethys Occidental; Extinción Pliensbaquiense-Toarciense.

Introduction

The Early Jurassic constituted a timespan that involved critical environmental perturbations affecting marine ecosystems. In the framework of the Central Atlantic Ocean opening, a late Sinemurian-early Pliensbachian tectonic event led to the collapse of the shallow-water platforms system well-established in the Western Tethys Ocean by rifting and subsequent drowning (Bernoulli & Jenkyns, 1974; Winterer & Bosellini, 1981; Vera, 2001). This triggered a high diversification on ecological niches and biotas and gave rise to the mostly stable environmental conditions of the Pliensbachian period. This phase took place just before the well-known early Toarcian mass extinction event often correlated with the Toarcian Oceanic Anoxic Event (T-OAE), also called Jenkyns Event (Müller *et al*., 2017; Reolid *et al*., 2020). This event represented one of the most critical ecological crisis in the whole Mesozoic, implying extinction and significant faunal turnovers in the nektonic/planktic and benthic biota (Hallam, 1986, 1987; Vörös, 1993, 2002; Little & Benton, 1995; Aberhan & Fürsich, 1997; Harries & Little, 1999; Macchioni & Cecca, 2002; Wignall *et al*., 2005; Wignall & Bond, 2008; Arias, 2009, 2013; Dera *et al*., 2010; García Joral *et al*., 2011; Caruthers *et al*., 2013; Reolid *et al*., 2014, 2019; Baeza-Carratalá *et al*., 2015, 2017). The Jenkyns Event is worldwide characterized by the record of a negative carbon isotopic excursion (CIE) also recorded in the South-Iberian Palaeomargin (Reolid *et al.,* 2014; Rodrigues *et al.,* 2019; Ruebsam *et al*., 2020) (Fig. 1).

The evolution of the Early Jurassic depositional environments and ecological conditions in the South-Iberian Palaeomargin are well understood, evolving from shallow carbonate platforms to an epioceanic swell/graben system with changing environmental conditions and ecospaces for the marine communities (Braga *et al.*, 1981; Rodríguez-Tovar

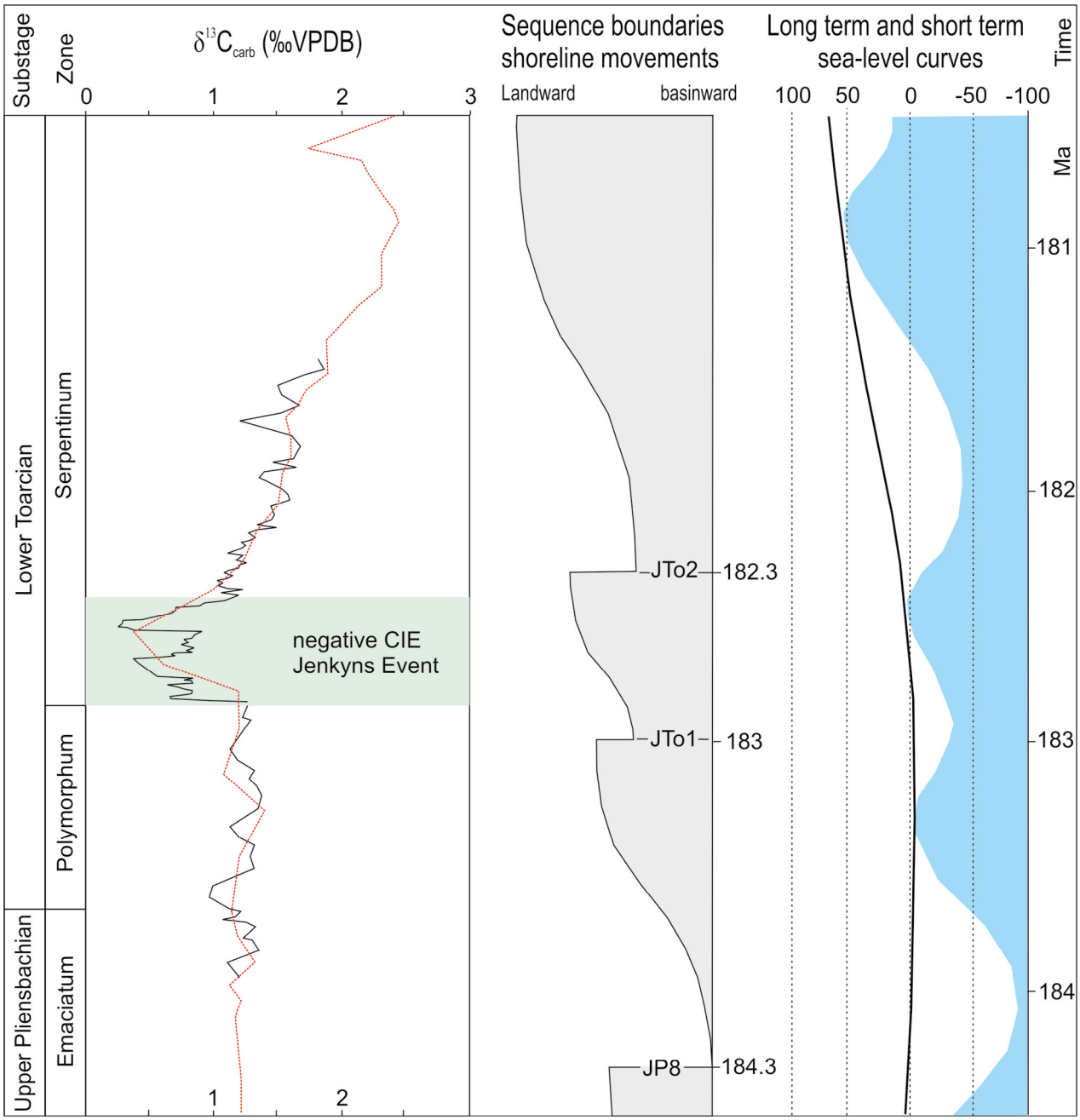

Figure 1.— Idealized isotopic $\delta^{13}C$ curve from bulk carbonate for the late Pliensbachian-early Toarcian interval in the South-Iberian Palaeomargin (Subbetic Domain) based on the records of Reolid *et al*. (2014, red dotted line) and Ruebsam *et al*. (2020, continuous line). Note the negative carbon isotopic excursion (CIE) that correlated with the Jenkyns Event that includes the T-OAE. The isotopic curve is correlated with the sequence boundaries and the sea-level curve after Haq (2018).

& Uchman, 2011; Sandoval *et al*., 2012; Reolid *et al*., 2014, 2015). Amidst these communities, the brachiopod fauna is widely documented in the South-Iberian Palaeomargin (Baeza-Carratalá, 2011, 2013; Baeza-Carratalá *et al*., 2014, 2015, 2016a, 2016b, 2018a) and shows fluctuations in which correlate with the major environmental perturbation events. In particular, the biotic crisis related to the Jenkyns Event represented the most important brachiopod faunal turnover during the Mesozoic and the Cenozoic worldwide (Hallam, 1996; Vörös, 2002; Ruban, 2004, 2009; García Joral *et al*., 2011; Bae-

za-Carratalá *et al*., 2015, 2017; Vörös *et al*., 2019; Baeza-Carratalá & García Joral, 2020).

Numerous high-resolution datasets of carbon and oxygen isotopes have been developed in order to elucidate episodes of warming and anoxia as the most probable causes for the early Toarcian biotic crisis (Jenkyns & Clayton, 1997; Hesselbo *et al*., 2000, 2007; Suan *et al*., 2008; Bodin *et al*., 2010; Littler *et al*., 2010; Reolid *et al*., 2012; Danise *et al*., 2013; Ait-Itto *et al*., 2017; Ruebsam *et al*., 2020; Ullmann *et al*., 2020). In the Pliensbachian-Toarcian deposits of the South-Iberian Palaeomargin, analysis of major and trace elements in bulk rock have been also performed (Rodríguez-Tovar & Reolid, 2013; Reolid *et al*., 2014) as well as the analysis of the O and C stable isotope composition in bulk rock (Rodríguez-Tovar & Reolid, 2013), fossil shells (Reolid, 2014) and organic matter (Rodrigues *et al*., 2019; Ruebsam *et al*., 2020), which pointed out changes in palaeoproductivity, water circulation, temperature, detrital input, and oxygenation degree. These changes were related to the biotic crisis that correlated with the T-OAE, although widespread anoxic conditions were not developed in the South-Iberian Palaeomargin (Reolid *et al*., 2015, 2018), being therefore more probably related to other effects of the Jenkyns Event such as a global warming episode (Reolid *et al*., 2020).

Calcite and aragonite readily incorporate trace elements during precipitation (Smrzka *et al*., 2019 and references therein). As the main source of many trace elements in calcite is seawater, the rate of trace element enrichment depends on bottom water renewal rates and residence times of the elements (Algeo & Lyons, 2006). Incorporation of trace elements into skeletal structures has been analysed in foraminifera (Boyle, 1981; Delaney & Boyle, 1982; Palmer, 1985; Russell *et al*., 1994; de Nooijer *et al*., 2007; Munsel *et al*., 2010; Keul *et al*., 2013; Wang *et al*., 2016), mollusk shells (Blanchard & Oakes, 1965) and corals (Scherer & Seitz, 1980; Swart & Hubbard, 1982; Shen & Dunbar, 1995; Sholkovitz & Shen, 1995; Akagi *et al*., 2004; Wyndham *et al*., 2004; Raddatz & Rüggeberg, 2019). Brachiopod shells consist of low-Mg calcite, and their growth is controlled at the mantle margin of both valves by a conveyor-belt system of outer epithelial secreting cells proliferating at the generative zone (e.g. Immel *et al*., 2015). Geochemical studies on extant brachiopods have revealed that element incorporation in calcite shells occurs in equilibrium with the seawater with only small or negligible "vital effects" (Bates & Brand, 1991; Brand *et al*., 2003; Simonet-Roda *et al.,* 2019) and constitutes a good indicator of surrounding environmental conditions if diagenetic overprint is negligible (e.g. Lee *et al*., 2004; Korte *et al*., 2005).

Carbonate minerals are highly prone to incorporate significant amounts of trace elements (Veizer, 1983; Smrzka *et al*., 2019) via co-precipitation and adsorption (Zachara *et al*., 1991; Paquette & Reeder, 1995). The calcite partition coefficient quantifies the incorporation of trace elements into the calcite structure and considers the trace element content in the water and its compatibility with calcium in the calcite structure in terms of the size/charge ratio. Thus, trace elements with an ion radius and charge similar to Ca^{2+} such as Co, Zn, Mn, and Fe will be more prone to be incorporate into the calcite structure via co-precipitation (Morse & Mackenzie, 1990). Co-precipitation is influenced by shell growth rate and surface structure (Reeder *et al*., 1999). For most of the trace elements, the partition coefficient increases with water temperature and consequently increases the incorporation of trace elements into calcite (Böttcher & Dietzel, 2010). Element adsorption on the mineral surface is the second major process enabling trace elements incorporation into calcite and is related to their size (ion radius) relative to the Ca^{2+} ion that is substituted within the lattice. The adsorption of cations is favoured with decreasing ionic radius, with the adsorption of free metals ions for divalent cations, or as complexed aqueous species for trivalent cations (Zachara *et al*., 1988; Cheng *et al*., 1999).

Trace element content in the water column shows a variable vertical distribution and is controlled by a complex interaction involving source strengths, their removal rates and water circulation patterns (Smrzka *et al*., 2019). Trace element concentration and distribution in seawater depends on continental influx, redox environmental conditions, suspended particulate matter, organic matter, volcanic and hydrothermal sources, atmospheric dust deposition, and diffusion from sediments (e.g. Tribovillard *et al*., 2006; Chester & Jickells, 2012). In particular, biological productivity in the ocean is strongly influenced by

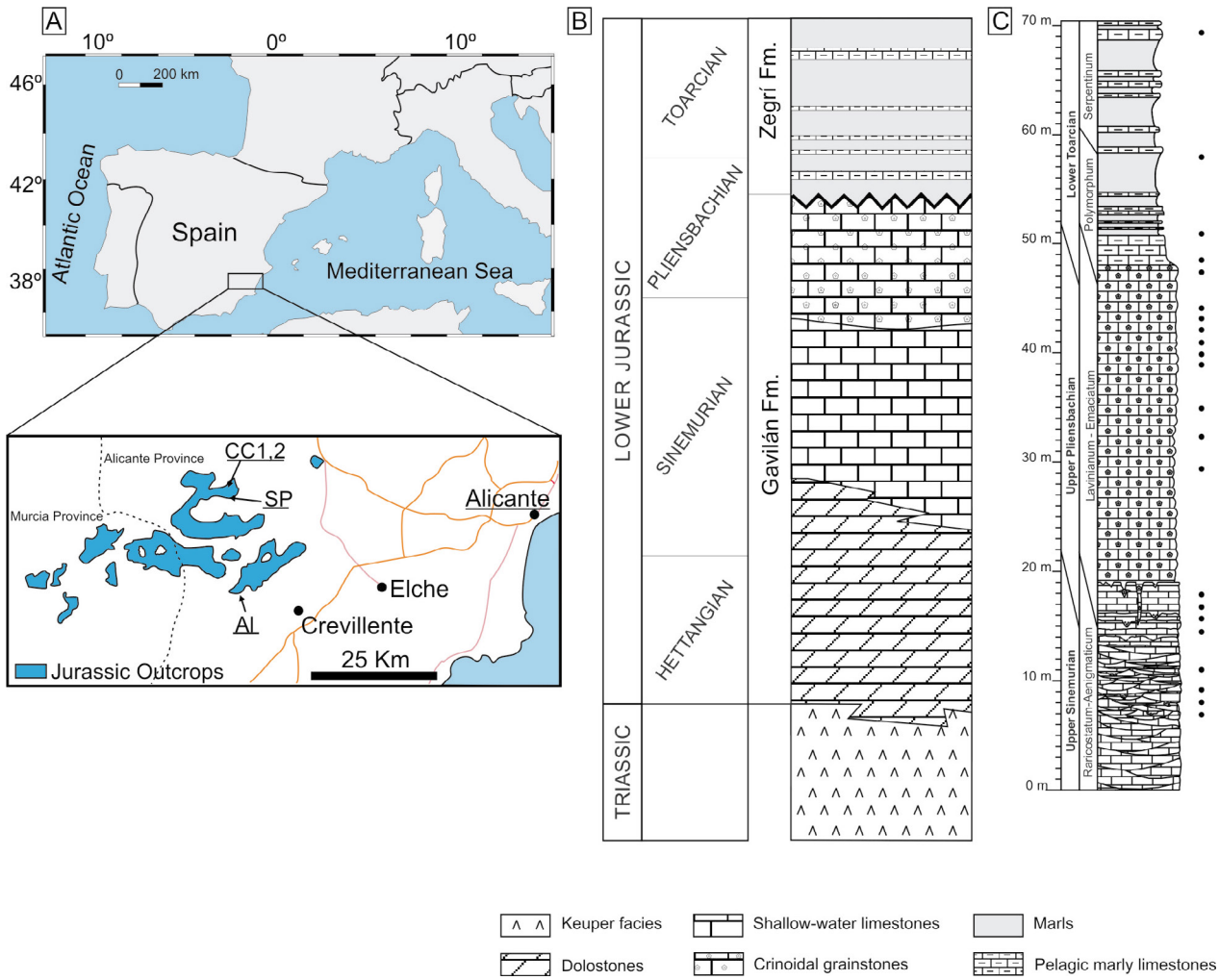

Figure 2.— A. Localization of the study sections (SP: Sierra Pelada, CC: Cerro de la Cruz, Al: Algueda) among the Jurassic outcrops from SE Spain; B. Synthetic stratigraphic sketch of the area and C. final composite section including the studied time interval (late Sinemurian–early Toarcian) and location of sampling beds (black points).

trace metal distribution, which generally exposes a nutrient-type depth pattern within the water column (Bruland, 1980; Bruland *et al*., 1991; Morel & Price, 2003; Tribovillard *et al.,* 2006; Smrzka *et al*., 2019).

For all the aforementioned reasons, geochemical analyses in shells can provide highly consistent proxies for the reconstruction of ancient palaeoenvironmental marine conditions (e.g. Popp *et al*., 1986; Korte *et al*., 2005, 2008; Grossman *et al*., 2008; Angiolini *et al*., 2012; Ullmann *et al*., 2014, 2016; Rasmussen *et al*., 2016; Harlou *et al*., 2016). The present work attempts to increase the fidelity of the brachiopod biotic signals related to the major Early Jurassic environmental shifts by analyzing the geochemical imprints on brachiopod shells. Brachiopods derived from the Eastern Subbetic (SE Spain) domain have been analyzed, emphasizing the possible relationship between changes in the trace elements content and environmental changes by assessing the diversity dynamics of the brachiopod fauna around the critical bioevents, mainly at the Sinemurian-Pliensbachian boundary and the Jenkyns Event from the Subbetic Domain (South-Iberian Palaeomargin).

Geological and stratigraphical setting

The brachiopod-bearing outcrops are located in the Crevillente and Reclot mountains in Alicante province, SE Spain (Fig. 2A), which are integrated in the Eastern Subbetic Domain of the External Betic Zone. The Mesozoic sedimentary rocks of this area

represent part of the South-Iberian Palaeomargin, located in the westernmost Tethys Ocean. During most of the Jurassic and Early Cretaceous, the Subbetic Domain was characterized by marine sedimentation with environments ranging from shallow carbonate platforms to pelagic troughs and swells (Azéma *et al*., 1979; Vera *et al*., 2004). In the Eastern Subbetic, the Lower Jurassic succession is typified by the Gavilán and Zegrí formations (e.g. García-Hernández *et al*., 1979; Ruiz-Ortiz *et al.*, 2004; Nieto *et al*., 2008) (Fig. 2B), which have been presented in the composite section herein arranged (Fig. 2C).

In the studied outcrops, the upper Sinemurian part of the Gavilán Formation consists of micritic and pseudo-oolithic whitish wackestone beds, showing lateral and upward transitions to oolithic grainstone/packstone levels with intraclasts and peloids. They were deposited in a proximal platform environment. The top of this lithostratigraphical unit shows intense extensional fissures. These were a consequence of an initial pre-rifting stage (Vera, 1988, 1998; Molina *et al*., 1999) interpreted as the first tectonic pulses and related to the drowning of the westernmost Tethyan platforms in the framework of the Central Atlantic Ocean opening (Ruiz-Ortiz *et al*., 2004).

The upper member of the Gavilán Formation (upper Pliensbachian) overlies these shallow-water platform facies. It consists of red crinoidal grainstone beds with abundant glauconite. Brachiopods, benthic foraminifera, peloids, and intraclasts are also common. These layers often show irregular tops with condensed pavements interpreted as omission surfaces or hardgrounds with ammonoids, belemnites, and brachiopods.

The onset of the marly sedimentation is represented by the Zegrí Formation, which dominates throughout the early–middle Toarcian in the basin, suggesting a pelagic depositional environment. This formation is made up by alternating yellowish to greenish marl/marly mudstone beds with calcarenites interspersed at the base of the formation, showing towards the top a continuous increase in the marly content.

Materials and methods

Brachiopods were collected from the Lower Jurassic succession of four outcrops of the Eastern Subbetic in close proximity (SP: Sierra Pelada; CC: Cerro de la Cruz: CC1, CC2; Al: Algueda sections in Fig. 2).

The Sierra Pelada section (coord. 38°21’29’’N, 0°55’07’’W) corresponds to the basal layers of the composite section, typifying the middle member of the Gavilán Formation. This unit mainly consists of massive micritic and oolithic wackestones, showing lateral and upward transitions to oolithic grainstone and packstone levels with intraclasts and micropellets. Faunal content mainly consists of brachiopod shell concentrations, sponge spicules, crinoids, and scarce gastropods and benthic foraminifera. Brachiopods are found in pocket-like accumulations and in thick cross-bedded deposits (Fig. 3A). This interval was assigned to the late Sinemurian-early Pliensbachian (Raricostatum-Aenigmaticum zones) (Baeza-Carratalá & García Joral, 2012; Baeza-Carratalá, 2013; Baeza-Carratalá *et al*., 2014). At the top of the section, crinoidal red limestone beds overly these deposits, infilling extensional fractures in the underlying white limestone layers.

The basal layers of the Cerro de la Cruz outcrops are found in the CC-1 section (coord. 38°21’37’’N, 0°54’58’’W) and can be stratigraphically correlated with the uppermost interval recorded in the Sierra Pelada section, i.e., nests of brachiopod concentrations infilling extensional fissures within white massive limestone beds. Upwards, the upper member of the Gavilán Formation is extensively developed in both CC-1 and CC-2 (coord. 38°21’43’’N, 0°54’52’’W) sections (Figs. 3B, C). This lithostratigraphic member consists of red crinoidal grainstones with abundant glauconite. Occasionally, calcarenites are interspersed. Fossil assemblages are dominated by crinoids, abundant brachiopods and benthic foraminifera. Sporadically, condensed pavements with ammonoids, belemnites, crinoids, and brachiopods, interpreted as omission or hardground surfaces, are recorded. The crinoidal grainstone deposits (Fig. 3B) are arranged in prograding lobes and, in the CC-2 section, a thinning-upward sequence is developed (Fig. 3C). The thin-bedded marly limestone layers of the Zegrí Formation overlie the crinoidal limestones, representing the top of both stratigraphic sections.

In the Algueda section (coord. 38°15’35’’N, 0°54’57’’W; Fig. 3D), the aforementioned red cri-

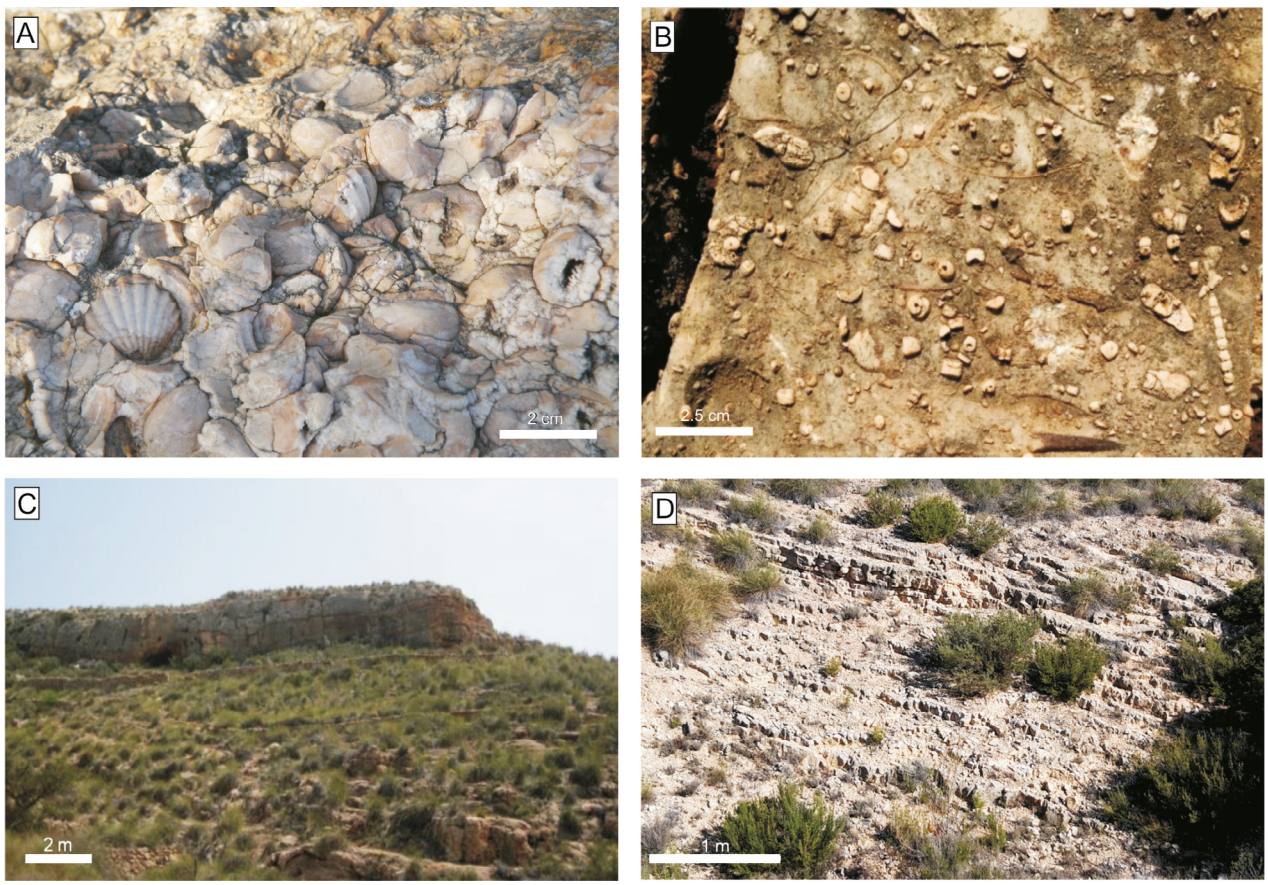

Figure 3.— Field view of the studied deposits. A. Skeletal concentrations made up of densely packed brachiopods of the Gavilán Formation in Sierra Pelada section. B. Crinoidal grainstone from the Gavilán Formation in the Cerro de la Cruz section 1 (CC-1) showing abundant crinoidal ossicles, brachiopods, and belemnite remains. C. Field view of the Cerro de la Cruz 2 section (CC-2) where the red crinoidal limestone beds rich in brachiopod crop out. d. Field view of the marl and marly limestone alternation beds of the Zegrí Formation (Serpentinum Zone), outcropping at the top of La Algueda section.

noidal grainstone deposits (about 30 m thick) belonging to the upper member of the Gavilán Fm., constitute the basal layers of the section. The top of this unit is represented by an irregular condensed pavement with ammonoids, belemnites, and brachiopods. Overlying these pavements are lenticular glauconitic sandy limestone deposits are recorded in a dark greyish matrix with abundant brachiopods, ammonoids, and gastropods. At the top of this carbonate sequence, the Zegrí Formation (35 m thick in this area) represents the onset of the marly sedimentation in the basin. In this outcrop the basal layers of the Zegrí Fm. consist of alternating yellowish and greenish marls and marly limestone, set out in thin beds with irregular top and bottom surfaces, where mudstone texture predominates. Levels of calcarenites and yellowish sandy marlstone beds are intercalated sporadically. The marly sedimentation dominates upwards up to the top of the section.

These sections have been summarized in a composite stratigraphical section (Fig. 2C), spanning the upper Sinemurian–lowermost Pliensbachian (Raricostatum-Aenigmaticum zones) to the lower Toarcian (Serpentinum Zone). The biostratigraphy of the studied Jurassic succession is based on the record of ammonites and brachiopods. The present study focuses on the analysis of trace elements from brachiopod shells recovered from this stratigraphic interval. Specimens are deposited in the collections of the Earth and Environmental Sciences Department (University of Alicante, Spain).

Taxonomic identification of brachiopods follow recent works on systematic data in the Subbetic Domain and neighboring basins of the Western Tethys

Table 1.— Arrangement of analysed brachiopod taxa in the samples of the composite section herein studied. Suprageneric taxonomical data are included to show the homogeneity (when possible) of the analysis. Total number of each taxon in the same level (nL) and total number of brachiopods recorded in the same level (ntL) are included to attest the representability of the selected taxa in each level.

Site	Level	Sample	Taxa	Author	Family	nL	ntL	Chronozone
Algueda	Z2 C2	Z2 C2-2g	*Telothyris pyrenaica*	Dubar, 1931	Lobothyrididae	14	17	Serpentinum-lowermost Bifrons (LT-MT)
Algueda	Z2.C2	Z2.C2-1g	*Telothyris pyrenaica*	Dubar, 1931	Lobothyrididae	14	17	Serpentinum-lowermost Bifrons (LT-MT)
Algueda	Z2.C1	Z2.C1-1g	*Soaresirhynchia bouchardi*	Davidson, 1852	Basiliolidae	3	3	Lower Serpentinum (LT)
Algueda	Z2.B	Z2.B-2g	*Lobothyris arcta*	Dubar, 1931	Lobothyrididae	3	7	Uppermost Emaciatum-Polymorphum (UP-LT)
Algueda	Z2.B	Z2.B-1g	*Lobothyris arcta*	Dubar, 1931	Lobothyrididae	3	7	Uppermost Emaciatum-Polymorphum (UP-LT)
Algueda	Z2.A	Z2.A-2g	*Prionorhynchia aff. polyptycha*	Oppel, 1861	Prionorhynchiidae	8	15	Lavinianum-Emaciatum (P)
Algueda	Z2.A	Z2.A-1g	*Prionorhynchia aff. polyptycha*	Oppel, 1861	Prionorhynchiidae	8	15	Lavinianum-Emaciatum (P)
Algueda	Z1.B	Z1.B-2g	*Prionorhynchia quinqueplicata*	Zieten, 1832	Prionorhynchiidae	49	168	Lavinianum-Emaciatum (P)
Algueda	Z1.B	Z1.B-1g	*Prionorhynchia quinqueplicata*	Zieten, 1832	Prionorhynchiidae	49	168	Lavinianum-Emaciatum (P)
Cerro Cruz 2	CC2.9	CC2.9	*Prionorhynchia quinqueplicata*	Zieten, 1832	Prionorhynchiidae	7	136	Lavinianum-Emaciatum (P)
Cerro Cruz 2	CC2.6	CC2.6-2g	*Prionorhynchia* quinqueplicata.	Zieten, 1832	Prionorhynchiidae	5	64	Lavinianum-Emaciatum (P)
Cerro Cruz 2	CC2.6	CC2.6-1g	*Prionorhynchia* sp.		Prionorhynchiidae	1	64	Lavinianum-Emaciatum (P)
Cerro Cruz 2	CC2.5	CC2.5-2g	*Cirpa briseis*	Gemmellaro, 1874	Wellerellidae	17	47	Lavinianum-Emaciatum (P)
Cerro Cruz 2	CC2.5	CC2.5-1g	*Cirpa briseis*	Gemmellaro, 1874	Wellerellidae	17	47	Lavinianum-Emaciatum (P)
Cerro Cruz 2	CC2.4	CC2.4-2g	*Cirpa* sp.		Wellerellidae	27	141	Lavinianum-Emaciatum (P)
Cerro Cruz 2	CC2.4	CC2.4-1g	*Cirpa* sp.		Wellerellidae	27	141	Lavinianum-Emaciatum (P)
Cerro Cruz 2	CC2.3	CC2.3-2g	*Cirpa* sp.		Wellerellidae	26	197	Lavinianum-Emaciatum (P)
Cerro Cruz 2	CC2.3	CC2.3-1g	*Cirpa briseis*	Gemmellaro, 1874	Wellerellidae	26	197	Lavinianum-Emaciatum (P)
Cerro Cruz 2	CC2.2	CC2.2-2g	*Cirpa briseis*	Gemmellaro, 1874	Wellerellidae	28	263	Lavinianum-Emaciatum (P)
Cerro Cruz 2	CC2.2	CC2.2-1g	*Cirpa briseis*	Gemmellaro, 1874	Wellerellidae	28	263	Lavinianum-Emaciatum (P)
Cerro Cruz 2	CC2.1	CC2.1-1g	*Prionorhynchia quinqueplicata*	Zieten, 1832	Prionorhynchiidae	71	210	Lavinianum-Emaciatum (P)
Cerro Cruz 2	CC2.0	CC2.0-2g	*Prionorhynchia* sp.		Prionorhynchiidae	25	210	Lavinianum-Emaciatum (P)
Cerro Cruz 2	CC2.0	CC2.0-1g	*Prionorhynchia quinqueplicata*	Zieten, 1832	Prionorhynchiidae	110	210	Lavinianum-Emaciatum (P)
Cerro Cruz 1	CC1.11	CC1.11-1g	*Liospiriferina* sp.		Spiriferinidae	2	34	Lavinianum-Emaciatum (P)
Cerro Cruz 1	CC1.10	CC1.10-2g	*Prionorhynchia* aff. *forticostata*	Böckh, 1879	Prionorhynchiidae	1	198	Lavinianum-Emaciatum (P)
Cerro Cruz 1	CC1.10	CC1.10-1g	*Prionorhynchia* aff. *gignouxi*	Jiménez de Cisneros, 1923	Prionorhynchiidae	3	198	Lavinianum-Emaciatum (P)
Cerro Cruz 1	CC1.8	CC1.8-2g	*Prionorhynchia gumbeli*	Oppel, 1861	Prionorhynchiidae	111	392	Lavinianum-Emaciatum (P)
Cerro Cruz 1	CC1.8	CC1.8-1g	*Prionorhynchia gumbeli*	Oppel, 1861	Prionorhynchiidae	111	392	Lavinianum-Emaciatum (P)
Cerro Cruz 1	CC1.6	CC1.6-2g	*Liospiriferina* sp.		Spiriferinidae	20	38	Lavinianum-Emaciatum (P)
Cerro Cruz 1	CC1.6	CC1.6-1g	*Liospiriferina* sp.		Spiriferinidae	20	38	Lavinianum-Emaciatum (P)
Cerro Cruz 1	CC1.1	CC1.1-1g	*Prionorhynchia regia*	Rothpletz, 1886	Prionorhynchiidae	11	311	Raricostatum-Aenigmaticum (US-LP)
Cerro Cruz 1	CC1.0	CC1.0-1g	*Calcirhynchia plicatissima*	Quenstedt, 1852	Wellerellidae	29	87	Raricostatum-Aenigmaticum (US-LP)
Sierra Pelada	BOL-1	BOL-1-1g	*Calcirhynchia plicatissima*	Quenstedt, 1852	Wellerellidae	44	309	Raricostatum-Aenigmaticum (US-LP)
Sierra Pelada	BOL-2	BOL-2-1g	*Calcirhynchia plicatissima*	Quenstedt, 1852	Wellerellidae	123	198	Raricostatum-Aenigmaticum (US-LP)
Sierra Pelada	EFC-0	EFC-0-1g	*Calcirhynchia plicatissima*	Quenstedt, 1852	Wellerellidae	78	187	Raricostatum-Aenigmaticum (US-LP)
Sierra Pelada	EFC-1	EFC-1-1g	*Calcirhynchia plicatissima*	Quenstedt, 1852	Wellerellidae	139	323	Raricostatum-Aenigmaticum (US-LP)
Sierra Pelada	EFC-2	EFC-2-1g	*Calcirhynchia plicatissima*	Quenstedt, 1852	Wellerellidae	215	515	Raricostatum-Aenigmaticum (US-LP)
Sierra Pelada	EFC- 3	EFC-3-1g	*Calcirhynchia plicatissima*	Quenstedt, 1852	Wellerellidae	48	118	Raricostatum-Aenigmaticum (US-LP)

(García Joral & Goy, 2000; Baeza-Carratalá, 2011, 2013; García Joral *et al*., 2011; Baeza-Carratalá *et al*., 2014). In order to minimize possible vital effects in the variation of trace elements, the minimal taxonomical assortment was favoured, selecting the same species/genus/family where possible (Table 1). Thus, the studied specimens are arranged in two families of rhynchonellides (Wellerellidae, genera *Calcirhynchia* and *Cirpa*; and Prionorhynchiidae, genus *Prionorhynchia*) and a single terebratulide Family (Lobothyrididae, genera *Lobothyris* and *Telothyris*). Other genera were used for those levels where these taxa were not recorded (paucity or occurrence of bioevents). In these cases, taxa were selected from groups for which vital effects in modern specimens are known to be negligible (Brand *et al*., 2003).

Ephebic/adult individuals were selected to avoid ontogenetic effect. Likewise, preservation of the shell was analysed near the mid-length. Possible signs of diagenetic alteration were studied on 45 samples with a binocular microscope and carried out by high-resolution microphotographs of acetate peels taken with a Nikon CFI60 600POL microscope. In addition, sections of the brachiopod shells were carbon coated and analysed with images of secondary electrons, cold cathodoluminescence and EDX (energy-dispersive X-ray spectroscopy) elemental mapping in a Merlin Carl Zeiss Scanning Electron Microscope (SEM) at the Centro de Instrumentación Científico-Técnica of the University of Jaén (Spain). Mn^{2+}, Mn^{4+}, Cr^{3+} and Pb^{2+} are the main activators of luminescence in carbonates (Machel & Burton, 1991; Machel *et al*., 1991), indicative of diagenetic recrystallization of brachiopod shell (Van Geldern *et al.,* 2006). Finally, non-luminescent shells were selected for geochemical analyses. The EDX elemental mappings show the Mn and Fe were below detection limit. Thus, diagenetic alterations of the microstructure of the secondary layer (dissolution and recrystallization) of the shell could be excluded in the analysed specimens (cf. Ullmann *et al*., 2020), selecting those with the unaltered leptinoid/eurinoid microstructure pattern (Fig. 4). Recrystallization of carbonates is commonly accompanied by changes, usually increase, in the content of Fe and Mn, which are mobilised during recrystallization by diagenetic reactions (McArthur *et al*., 1994). However, there is no stablished threshold in element concentration working as diagnostic of alterations. McArthur *et al.* (1994) proposed 500 ppm for Fe and 300 ppm for Mn. The selected specimens are mostly < 500 ppm for Fe and mostly < 100 ppm of Mn.

Therefore, a total of 38 specimens have been analysed assuming that biogenic calcite from the secondary layer of these brachiopod shells and consequently their shifts in trace elements content reflect variations in concentration in the water column. This is consistent with several studies (Popp *et al*., 1986; Veizer *et al*., 1999; Korte *et al*., 2017) showing the low-Mg calcite of brachiopod shells to be resistant to diagenesis. Therefore, in the present study geochemical data have been obtained from 8 specimens of *Calcirhynchia*, 7 *Cirpa*, 15 *Prionorhynchia*, 2 *Lobothyris*, 2 *Telothyris*, 1 *Soaresirhynchia*, and 2 *Liospiriferina*.

Texturally well-preserved brachiopod shells (Fig. 4) were prepared for an acid dissolution mainly following the method described in Brazier *et al.* (2015). The shells of 38 selected specimens were carefully washed with deionized water and the primary layer was removed with a dental scraper under a binocular microscope (cf. Ullmann *et al*., 2020). Shells were individually studied from each sampling bed in the Applied Petrology Laboratory of the University of Alicante. Every powdered shell sample (100 mg), was obtained by means a microdrill tool, also avoiding the posterior cardinal area. Subsequently every sample was directly dissolved in 3.5N HNO_3 for 48 hours. Trace elements were analysed using inductively coupled plasma-mass spectrometry (ICP-MS Agilent 7700x, using SCP33MS multi-element and REE standard solution, SCP Science at the Research Technical Services of the University of Alicante), whereas calcium concentration was determined with an inductively coupled plasma atomic emission spectrometer (ICP-AES, Perkin Elmer, Optima 7400DV, with a 7300DV standard solution, Perkin Elmer at the Research Technical Services of the University of Alicante). The trace element contents, mainly for studying stratigraphic fluctuations, have not been normalized to aluminum since this is common for geochemical studies of bulk rock where some trace elements may be related to aluminosilicates (Calvert, 1990; Calvert & Pedersen, 1993) but in the present study the analyses are performed

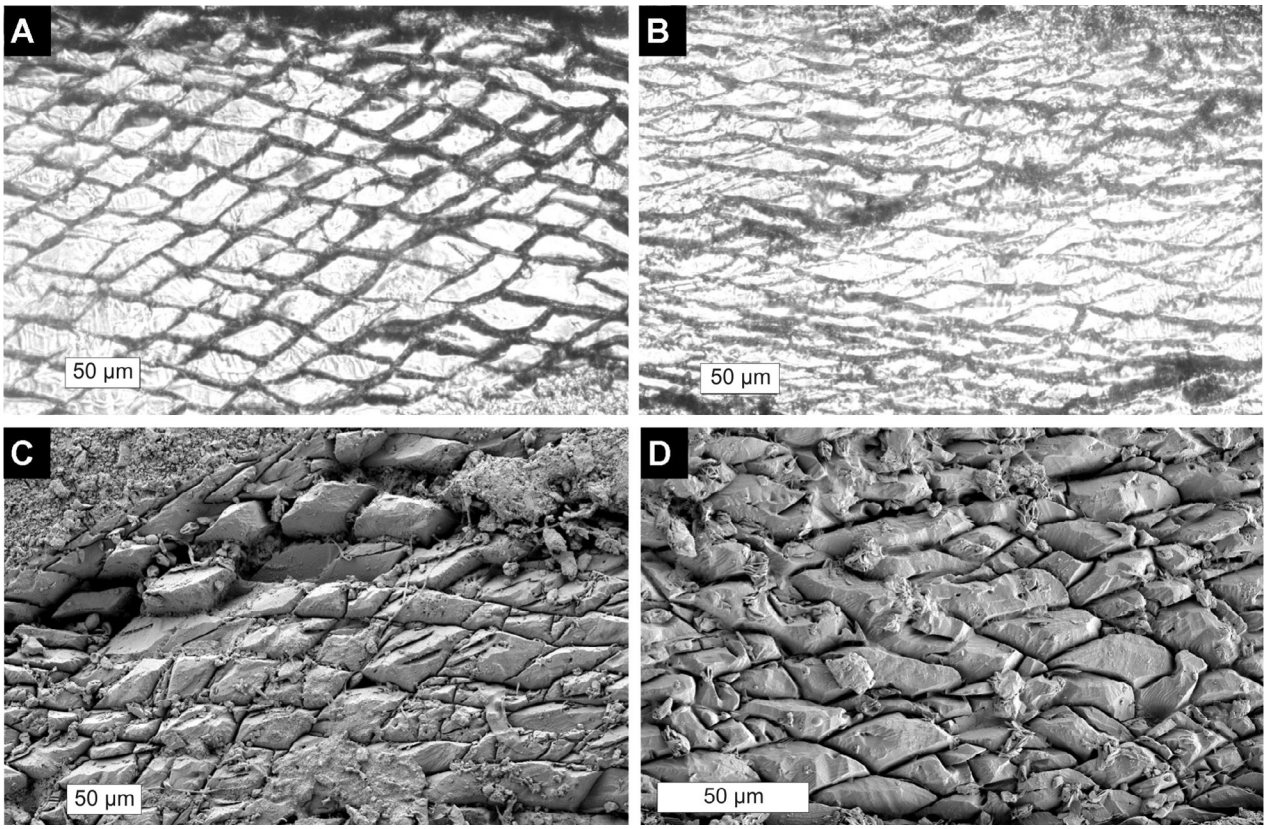

Figure 4.— Microstructure preservation of the secondary layer of the shell of some representative brachiopod species analysed. Diagenetic alteration is absent as shown by the excellent preservation of the calcite fibres. A Microphotograph of a section performed in *Soaresirhynchia bouchardi* (Sb2.Z2.C1 specimen) at 1.10 mm from the apex, evidencing eurinoid microstructure pattern. B Microphotograph of a section performed in *Prionorhynchia quinqueplicata* (pQ1.CC2.0 specimen) at 5.10 mm from the apex, evidencing leptinoid microstructure pattern. C SEM image showing the eurinoid ultrastructure in a section at 3.60 mm from the apex in *Cirpa briseis* (CC2.5-2g specimen). D SEM image showing the leptinoid ultrastructure in a section at 2.90 mm from the apex in *Prionorhynchia gumbeli* (CC1.8-2g specimen).

on the brachiopod shells. The Mg/Ca ratio has been applied to selected shells. According to Brand *et al*. (2013) brachiopods exhibit a Mg/Ca ratio that is temperature dependent, but it is not clear from calibration studies if there is an exponential relationship between temperature and Mg/Ca ratio (Anand *et al*., 2003; Regenberg *et al*., 2009) or a linear one (Quillmann *et al*., 2012). Here we use this ratio for determining relative trends in temperature.

A statistical analysis was applied using SPSS vs. 26 (IBM). Descriptive statistics summarize features of trace elements in the brachiopod shells. Concentration profiles and variations of trace elements were plotted against the stratigraphical section. Finally, a Principal Component Analysis (PCA) applied to the database, as exploratory method for variable reduction, to establish the structure of the variable dependence and interrelationship between trace elements. PCA evaluates variable groupings within multivariate data by calculating principal components for a given percentage of the total variance. These components are computed by coefficients or scores, which include: (1) the absolute value of the coefficients (high values in several coefficients of the same principal component show a close relationship between them) and (2) the sign of the coefficients (the same or opposite sign of several coefficients shows the direct or inverse relationship between them).

Brachiopod biochronostratigraphy

In the lowermost deposits (samples EFC3 to CC1.0), the analysed brachiopod shells predominantly belong to *Calcirhynchia plicatissima* (Table 1, Fig. 6), which shows a continuous record in these

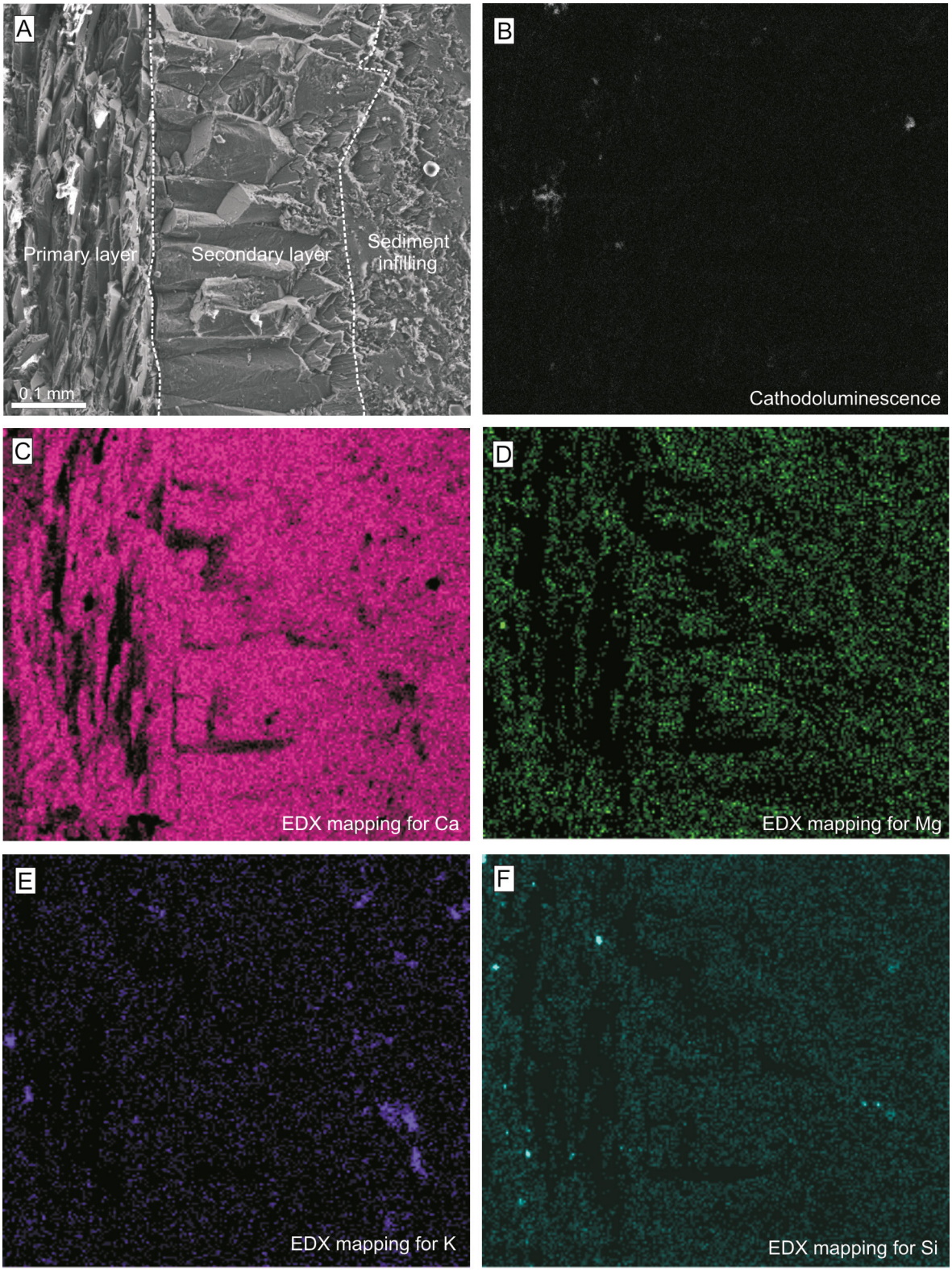

Figure 5.— SEM images of primary and secondary layers of the shell of a *Prionorhynchia gumbeli* under SEM. Diagenetic alteration is discarded as shown by the absence of cathodoluminescence. The EDX elemental mapping only recognised C, O, Ca, Mg, Na, K and Si. Other elements are very scarce and they are only detected with ICP-MS. A. Secondary electron image. B. Cathodoluminiscence image. C – F. Selected EDX elemental maps for Ca, Mg, K and Si.

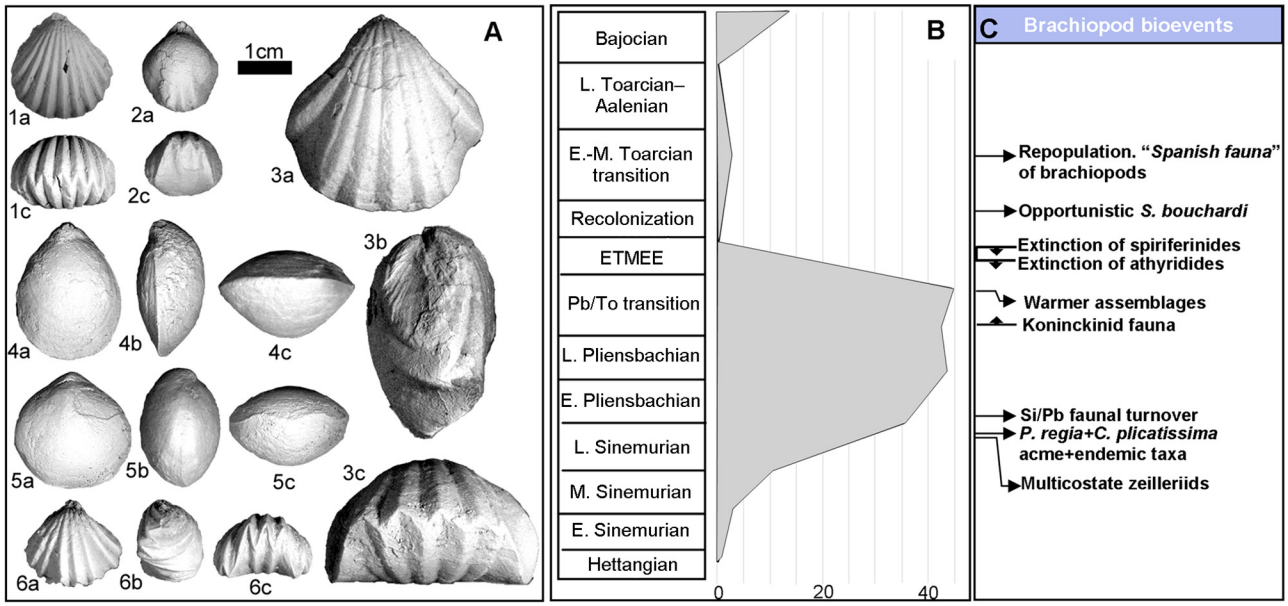

Figure 6.—A. Some representative taxa selected to carry out the geochemical analysis. 1. *Calcirhynchia plicatissima* (Quenstedt), specimen O.15.8.4; 2. *Soaresirhynchia bouchardi* (Davidson), specimen Z2.Al.Bo.1; 3. *Prionorhynchia quinqueplicata* (Zieten), specimen O.9.2.1; 4. *Lobothyris arcta* (Dubar), specimen Z2.Al.Ar.4; 5. *Telothyris* gr. *pyrenaica* (Dubar), specimen Z2C.Al.Py.4; 6. *Cirpa briseis* (Gemmellaro), specimen CC.A8.Cb.1. All specimens were coated with magnesium oxide prior to photographing. Views of each specimen are ordered consecutively in (a) dorsal, (b) lateral, and (c) anterior views. B. Diversity dynamics at species level in the brachiopod assemblages in the Lower Jurassic from the Eastern Subbetic (modified after Baeza-Carratalá, 2011). Abundance data is given in absolute quantitative number of species. C. Main faunal turnover and critical brachiopod bioevents recorded in the Eastern Subbetic.

sediments. The acme of this species, together with that of *Prionorhynchia regia* and *Gibbirhynchia curviceps,* plus the first occurrence of multicostate zeilleriids and the genus *Securina*, typify the Assemblage 1 of brachiopods in the easternmost Subbetic (Baeza-Carratalá, 2013). This assemblage is assigned to the Sinemurian-Pliensbachian transition (Raricostatum-Aenigmaticum zones).

In the middle part of the Lower Jurassic succession, the analysed shells are among the prevailing taxa of Assemblage 2 (Baeza-Carratalá, 2013). Thus, several species of *Prionorhynchia* and *Cirpa* are selected for geochemical analyses (Table 1), since they occur profusely in the upper member of the Gavilán Formation. In these deposits, spiriferinides acquire great diversity and abundance as well, and they were selected for analyses only when multicostate rhynchonellides were not available. Data from ammonite faunas in these sediments range in age from the lower (Demonense Zone) up to the upper (Algovianum Zone) Pliensbachian (Braga, 1983; Iñesta, 1988; Tent-Manclús, 2006).

The biochronological control of brachiopods prior to and after the Jenkyns Event is more accurate if the Subbetic record is correlated with that of the nearby Iberian basin, where an extensive succession of ammonites allows for a precise calibration. Thus, *Lobothyris arcta* is recorded prior to the Jenkyns Event in the Emaciatum-Polymorphum zones (García Joral *et al*., 2011, Baeza-Carratalá, 2013) together with several spiriferinid (*Calyptoria vulgata*) and athyridide representatives (the so-called Koninckinid fauna; Fig. 6), which became extinct in the earliest Serpentinum Zone as an effect of the Jenkyns Event (Ager, 1987; Vörös, 2002; Comas-Rengifo *et al*., 2006; Baeza-Carratalá *et al*., 2015, 2018a; Vörös *et al.*, 2016, 2019). After this event, *Soaresirhynchia bouchardi* led the repopulation interval in many Western Tethyan basins (Fig. 6), constituting monospecific assemblages in the Elegantulum Subzone of the Serpentinum Zone (García Joral & Goy, 2000; García Joral *et al*., 2011; Baeza-Carratalá *et al*., 2011, 2017; Comas-Rengifo *et al*., 2013, 2015). Therefore, *Soaresirhynchia bouchardi* was selected for geochemical analyses of this stratigraphic post-crisis interval (Table 1).

Finally, *Telothyris pyrenaica* is selected (Table 1) as representative for the lower-middle Toarcian,

Serpentinum–lowermost Bifrons zones (García Joral & Goy, 1984, 2000; García Joral *et al*., 2011; Baeza-Carratalá *et al*., 2016c), signifying the re-establishment of the background conditions after the extinction event.

Trace element geochemistry and potential sources

Stratigraphic fluctuations

Concentration values of the trace elements and their distribution by samples have been displayed in boxplots Fig. 7 and Table 2. Mg, Al, and Fe are present in high values in the shells, followed by Sr. Among trace elements, Cr, Zn, and Ni show the highest values. The REEs show very low concentrations with the highest values corresponding to La, Ce, and Nd (Fig. 7). According to the brachiopod taxa analysed, the concentrations of elements are slightly different among the most common genera, *Calcirhynchia* and *Prionorhynchia.* Values of Ti, Cr, Fe, Co, Ni, Cu, Zn, Mo, Ba, and Pb are relatively higher in the shells of *Calcirhynchia* whereas Al, V, Mn, Th, and U show higher values in the shells of *Prionorhynchia.*

Selected trace element contents have been plotted against the stratigraphic composite section and the biochronostratigraphic framework (Figs. 8, 9) to elucidate the variation of contents over time, correlated with key events in the fossil and stratigraphic record. These selected trace elements are related to biological cycling or complexed in particulate organic matter (Mo, Ni, Zn, Cu, Co, Cd, and U) most of them

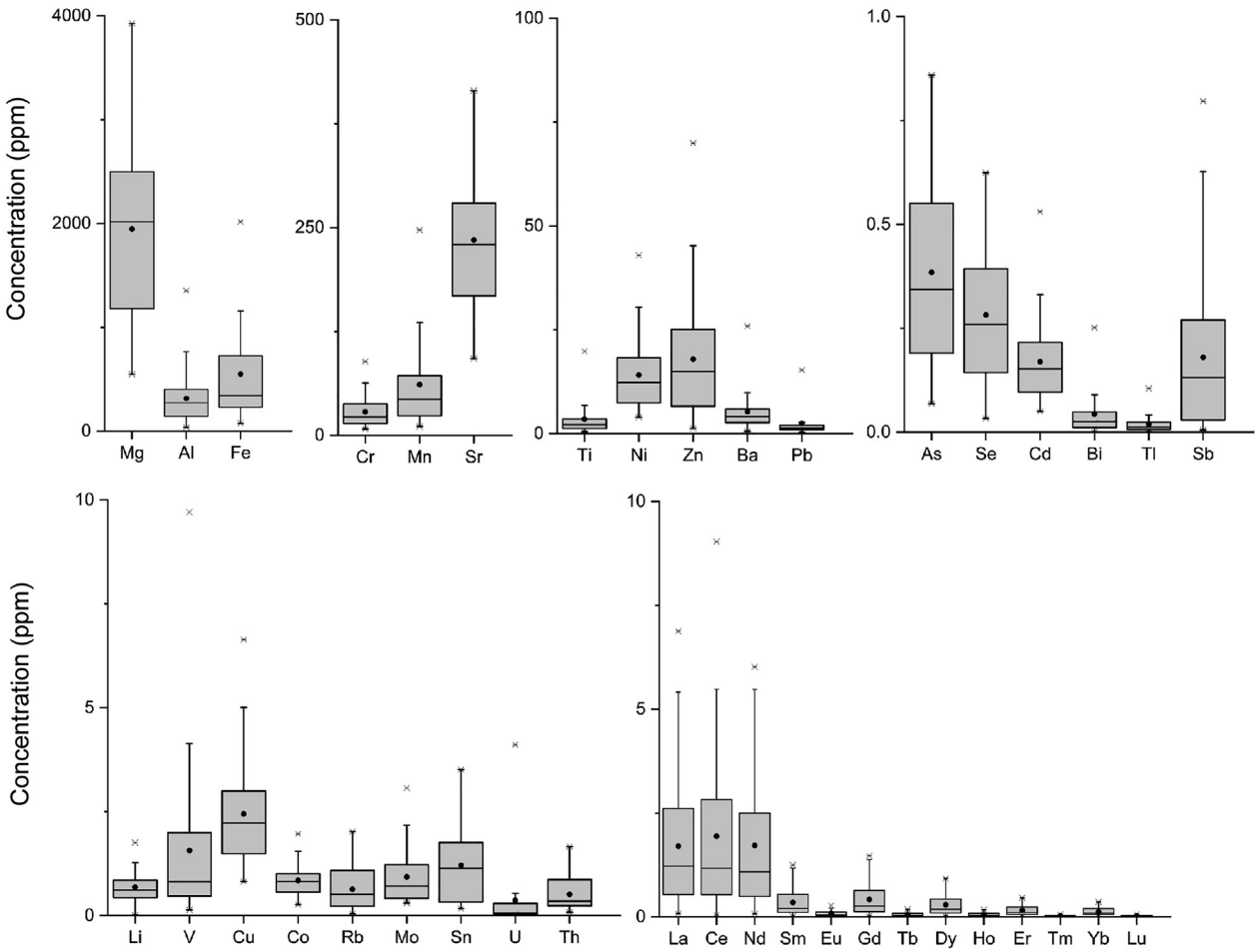

Figure 7.— Boxplot diagram representing the concentration of the trace elements in all the analysed samples. Boxes range from lower to upper quartiles, and the median is shown with a horizontal line inside the box, and whiskers denote minimum and maximum values unless they are considered outliers (denoted by crosses).

Table 2.— Chemical composition of studied specimens in ppm.

Specie	Sample Name	Ca	Li	Mg	Al	Ti	V	Cr	Mn	Fe	Co	Ni	Cu	Zn	As	Se	Rb
Telothyris pyrenaica	Z2C2-2g	2680	1,272	3119,207	576,110	1,511	2,527	14,428	85,239	947,400	1,547	8,069	2,298	8,893	0,568	0,417	1,285
Telothyris pyrenaica	Z2C2-1g	2466,44	0,516	2498,053	552,400	8,028	1,989	13,144	71,595	1084,134	1,309	7,791	1,492	9,078	0,606	0,461	1,130
Soaresirhynchia bouchardi	Z2C1-1g	754,52	0,367	2473,061	558,334	8,920	2,011	31,803	88,051	991,866	1,087	16,092	2,994	22,832	0,550	0,443	1,299
Lobothyris arcta	Z2B-2g	2070,00	0,746	2365,311	402,645	1,541	3,555	17,860	68,328	2017,471	0,760	7,680	3,085	18,939	0,774	0,341	0,986
Lobothyris arcta	Z2B-1g	539,99	1,757	3360,184	386,367	6,824	2,198	59,946	88,685	1157,010	1,067	29,775	4,948	54,127	0,442	0,552	1,081
Prionorhynchia aff. *polyptycha*	Z2A-2g	2660,00	0,719	2782,539	302,514	1,272	4,140	20,251	247,076	1016,647	0,921	5,691	1,179	13,260	0,307	0,255	0,639
Prionorhynchia aff. *polyptycha*	Z2A-1g	1985,39	0,852	2645,362	203,885	2,815	2,793	18,763	177,945	657,151	0,754	9,990	2,005	15,014	0,560	0,226	0,519
Prionorhynchia quinqueplicata	CC 2.9	3263,55	0,493	1047,500	143,051	1,742	0,457	9,969	32,149	145,314	0,425	4,605	1,951	4,828	0,106	0,128	0,225
Prionorhynchia quinqueplicata	CC 2.6-2g	2440,00	0,670	2410,213	378,689	1,430	0,873	17,640	131,913	316,998	1,003	9,999	2,176	3,733	0,191	0,276	0,742
Prionorhynchia sp.	CC 2.6-1g	1280,41	1,187	2486,321	588,409	8,367	1,308	27,748	56,876	473,038	0,901	16,626	2,912	10,723	0,534	0,393	1,414
Cirpa briseis	CC 2.5-1g	2325,84	0,435	736,626	187,437	2,465	0,471	12,524	16,299	170,529	0,566	6,441	1,230	3,492	0,301	0,091	0,251
Cirpa sp.	CC 2.4-2g	2230,00	0,621	2451,784	291,754	1,136	0,992	16,398	22,456	230,799	0,771	8,034	1,585	16,229	0,537	0,324	0,567
Cirpa sp.	CC 2.4-1g	920,77	0,360	1089,895	252,991	3,400	0,702	28,546	45,187	317,990	0,711	13,810	2,424	20,096	0,427	0,178	0,894
Cirpa sp.	CC 2.3-2g	2410,00	0,562	1733,885	314,556	1,208	0,683	14,652	23,851	228,440	0,815	7,442	1,448	3,819	0,416	0,378	0,500
Cirpa briseis	CC 2.3-1g	1138,59	1,046	2124,458	626,939	7,880	1,260	42,627	43,209	634,408	1,202	20,070	3,518	18,709	0,857	0,264	1,095
Prionorhynchia quinqueplicata	Z1B-2g		0,607	2565,395	224,262	3,512	6,891	13,748	222,814	1639,107	1,043	5,652	1,222	14,822	0,322	0,227	0,471
Prionorhynchia quinqueplicata	Z1B-1g	1204,45	0,837	2009,469	659,261	9,901	9,708	51,390	43,488	970,315	0,959	16,100	2,529	25,078	0,839	0,544	1,139
Cirpa briseis	CC 2.2-2g	2830,00	0,908	3586,443	464,002	2,425	1,780	20,569	49,325	417,371	1,292	12,778	1,906	26,007	0,688	0,439	0,760
Cirpa briseis	CC 2.2-1g	3584,54	0,301	834,531	41,038	0,545	0,136	10,382	12,825	88,774	0,431	4,878	0,818	4,129	0,107	0,103	0,050
Liospiriferina sp.	CC 1.11-1g	853,00	0,346	2551,152	381,971	5,614	1,287	49,954	64,397	583,388	0,863	30,042	3,159	16,945	0,473	0,539	1,493
Prionorhynchia quinqueplicata	CC 2.1-1g	1851,73	0,412	1559,939	160,748	2,135	0,385	16,224	45,212	233,793	0,567	7,694	1,273	6,201	0,306	0,126	0,367
Prionorhynchia aff. *forticostata*	CC 1.10-2g	2460,00	0,581	2025,128	293,435	0,894	0,925	9,378	35,902	200,755	0,634	6,929	1,146	4,448	0,348	0,290	0,610
Prionorhynchia aff. *gignouxi*	CC 1.10-1g	774,19	0,007	1242,296	88,918	1,272	0,369	29,937	34,070	262,466	0,464	19,089	2,174	6,582	0,151	0,098	0,160
Prionorhynchia sp.	CC 2.0-2g	3320,00	0,434	910,023	304,298	1,234	0,760	10,177	119,619	203,825	0,905	5,365	1,384	17,061	0,447	0,243	0,270
Prionorhynchia quinqueplicata	CC 2.0-1g	2355,41	0,173	548,274	37,772	0,492	0,145	7,708	25,354	75,924	0,264	3,946	1,603	1,241	0,074	0,045	0,041
Prionorhynchia gumbeli	CC 1.8-2g	3420,00	0,546	2185,185	205,858	1,008	0,554	10,229	23,395	191,984	0,715	5,222	1,279	3,718	0,215	0,271	0,414
Prionorhynchia gumbeli	CC 1.8-1g	789,97	0,887	1679,184	115,466	2,143	0,586	28,903	61,176	277,794	0,874	16,184	2,051	7,128	0,384	0,200	0,270
Liospiriferina sp.	CC 1.6-2g	2060,00	1,206	3925,997	765,832	3,292	1,989	23,618	43,219	724,987	1,283	12,252	2,703	13,049	0,685	0,600	1,429
Liospiriferina sp.	CC 1.6-1g	1432,11	0,798	3103,800	329,610	4,907	1,345	25,364	56,979	513,376	0,683	12,359	2,277	8,406	0,340	0,166	0,658
Calcirhynchia plicatissima	CC 1.1-2g	2170,00	0,744	1710,425	144,382	1,501	0,479	16,642	35,638	220,839	1,005	8,755	1,600	29,784	0,104	0,277	0,165
Prionorhynchia regia	CC 1.1-1g	866,61	0,579	745,207	38,901	0,944	0,346	37,632	10,586	247,396	0,564	20,865	3,042	69,914	0,088	0,129	0,075
Calcirhynchia plicatissima	CC.1.0-1g	789,97	0,595	750,643	35,751	1,033	0,288	30,357	11,521	214,929	0,444	15,000	2,403	22,741	0,075	0,082	0,091
Calcirhynchia plicatissima	BOL-1-1g	719,95	0,801	1320,683	87,094	2,199	0,646	41,483	20,888	360,102	0,712	20,619	3,064	28,901	0,190	0,178	0,131
Calcirhynchia plicatissima	BOL-2-1g	286,13	0,333	2132,527	1352,364	19,847	3,126	88,892	135,622	1538,479	1,964	42,947	6,642	45,284	0,859	0,625	2,020
Calcirhynchia plicatissima	EFC-0-1g	482,24	1,275	1516,373	145,575	2,466	0,638	62,941	24,329	460,403	0,853	30,451	5,315	30,108	0,167	0,390	0,329
Calcirhynchia plicatissima	EFC-1-1g	515,99	0,194	1180,938	123,855	2,394	0,595	62,859	18,277	452,778	0,828	30,297	5,008	35,334	0,299	0,246	0,178
Calcirhynchia plicatissima	EFC-2-1g	856,47	1,015	1606,679	38,215	1,119	0,264	38,048	12,918	267,023	0,538	18,264	2,667	31,274	0,068	0,144	0,090
Calcirhynchia plicatissima	EFC-3-1g	556,37	0,791	913,236	149,455	3,097	0,397	37,650	15,429	325,954	0,551	18,211	2,434	9,812	0,214	0,033	0,251

	Sr	Mo	Cd	Sn	Sb	Ba	Pb	Bi	Th	U	La	Ce	Nd	Sm	Eu	Gd	Tb	Dy	Ho	Er	Tm	Yb	Lu	Tl
	385,260	0,398	0,108	0,289	0,060	4,390	1,398	0,142	0,862	0,537	3,724	6,373	5,479	1,168	0,260	1,377	0,180	0,925	0,172	0,462	0,058	0,352	0,056	0,072
	235,970	0,445	0,131	0,628	0,104	8,180	4,914	0,022	0,877	0,343	3,210	5,191	4,689	1,083	0,210	1,218	0,150	0,790	0,134	0,371	0,042	0,258	0,040	0,021
	166,230	1,066	0,149	1,674	0,270	12,328	9,808	0,041	0,933	0,144	3,061	5,481	3,778	0,812	0,172	0,984	0,117	0,655	0,115	0,333	0,041	0,246	0,037	0,030
	230,876	0,373	0,103	0,324	0,045	4,514	1,218	0,089	0,730	0,270	3,636	4,558	4,367	0,748	0,161	0,852	0,108	0,544	0,101	0,274	0,037	0,231	0,039	0,041
	365,554	1,982	0,116	2,723	0,291	7,699	4,516	0,045	1,334	0,413	3,217	4,559	3,563	0,742	0,160	0,947	0,110	0,628	0,110	0,326	0,040	0,255	0,037	0,028
	231,469	0,300	0,143	0,198	0,018	4,000	1,531	0,048	0,306	1,190	1,923	1,529	1,539	0,283	0,070	0,360	0,049	0,269	0,055	0,159	0,022	0,149	0,026	0,008
	279,466	0,571	0,177	0,835	0,129	4,646	11,371	0,023	0,416	0,520	1,373	1,069	1,055	0,189	0,044	0,244	0,032	0,186	0,037	0,115	0,015	0,104	0,017	0,009
	167,856	0,331	0,138	0,484	0,084	2,787	1,275	0,010	0,164	0,033	0,827	0,575	0,584	0,110	0,026	0,145	0,018	0,113	0,021	0,066	0,009	0,057	0,009	0,005
	199,025	0,548	0,204	0,334	0,011	3,402	0,905	0,036	0,279	0,038	0,904	1,270	0,914	0,187	0,043	0,239	0,032	0,168	0,032	0,089	0,012	0,074	0,012	0,007
	174,186	0,989	0,220	1,509	0,231	4,204	1,860	0,051	0,877	0,062	2,348	2,825	2,496	0,544	0,113	0,636	0,082	0,428	0,081	0,239	0,031	0,182	0,026	0,033
	214,208	0,468	0,077	0,725	0,145	2,071	0,729	0,026	0,221	0,025	0,547	0,533	0,537	0,108	0,025	0,124	0,016	0,093	0,017	0,053	0,007	0,041	0,007	0,016
	148,669	0,489	0,262	0,297	0,012	2,514	1,217	0,038	0,281	0,050	1,569	1,512	1,433	0,268	0,062	0,334	0,042	0,231	0,046	0,129	0,018	0,107	0,019	0,028
	131,825	1,029	0,331	1,942	0,408	4,811	3,646	0,090	0,633	0,069	1,203	1,379	1,113	0,215	0,049	0,284	0,035	0,182	0,034	0,097	0,013	0,078	0,013	0,055
	263,572	0,466	0,205	0,289	0,014	2,742	0,829	0,023	0,192	0,035	1,157	1,014	1,111	0,224	0,055	0,277	0,037	0,200	0,039	0,110	0,015	0,088	0,015	0,014
	261,711	1,580	0,291	3,124	0,774	6,382	2,702	0,199	1,079	0,148	1,623	1,977	1,577	0,329	0,072	0,419	0,052	0,272	0,054	0,151	0,022	0,124	0,024	0,106
	207,811	0,334	0,074	0,239	0,032	2,974	1,472	0,036	0,116	3,064	1,242	0,846	0,776	0,136	0,036	0,185	0,024	0,134	0,029	0,090	0,013	0,093	0,018	0,003
	261,692	1,080	0,297	1,738	0,288	4,980	1,466	0,052	0,894	4,109	5,410	4,003	4,021	0,755	0,160	0,976	0,122	0,745	0,137	0,437	0,054	0,358	0,055	0,020
	332,723	0,776	0,314	0,629	0,019	9,846	1,212	0,033	0,380	0,095	2,608	2,045	2,281	0,440	0,111	0,529	0,071	0,393	0,080	0,225	0,031	0,195	0,035	0,010
	228,592	0,411	0,068	0,953	0,264	1,329	0,307	0,050	0,288	0,033	0,347	0,167	0,295	0,051	0,012	0,064	0,009	0,051	0,010	0,030	0,004	0,024	0,005	0,016
	328,847	1,712	0,216	2,105	0,329	4,351	1,279	0,016	0,888	1,233	3,669	4,193	4,987	1,085	0,207	1,090	0,136	0,732	0,123	0,330	0,035	0,215	0,033	0,015
	169,645	0,649	0,097	1,888	0,627	1,846	0,729	0,122	0,852	0,053	0,743	0,786	0,771	0,161	0,033	0,197	0,025	0,147	0,027	0,086	0,011	0,069	0,011	0,009
	148,428	0,316	0,227	0,201	0,005	3,250	2,013	0,016	0,251	0,062	2,017	1,450	1,804	0,345	0,082	0,401	0,055	0,299	0,059	0,166	0,022	0,134	0,024	0,012
	125,042	0,981	0,085	1,339	0,133	2,107	0,891	0,011	0,354	0,041	0,746	0,769	0,651	0,123	0,030	0,171	0,021	0,129	0,023	0,081	0,010	0,065	0,010	0,007
	190,612	0,323	0,176	0,163	0,014	13,246	1,452	0,030	0,116	0,028	0,670	0,785	0,606	0,123	0,044	0,165	0,022	0,118	0,024	0,072	0,010	0,061	0,011	0,004
	92,366	0,417	0,073	1,759	0,797	0,566	0,510	0,252	1,664	0,040	0,240	0,457	0,262	0,051	0,011	0,076	0,009	0,048	0,009	0,029	0,004	0,026	0,004	0,002
	271,498	0,313	0,184	0,219	0,011	2,256	0,963	0,012	0,163	0,084	1,446	1,346	1,294	0,251	0,059	0,312	0,043	0,226	0,046	0,131	0,017	0,104	0,020	0,004
	260,131	1,169	0,096	1,296	0,121	2,652	1,173	0,009	0,268	0,029	0,941	0,693	0,754	0,143	0,037	0,182	0,024	0,144	0,029	0,088	0,011	0,068	0,012	0,024
	289,931	0,649	0,220	0,427	0,029	12,216	2,258	0,025	0,563	0,478	2,909	2,909	2,913	0,593	0,149	0,732	0,099	0,534	0,104	0,289	0,038	0,232	0,041	0,011
	157,982	0,871	0,213	0,979	0,157	5,922	3,892	0,009	0,341	0,295	1,674	1,477	1,177	0,239	0,056	0,297	0,039	0,221	0,045	0,138	0,019	0,128	0,019	0,016
	362,048	0,550	0,196	0,295	0,010	4,612	1,115	0,014	0,072	0,048	0,513	0,491	0,397	0,082	0,024	0,105	0,014	0,082	0,018	0,053	0,007	0,044	0,008	0,004
	377,770	1,221	0,051	1,602	0,153	2,662	0,988	0,015	0,295	0,019	0,077	0,039	0,070	0,013	0,004	0,017	0,003	0,017	0,004	0,012	0,002	0,010	0,002	0,009
	271,973	0,981	0,050	1,282	0,147	2,604	1,375	0,008	0,238	0,024	0,162	0,181	0,153	0,032	0,008	0,043	0,005	0,034	0,007	0,020	0,003	0,020	0,004	0,007
	415,005	1,581	0,072	1,790	0,193	3,548	1,202	0,000	0,212	0,031	0,535	0,373	0,394	0,080	0,023	0,101	0,014	0,084	0,018	0,061	0,007	0,055	0,009	0,006
	98,378	3,071	0,531	3,515	0,277	25,849	15,303	0,031	1,059	0,065	6,877	9,031	6,018	1,247	0,272	1,470	0,174	0,916	0,147	0,425	0,048	0,314	0,043	0,032
	223,175	1,965	0,156	2,500	0,274	4,269	1,804	0,010	0,450	0,046	0,535	0,552	0,493	0,106	0,027	0,142	0,019	0,112	0,021	0,074	0,009	0,063	0,012	0,021
	300,356	2,172	0,156	2,452	0,167	8,012	1,221	0,007	0,365	0,026	0,232	0,373	0,253	0,057	0,021	0,074	0,011	0,066	0,014	0,033	0,004	0,028	0,005	0,013
	216,659	1,368	0,128	1,600	0,093	1,897	0,886	0,001	0,204	0,028	0,342	0,264	0,243	0,038	0,011	0,081	0,010	0,068	0,014	0,053	0,007	0,050	0,008	0,006
	151,602	1,348	0,107	1,532	0,117	3,932	1,859	0,005	0,249	0,028	0,469	0,527	0,393	0,079	0,020	0,107	0,014	0,085	0,017	0,053	0,007	0,043	0,005	0,007

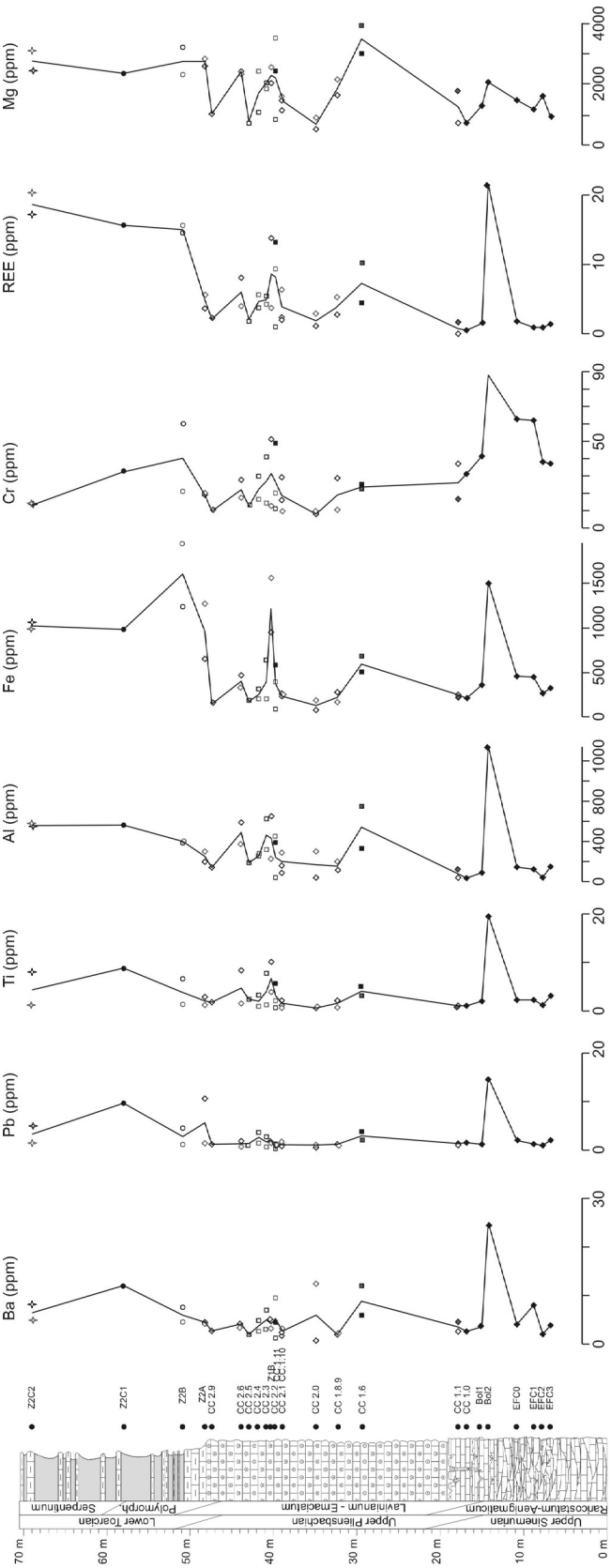

Figure 8.— Stratigraphic distribution of trace elements from brachiopod shells regularly related to biological cycling or complexed in particulate organic matter, throughout the studied stratigraphic section. All concentration values are given in ppm.

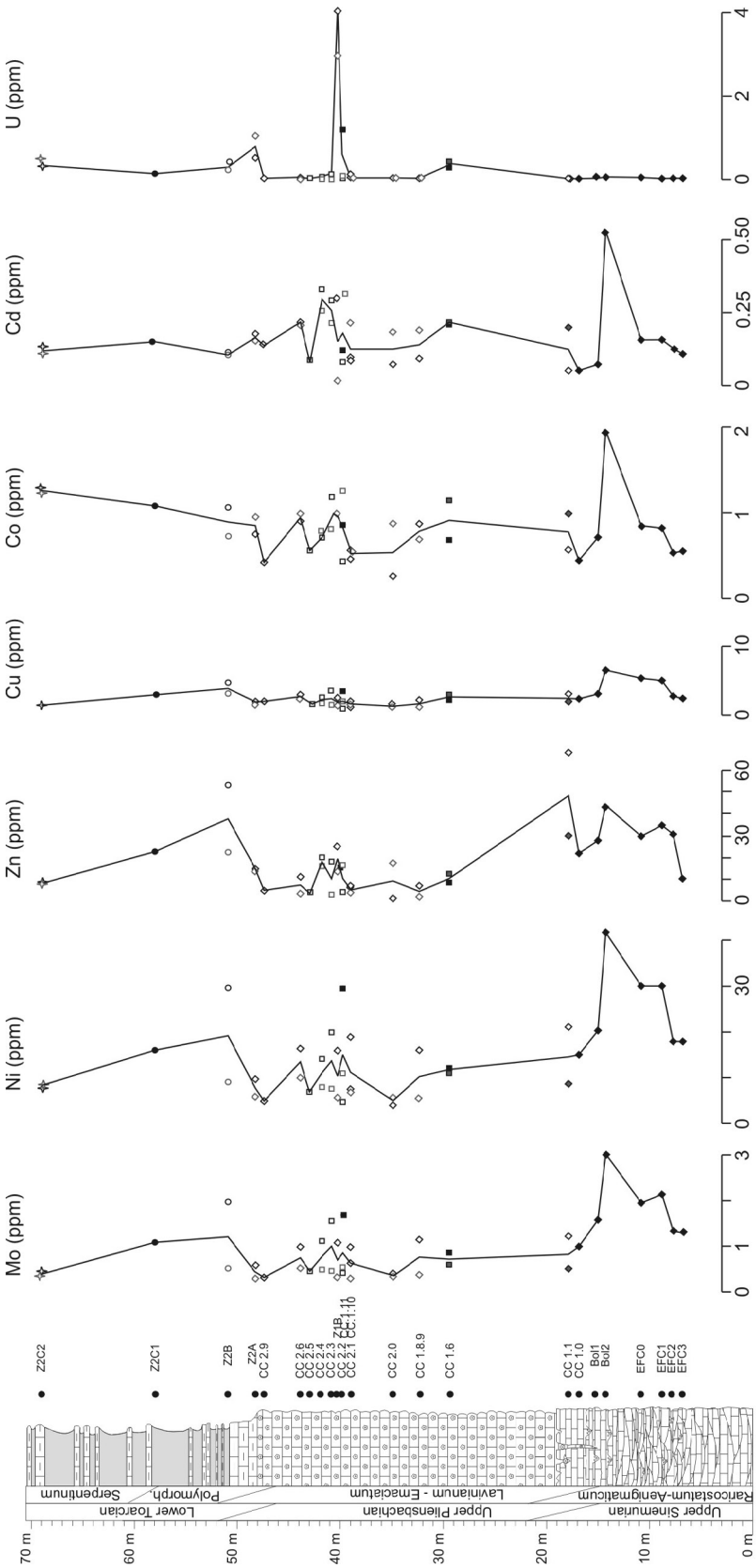

Figure 9.— Stratigraphic distribution of trace elements from brachiopod shells, regularly related to continental influx, throughout the studied stratigraphic section. All concentration values are given in ppm.

representing redox-sensitive elements, and related to continental influx (Al, Fe, Ti, Cr, Pb, Ba, and REE) (e.g. Tribovillard *et al*., 2006; Chester & Jickells, 2012; Zaky *et al*., 2016).

A first positive excursion has been detected at the Sinemurian-Pliensbachian transition in the *Calcirhynchia* shells for Al, Fe, and Mg and trace elements such as Mo, Ni, Cr, Ba, Pb, Ti, and Cd (Figs. 8, 9) and for REE (Fig. 8). The redox sensitive elements (Cr, Co, Ni, Mo, and Cd) show a first increase followed by a decrease in the uppermost part of this interval (Figs. 8, 9). Mg/Ca ratio increase close to the Sinemurian-Pliensbachian transition (Fig. 10). Subsequently, values are kept low for all the aforementioned elements upwards except for Mg (sample CC.1.6) in the Pliensbachian samples, up to the Pliensbachian-Toarcian transition (uppermost Emaciatum-lower Polymorphum zones), where several small positive peaks are detected in the pre-extinction interval (Mo, Ni, Cr, Zn, Ba, Ti, Fe, and U) in the shells of the genus *Cirpa* (Figs. 8, 9).

An important positive excursion for Mg, Fe, Mo, Ni, Cr, Zn, and Pb is recorded in *Cirpa* shells just in correspondence with the Z2B sampling level (first marly beds of the Polymorphum Zone) which can be related with the onset of the Jenkyns Event interval. The Mg/Ca ratio also increase in the base of the marls of the Toarcian (Fig. 10). The values obtained from *Soaresirhynchia* recorded in the marls of the base of the Serpentinum Zone evidence a clear enrichment in Ba and Pb and a decrease in Mo, Ni, Cr, and Zn. Then, element concentrations gradually go back to normal low values except for Fe, Co, and REE (Figs. 8, 9).

Principal Component Analysis

The Principal Component Analysis (PCA) establishes the structure of the variable dependence and therefore the correlations between the different trace elements. Three principal components axes (PC) were extracted which accounted for 83.13 % of the total variance. Fig. 11 and Table 3 display the trace elements grouping for the extracted principal components.

PC1 axis accounts for 61.37 % of the total variation and is associated with the Mg, Al, Ti, Fe, Co,

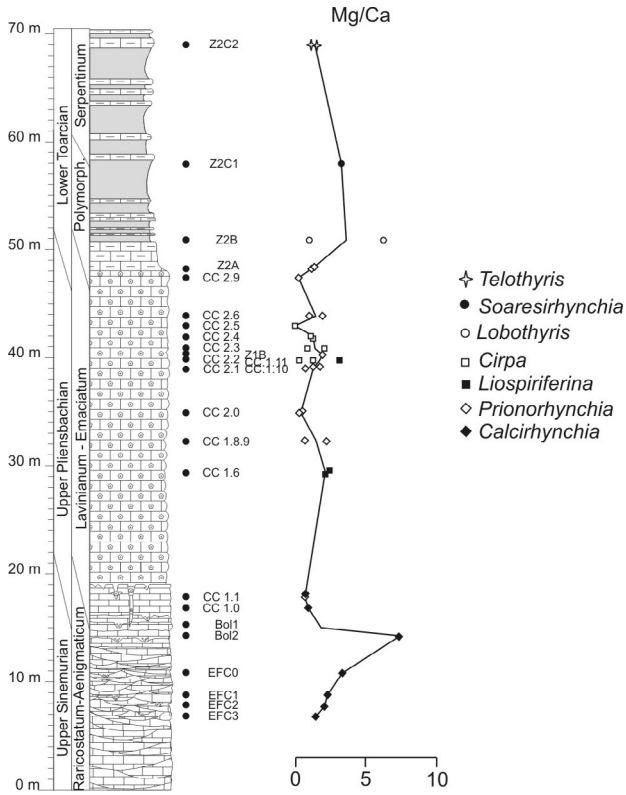

Figure 10.— Stratigraphic distribution of Mg/Ca ratio from brachiopod shells, throughout the studied stratigraphic section.

Rb, Cd, Ba, Pb, and REEs. PC2 axis accounts for 15.22 % of the total variation and links Cr, Ni, Cu, Zn, and Mo, whereas PC3 axis includes V, Mn, and U with a total variation of 6.54 %.

The axis PC1 reveals a strong interaction between Mg, Al, Ti, Fe, Co, Rb, Cd, Ba, Pb, and REEs, suggesting a common source for these elements (Fig. 11). PC2 and PC3 comprise the redox-sensitive trace elements. V and U are redox-sensitive elements in PC3 that present a common geochemical behaviour, different to that of other redox-sensitive trace metals found in PC2 (Zn, Mo, Ni, Cr, and Cu). In fact, U and V are reduced and can be eliminated from seawater under denitrifying conditions (Tribovillard *et al*., 2006) whereas Ni, Cr, Cu, Zn, and Mo (represented in the PC2 axis, Fig. 11) are removed mainly under sulphate-reducing conditions (Tribovillard *et al*., 2006). Fe is an element that is redox-sensitive as well but the PCA indicate a behaviour common with other elements typically derived from terrigenous detrital input such as Al, Ti and Rb (Hamroush

Table 3.— Coefficients of the different variables in the three components obtained by principal component analysis (PCA).

	PC1	PC2	PC3
Mg	**0.653**	-0.316	0.048
Al	**0.905**	0.064	-0.083
Ti	**0.791**	0.374	0.077
V	0.562	-0.307	**0.723**
Cr	0.441	**0.828**	0.203
Mn	0.35	-0.253	**0.564**
Fe	**0.736**	-0.095	0.431
Co	**0.833**	0.078	0.006
Ni	0.408	**0.856**	0.061
Cu	0.48	**0.804**	0.055
Zn	0.237	**0.666**	0.273
Rb	**0.936**	-0.027	-0.115
Mo	0.355	**0.896**	0.066
Cd	**0.579**	0.259	-0.094
Ba	**0.693**	0.394	-0.064
Pb	**0.589**	0.342	0.033
U	0.346	-0.33	**0.757**
La	**0.968**	-0.061	0.029
Ce	**0.965**	-0.006	-0.139
Nd	**0.958**	-0.14	-0.141
Sm	**0.952**	-0.121	-0.181
Eu	**0.964**	-0.125	-0.174
Gd	**0.967**	-0.12	-0.153
Tb	**0.961**	-0.158	-0.162
Dy	**0.966**	-0.152	-0.129
Ho	**0.958**	-0.207	-0.119
Er	**0.963**	-0.191	-0.074
Tm	**0.952**	-0.237	-0.056
Yb	**0.955**	-0.225	-0.005
Lu	**0.928**	-0.292	0.008
% varianza	61.37	15.22	6.54

& Stanley, 1990; Calvert, 1990; Calvert & Pedersen, 1993; Chester & Jickells, 2012; Reolid *et al.*, 2012; Rodríguez-Tovar & Reolid, 2013)

Discussion

Brachiopod shells and geochemical record

Assessing possible disparities due to different vital effects in the incorporation of the trace elements in the shell of the most representative genera analyzed, i.e. *Cirpa*, *Calcirhynchia,* and *Prionorhynchia,* is important to discard possible interferences in the geochemical signals. Seemingly, these taxa are structurally influenced by similar factors with minor variations: external characters are practically comparable in outline, folding, ribbing multicostate pattern, and beak features, all of them showing minute pedicle foramen pointing to rhizo-pedunculate shells. Regarding the internal architecture, representatives of the Wellerellidae (*Cirpa* and *Calcirhynchia*) are typified by well-developed hamiform crural developments whereas *Prionorhynchia* shows a simpler raduliform crura. On the other hand, these taxa show differences in the microstructural pattern of the secondary layer of the shell. In *Cirpa* and *Calcirhynchia* microstructure is characterized by coarse calcite fibres forming the eurinoid pattern whereas *Prionorhynchia* shows thinner and anvil-like calcite fibres typifying the leptinoid pattern (Fig. 4). According to Simon *et al.* (2018) the eurinoid type seemingly requires more

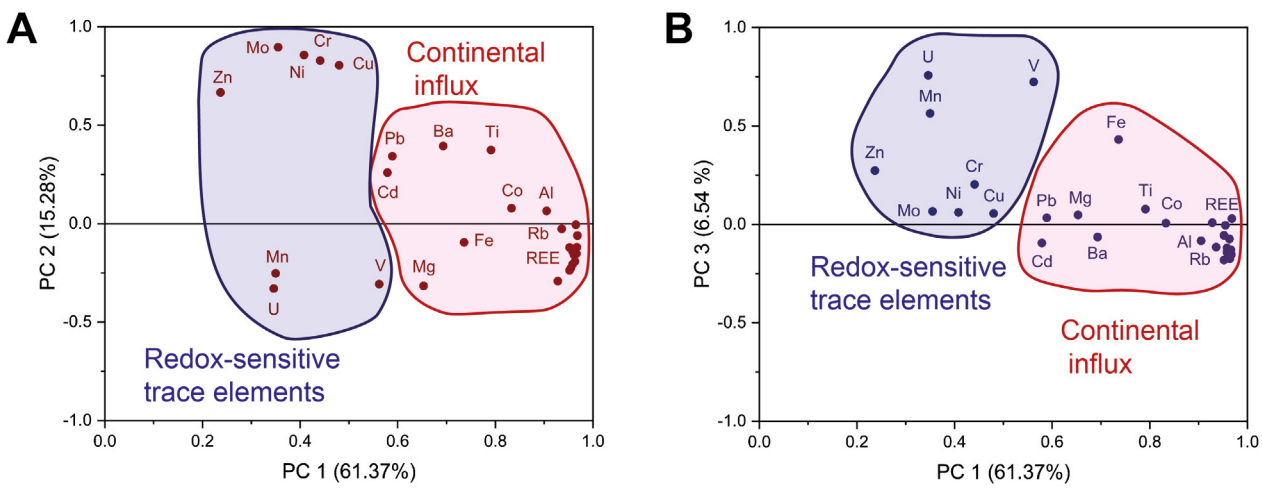

Figure 11.— Scatter plots of the studied samples according the results of the PCA analysis. Trace elements scores clustered in terms of their possible source.

metabolic energy and oxygenated habitats to construct coarser fibres than the leptinoid pattern. Thus, a theoretical approach could relate these differences among taxa to adaptive strategies or to dissimilar metabolism and feeding. However, these genera are recorded together virtually in the same ecospace and with similar body size, as inhabitants of the shallow platforms in the background conditions of the Sinemurian-Pliensbachian transition, and later in their Pliensbachian heyday under hemipelagic conditions (Baeza-Carratalá, 2013).

Regarding the incorporation of trace elements in these taxa, there is not a great difference in the content of trace elements among the most analysed genera *Cirpa*, *Calcirhynchia,* and *Prionorhynchia* (Figs. 12, 13). The axis PC1 reveals a strong interaction between Mg, Al, Ti, Fe, Co, Rb, Cd, Ba, Pb, and REEs which could be related to continental influx (e.g. Chester *et al*., 1977; Pye, 1987; Tribovillard *et al.,* 2006; Chester & Jickells, 2012; Zaky *et al.,* 2016) whereas PC2 and PC3 are related to redox sensitive elements (e.g. Calvert & Pedersen, 1997; Tribovillard *et al*., 2006).

The most common elements in the shells (excluding Ca) are Mg, Al, and Fe (Fig. 7). In marine environments these elements may be related to detrital inputs from emerged lands, mainly in the case of Al and Fe (Fig. 11). Brachiopod shells consist of low-Mg calcite, which explains the abundance of Mg in the shells compared to other elements (Fig. 7). Fe is included in the biological cycling (Bruland *et al*., 1991; Morel & Price, 2003; Smrzka *et al*., 2019), and is complexed in the particulate organic matter that is consumed by brachiopods. Iron is a micronutrient, and present high reactivity with oxygen as Fe^{2+} and low solubility as Fe^{3+} (and would not be incorporated into shell lattice except during diagenesis). Fe^{2+} facilitates electron transport in chloroplasts, mitochondria and bacteria. The Fe^{2+} can enter in the brachiopod metabolism through feeding and incorporate via coprecipitation because present octahedral coordination as Ca in calcite. The Sr is the following most abundant element in the studied shells, independently of the eurinoid or leptinoid microstructure pattern (Fig. 7). Sr and Mg replace Ca via adsorption of cations within the lattice with an initial surface uptake (Comans & Middelburg, 1987; Stipp & Hochella, 1991; Smrzka *et al*., 2019).

In the peri-Iberian platforms system, recent analysis performed in different macroinvertebrate taxa by Ullmann *et al.* (2020) provides a very comprehensive geochemical database for the upper Pliensbachian-lower Toarcian brachiopods derived from two stratigraphical sections from the Iberian Range (Spain) and the Lusitanian Basin (Portugal). The brachiopod taxa from the Subbetic, herein analysed, shows lower values in Sr and Mg if compared with their Portuguese or Central Iberian counterparts analysed by Ullmann *et al.* (2020). It would be attributable to the different environmental conditions and ecological setting prevailing in the different Iberian palaeomargins (Rodríguez-Tovar & Uchman, 2011; Rodríguez-Tovar & Reolid, 2013; Reolid *et al*., 2015, 2018). The depositional environment for the mainly Mediterranean *Cirpa briseis* (Pliensbachian) in the Subbetic consists of epioceanic and well-oxygenated platforms typified by crinoidal grainstone beds with abundant brachiopods, benthic foraminifera, peloids, and intraclasts. In addition, specimens of the Lusitanian Basin constitute a considerably younger occurrence than in the Subbetic area, since *C. briseis* is recorded in the Pliensbachian (Lavinianum-Emaciatum zones). On the other hand, the dataset of the Portuguese *Cirpa fallax* (lower Toarcian) collected by Ullmann *et al*. (2020) is the inhabitant of a low-energy, distal homoclinal ramp typified by hemipelagic sequences and organic matter rich facies (Duarte, 2007) where alternation of marlstone and argillaceous limestone beds prevailed (Duarte, 2007; Comas-Rengifo *et al*., 2013; Ullmann *et al*., 2020). Moreover, *C. fallax* is recorded in the Toarcian (Semicelatum Subzone, Polymorphum Zone) coevally with the representative components of the koninckinid fauna from the NW-European palaeobioprovince (Alméras *et al*., 1988, 1996; Alméras & Elmi, 1993, Comas-Rengifo *et al*., 2013), which is substantially different to the koninckinid fauna from the Mediterranean palaeobioprovince (Baeza-Carratalá *et al*., 2015). Therefore, differences in the Sr and Mg content between brachiopods from different Iberian palaeomargins may be related to different age, faunas and environmental conditions.

Following with the most abundant trace elements, Cr, Ni, and Zn, included in the PC2 axis (Fig. 11), usually present content < 60 ppm (Fig. 7). The con-

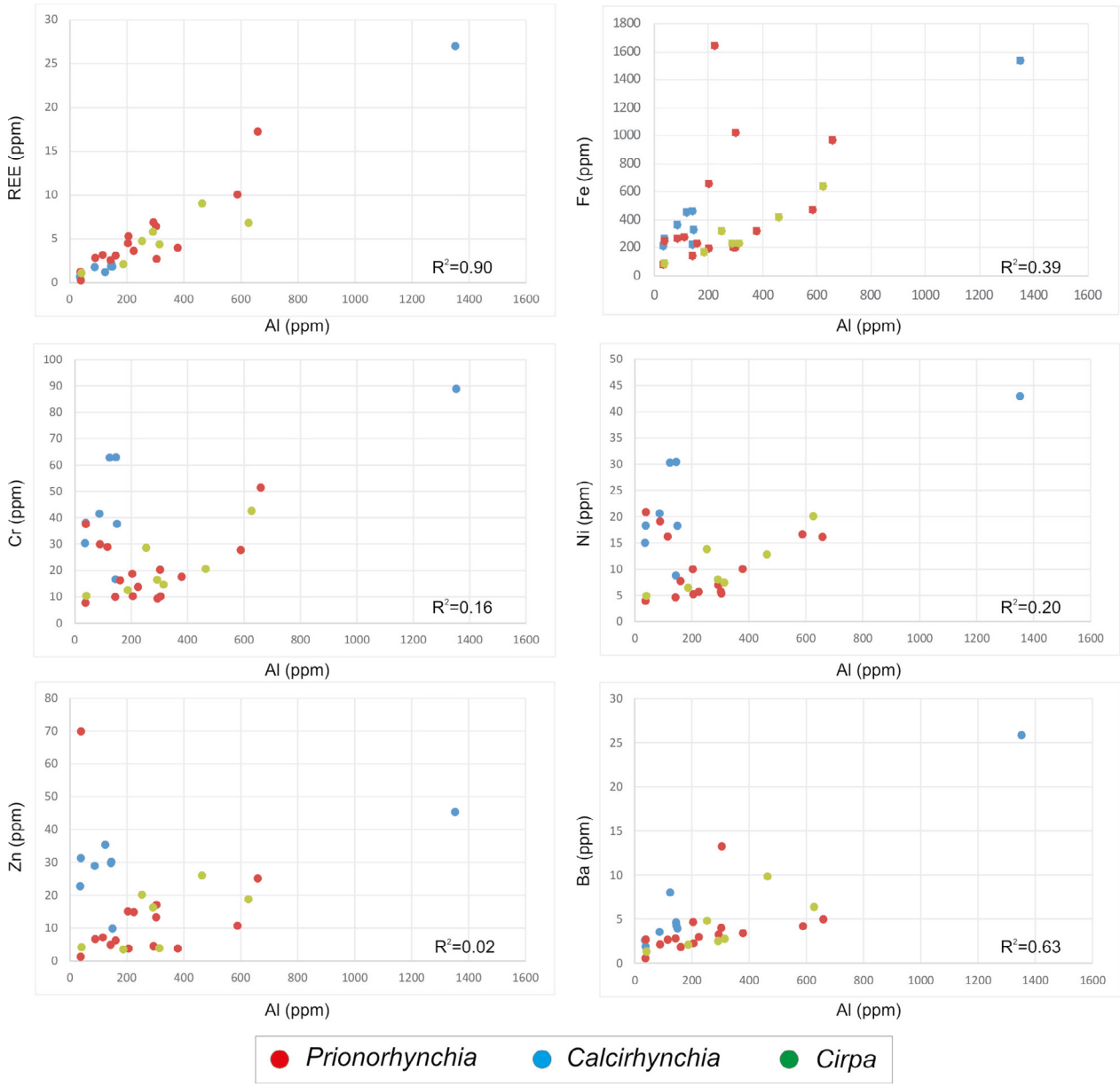

Figure 12.— Cross plots of selected trace elements from brachiopod shells of the three main genera plotted against to Al, which is clearly related to continental influx in marine environments (Calvert & Pedersen, 1993). Fe, REE, and Ba present a high correlation coefficient, congruent with an origin from detrital input from continental influx but also with a same behaviour in the incorporation to the brachiopod shell. Ni, Zn, and Cr present a different way of incorporation to the shell compared to Al as indicated by the low correlation coefficients. There is not a clear differentiation according to the taxa, except for a slight variation for *Calcirhynchia* (Zn, Cr, and Ni).

centration of these elements is slightly higher in *Calcirhynchia* shells (Fig. 12 and 13). Ni and Zn are micronutrients. Nickel constitutes a micronutrient required by phytoplankton growth in the photic zone (Calvert & Pedersen, 1993; Dupont *et al.,* 2010) and, under oxic conditions, is dissolved as Ni^{2+} (Fig. 14). Zinc is required for biological cycling by eukaryotes and this element exhibits a nutrient-type profile in modern oceans with surface water depletion (Zhao *et al*., 2014). Under oxic conditions Zn^{2+} appears as dissolved phase (Fig. 14).

The next most abundant elements in the brachiopod shells are Ti and Ba (< 10 ppm, Fig. 6), which are included in the PC1 axis related to continental

influx (Figs. 11, 14). Among the elements with minority content (commonly < 5 ppm), the Cu, Pb, V, Co, Mo, Cd, U, and REE are remarkable (Fig. 7), most of them considered redox sensitive elements. Molybdenum species in oxic seawater is molybdate (MoO_4^{2-}) that is reduced and subsequently enriched in sediments in close association with dissolved sulfides (e.g. Helz *et al*., 2011) (Fig. 14). In oxygen depleted conditions, molybdenum is incorporated into pyrite. In oxic waters, molybdenum concentrations are controlled by co-precipitation and adsorption onto Fe and Mn (oxy)hydroxides (Algeo & Rowe, 2012). However, the correlation coefficient indicates a similar way of incorporation in the shell for Zn and Mo ($R^2 = 0.64$) in the brachiopod shells (Fig. 13), showing Zn a nutrient-type profile in marine environments (Zhao *et al*., 2014).

Copper and vanadium are also essential nutrients for marine plankton as well (Smrzka *et al*., 2019) and they are constituents of numerous enzymes (Nalewajko *et al*., 1995; Moore *et al*., 1996) being as a dissolved phase under oxic conditions ($CuCO_3$, $VO_2(OH)_3^{2-}$ and $H_2VO_4^-$) (Fig. 14). Vanadium (PC3) and molybdenum (PC2) show a high affinity for hydrogen sulfide and are co-enriched in anoxic sediments (e.g. Tribovillard *et al*., 2006; Reolid *et al*., 2012), but V is commonly present in the organic matter and absent in pyrite (Algeo & Maynard, 2004) (Fig. 14). On the other hand, Co, Cr, and REE in sediments are derived from terrigenous detrital input (Fig. 14), but Cr appears in the PCA with a higher interaction with redox sensitive elements (PC2 axis, Fig. 11).

With respect to the Cd (PC1 axis), Tribovillard *et al.* (2006) stated that Cd, in contrast to Ni, Cu, and Zn (PC2 axis), presents one coordination state (Cd (II)) in the water column and sediments and has a nutrient-like role and, consequently, it implies a relatively short residence time in the water column. Cadmium is present as a dissolved phase ($CdCl^+$) in the seawater, showing photic zone depletion and deep-water enrichment. It is primarily transported to sea bottom via $CaCO_3$ particles and associated to organic carbon particles. The phytoplankton and organic matter present high content of Cd compared

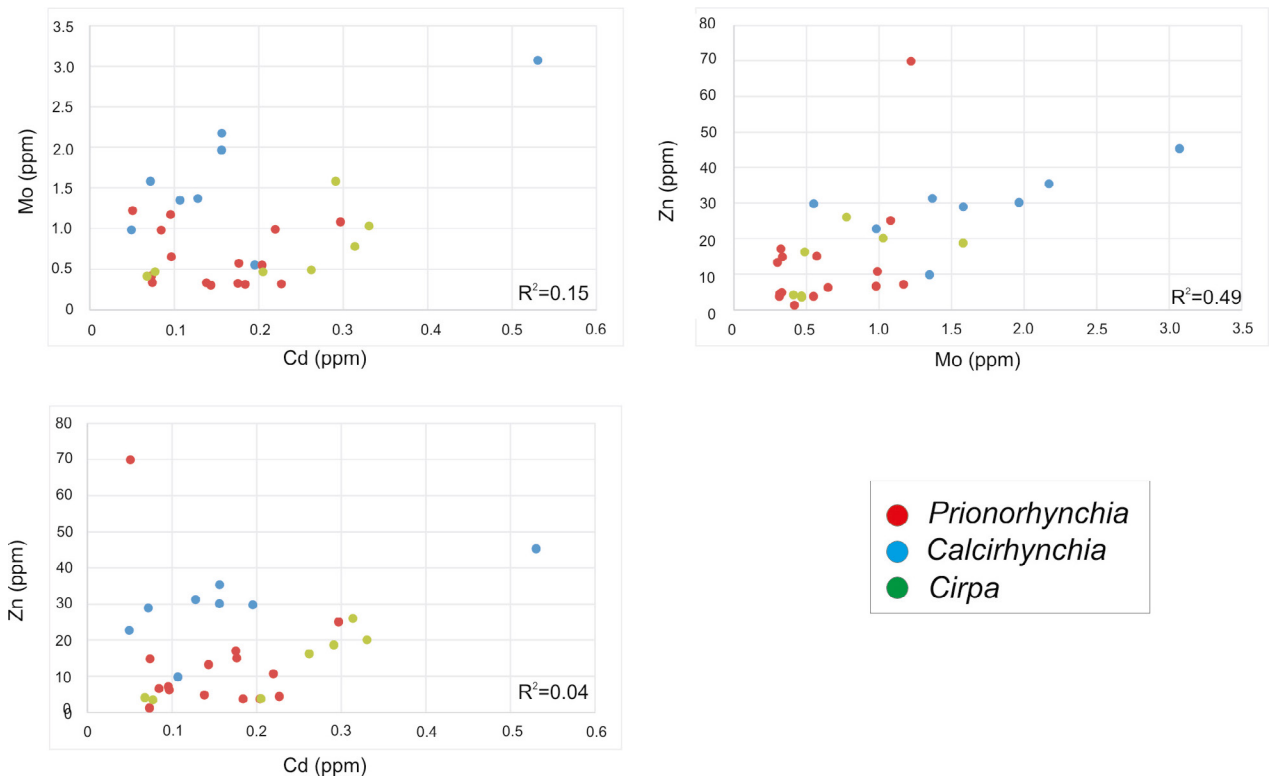

Figure 13.— Cross plots of the elements working as micronutrients. *Calcirhynchia* shows relatively higher values of Zn and lower values of Cd than *Prionorhynchia* and *Cirpa*, maybe related to the type of trophic resources or the geochemical conditions during the late Sinemurian. The correlation coefficient indicates a similar way of incorporation in the shell for Zn and Mo in the three studied genera.

with terrigenous material, thus making Cd a useful tracer for primary productivity (Gendron *et al*., 1996; Piper & Dean, 2002).

With respect to the REE, the main sources to the modern oceans are river inputs and atmospheric dust (Greaves *et al*., 1994; Holser, 1997). Because the Al content in marine sedimentary environments is controlled by continental influx (Calvert & Pedersen, 1993), the presence of Al in the shells has been plotted versus other elements (Fig. 10). Some elements present a high correlation coefficient with respect to Al, which is the case for REE (R^2= 0.90) and Ba (R^2=0.63), and lower correlation for Fe (R^2=0.39). Other elements, such as Cr, Zn, and Ni have a very low correlation index (< 0.20, Fig. 12) which is congruent with the PCA (Fig. 11) where they are grouped along the PC3 axis group (redox sensitive elements). However, this approach takes into account the behaviour of the trace elements in the seawater using data of concentration in the brachiopod shells. But we cannot discard other factors which can influence the co-precipitation and absorption processes of these elements in the calcite structure.

Biotic and environmental changes reflected in the brachiopod diversity pattern

In the Eastern Subbetic domain, the brachiopod fauna shows a progressive diversification from the Sinemurian to the late Pliensbachian-early Toarcian

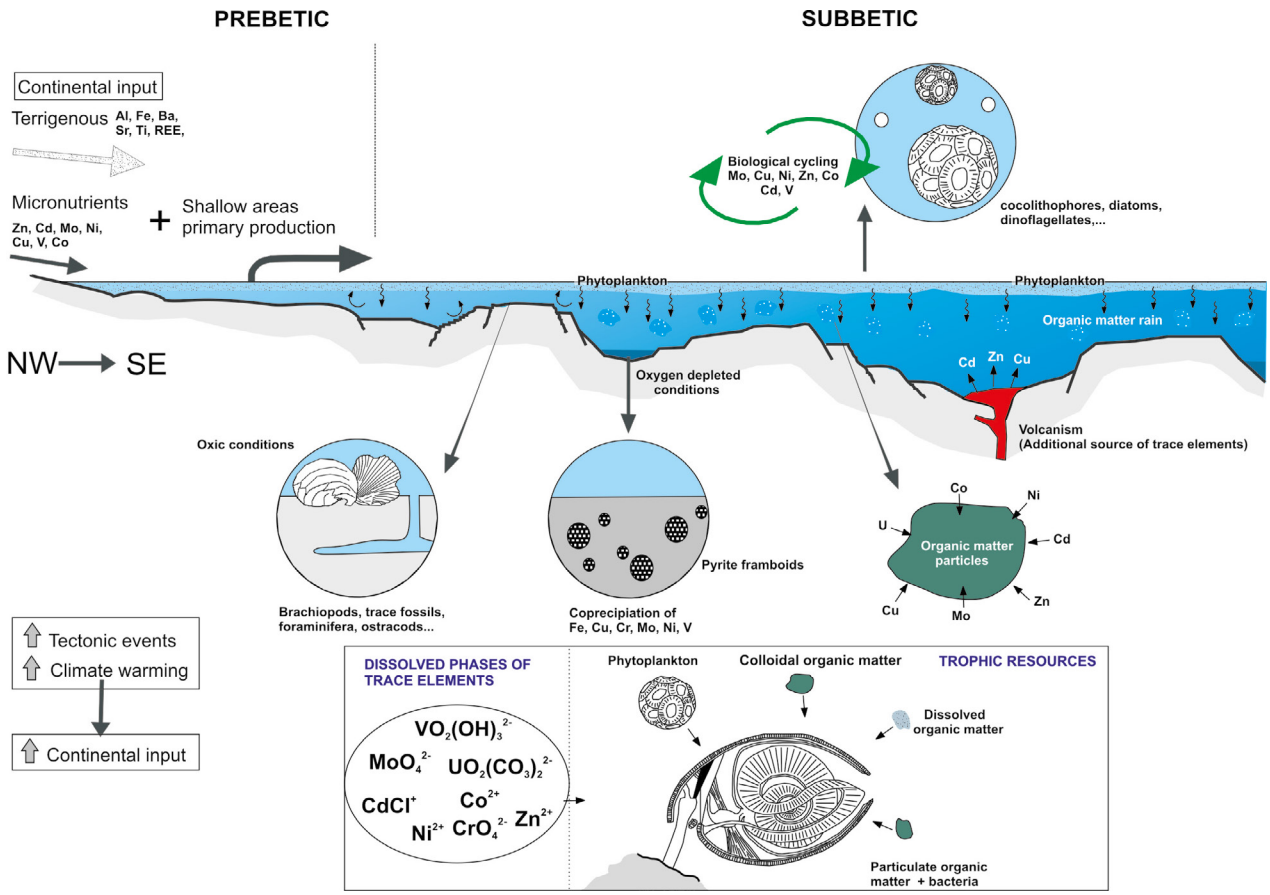

Figure 14.— Schematic model for trace element sources in the South-Iberian Palaeomargin. Continental input (affected by tectonic events as well as climate changes) would be the main supplier of trace elements to the ocean (included micronutrients). Volcanism as that recorded in the Median Subbetic (Comas *et al*., 1986; Reolid & Abad, 2014) would be an additional source. Micronutrients promote the benthic primary productivity in shallow areas and phytoplankton productivity in the epioceanic context through the biological cycling. Both, phytoplankton and labile organic matter sunk (organic matter rain) to the sea-floor (particulate organic matter, colloids and dissolved organic matter were trophic resources for brachiopods; Rosenberg *et al*., 1988; Tkachuck *et al*., 1989; James *et al*., 1992). Trace elements dissolved in oxic conditions and included in the organic matter were incorporated to the calcite shell through metabolism (breathing and feeding). Small sub-basins in the fragmented palaeomargin developed oxygen depleted conditions during the early Toarcian (Reolid *et al*., 2018) and were barren of brachiopods.

interval, punctuated by several critical episodes that conditioned the diversity dynamics of this group in the basin. The homogeneous platform system, established in the Western Tethys during the earliest Jurassic, subsequently drowned related to the Central Atlantic Ocean opening (Bernoulli & Jenkyns, 1974; Winterer & Bosellini, 1981). After an earlier diversification stage probably ongoing from the early Sinemurian (Baeza-Carratalá *et al*., 2018b), a speciation burst and radiation event during the Sinemurian–Pliensbachian transition (Raricostatum-Aenigmaticum zones) led to a bloom in brachiopod diversity from the late Sinemurian onwards. This peak of prosperity was probably related to an incipient pre-rifting stage of the westernmost Tethyan platform system. In the Sinemurian, the initial tectonic pulses of disintegration of the South-Iberian Palaeomargin (Vera, 1988, 1998; Molina *et al*., 1999) (Fig. 15) played an important role diversifying the ecological niches and facilitating the establishment and renewal of brachiopod communities (Baeza-Carratalá, 2013). This event of speciation in the Sinemurian–Pliensbachian transition concurred with the clear disconnection of the Mediterranean/Euro-Boreal brachiopod bioprovinces in the Betic Domain, since the sudden increase of the bathymetry makes achievable the diversification not only for brachiopod communities but also for necto-planktic fauna (e.g. Sandoval *et al.,* 2001). In other Tethyan basins this initial disintegration phase was also detected around the Sinemurian–Pliensbachian boundary, triggering greater diversification of depositional conditions in the late Sinemurian, which resulted in a great increase in diversity of the brachiopod fauna (cf. Hallam, 1981; Delance & Laurin, 1983).

The definitive extensional collapse of the platform system is evidenced in the South-Iberian Palaeomargin by faulting and blocks tilting (Rey, 1998; Tent-Manclús, 2006) (Fig. 13). The transition to more pelagic facies and the progressive establishment of epioceanic environments during the Pliensbachian produced changes in the environmental and depositional conditions. This also entailed alteration of the benthic biota, greatly influenced by substrate. A virtually complete renewal episode from the Sinemurian–Pliensbachian transition onwards meant the extinction of all endemic Sinemurian taxa together with several index-groups in the basin such as multicostate zeilleriids (Baeza-Carratalá, 2011, 2013; Baeza-Carratalá & García Joral, 2012) and the replacement of the prolific *Prionorhynchia regia* and *Calcirhynchia plicatissima* stocks by new Pliensbachian multicostate rhynchonellides (*Prionorhynchia* spp., *Cirpa* spp.), herein selected for the analysis (Table 1, Fig. 6A). Haq (2018) proposed a maximum flooding episode in the Sinemurian/Pliensbachian transition, just between the JSi5 and JPl1 events. Thus, the replacement of the Pliensbachian assemblages of the Mediterranean bioprovince, better adapted to epioceanic environments, was produced by the continuous deepening of the basin around the Sinemurian/Pliensbachian boundary.

The late Pliensbachian interval coincides with the great speciation phase of the benthic biota in the Western Tethys as a whole (cf. Hallam, 1981). The decrease in the faulting activity allowed the irregularities of the sea floor to be smoothed out enabling the spreading of brachiopods. With the settlement of polyspecific and very prolific communities, with profusion of genera such as *Prionorhynchia, Cirpa,* and *Liospiriferina*, a maximum in biodiversity and abundance was reached in the Pliensbachian–Toarcian transition (Figs. 6B, C), due to the favourable environments and the arrival of taxa from closer Euro-Boreal basins (e.g. *Lobothyris arcta*). A similar significant turnover in the Pliensbachian/Toarcian boundary was also noticed in ammonoids (Sandoval *et al*., 2001, 2012) linked to a relative drop in the sea level (JPl8 regressive event in Haq (2018); Fig. 1), prior to the onset of the Toarcian transgression. This interval is also partly concurring with a global cooling episode during the late Pliensbachian (Suan *et al*., 2010; Korte & Hesselbo, 2011; Korte *et al*., 2015; Gómez *et al*., 2016; Bougeault *et al*., 2017; De Lena *et al*., 2019; Storm *et al*., 2020).

The early Toarcian mass extinction event (Fig. 6) was preceded by several biotic changes, especially noticeable in the brachiopod assemblages. The progressive warming of the seawater and sea-level rise from the latest Pliensbachian onwards (Danise *et al*., 2013) led to several brachiopod clades to perform global adaptive strategies also noticed in the Subbetic brachiopod occurrences. During the pre-extinction interval, assemblages suffered a replacement

by taxa better adapted to warmer conditions, with *L. arcta, C. vulgata,* and *Pseudogibbirhynchia*? *moorei* as foremost representatives (cf. García Joral *et al*., 2011, Baeza-Carratalá, 2013; Baeza-Carratalá *et al*., 2015, 2018a). On the other hand, koninckinid fauna (with *Koninckella* and *Koninckodonta* recorded together with the usually associated *Nannirhynchia* and *Pseudokingena* species) occurs in the Subbetic area prior to the sudden increase in temperature reached in the Jenkyns Event. In this biotic crisis, the worldwide global extinction of orders Athyridida and Spiriferinida (Vörös, 2002; Comas-Rengifo *et al*., 2006; García Joral *et al*., 2011; Baeza-Carratalá *et al*., 2015; Vörös *et al*., 2016, 2019) is recorded in the Subbetic as well. In this sense, one of the last spiriferinid representatives (*Calyptoria vulgata*) suddenly appears in the Subbetic just prior to the Jenkyns Event, as a result of its long-term migration from the Arab-Madagascan margins to the epicontinental peri-Iberian ones triggered by increasing temperatures (Baeza-Carratalá *et al*., 2018a).

The lowermost Serpentinum hyperthermal event coinciding with the biotic crisis (Reolid *et al*., 2021) led to the total demise of brachiopod fauna in the basin (Fig. 15). Rodrigues *et al.* (2019), also from outcrops of the Subbetic, proposed a decreased ^{13}C fractionation during photosynthesis in C3 plants and arid environments from the Iberian Palaeomargin. Based on differences in the magnitude of the CIE recorded in land plants and marine substrates in the External Subbetic, Ruebsam *et al.* (2020) infer that the early Toarcian warming was paralleled by an increase in atmospheric CO_2 levels from ~500 ppmv to ~1000 ppmv. According to Rodrigues *et al.* (2019)

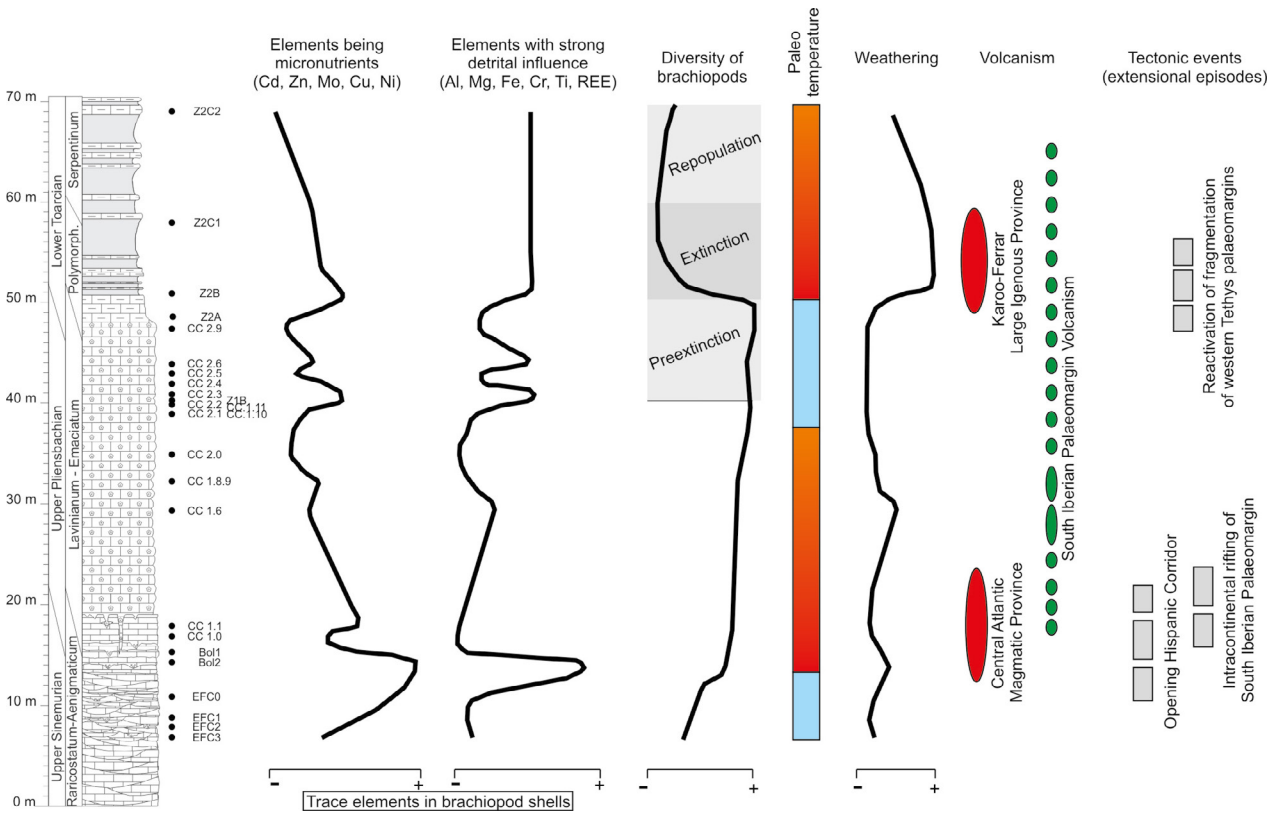

Figure 15.— Stratigraphic distribution of the trace elements content in the brachiopod shells, being micronutrients in the biological cycling and those specially linked to detrital input (average trends), compared with the diversity of brachiopods (Baeza-Carratalá, 2011). The extinction interval of the early Toarcian is preceded by environmental perturbations, as recorded in the content of trace elements in the shells during the so-called pre-extinction phase. Maximum values of trace elements in the shells are also related to: a) palaeotemperature-weathering interaction (blue for cooling and orange for warming; Deconinck *et al*., 2003; Them *et al*., 2017); b) volcanism of Central Atlantic Magmatic Province (Ruhl *et al*., 2016; Storm *et al*., 2020), Karoo-Ferrar Large Igneous Province (Pálfy & Smith, 2000) and South-Iberian Palaeomargin volcanisms (Comas et al., 1986); and c) tectonic events related to the opening of the Hispanic Corridor (Aberhan, 2002; Korte *et al*., 2015) and the extensional episodes affecting the South-Iberian Palaeomargin (Ruiz-Ortiz *et al*., 2004; Reolid *et al*., 2018).

and Ruebsam *et al.* (2020) the climatic belts in the South-Iberian Palaeomargin displaced to the north, turning more arid in this area.

After the Jenkyns Event, the repopulation began with *Soaresirhynchia bouchardi* as opportunistic taxa (García Joral & Goy, 2000; Gahr, 2005; García Joral *et al*., 2011; Baeza-Carratalá *et al*., 2017) probably related to its alleged low metabolic rate (Ullmann *et al*., 2020). The subsequent post-Jenkyns Event recovery during the Serpentinum–Bifrons zones was due to the stabilization of temperatures, which facilitated the settlement of the so-called "Spanish Bioprovince" of brachiopods (García Joral & Goy, 1984, 2000; Alméras & Fauré, 1990; García Joral *et al*., 2011), with the herein analysed *Telothyris* gr. *pyrenaica,* characterizing the background conditions and the well-oxygenated environments.

Coupling of trace elements and biotic signals

The increase in concentration of the analyzed trace elements in brachiopod shells could be mainly related to: oxygenation degree, external inputs and productivity:

a) Oxygen depleted conditions: Some of these trace elements are redox sensitive and are related to sulfides and organic matter, which preservation is favoured under reduced conditions;
b) External inputs: The higher concentration in the seawater as dissolved phase would result from increased inputs from emerged areas or proliferation of submarine volcanic activity;
c) Increase in productivity: Some of these trace elements are strongly complexed by dissolved organic matter and particulate organic matter used for brachiopod feeding.

These possibilities are analyzed below.

The first option, enrichment in redox sensitive elements related to oxygen depleted conditions is herein discarded. In fact, macrobenthic organisms including brachiopods, disappear in suboxic and anoxic conditions but these conditions did not occur in the studied area. In addition, the prolific brachiopod-bearing Sinemurian to Pliensbachian facies in the Subbetic area consist of oolithic grainstone to packstone and crinoidal grainstone sediments, thus confirming current activity and oxygenation. The growth of brachiopod calcitic shells, like other marine organisms with mineral skeletons, is produced by epithelial secreting cells at the mantle margin that obtain the Ca^{2+} and CO_3^{2-} through metabolism (breathing and feeding). For this reason, increasing values of redox sensitive elements in the sediments detected in other Toarcian outcrops of the Iberian margins (Rodríguez-Tovar & Reolid, 2013; Reolid *et al*., 2014) and related to precipitation under oxygen depleted conditions do not necessarily reach the metabolism of benthic organisms with the same intensity.

The biological cycling mostly affects to Mo, Cu, Ni, Zn, Cd, Co, Fe, and V (Bruland *et al*., 1991; Morel & Price, 2003; Smrzka *et al*., 2019), which are complexed in the particulate organic matter that is consumed by brachiopods, such as U typically related to organic matter (McManus *et al*., 2005). Therefore, the active incorporation via co-precipitation during the growth of shells is facilitated for Co, Zn, and Fe that can enter in the metabolism through feeding and are ions with the octahedral coordination, the same as Ca in calcite (Fig. 12). Other elements usually present in calcitic shells such as Mg, Ba, Sr, and U (Delaney & Boyle, 1982; Russell *et al*., 1994; Thébault *et al*., 2009; Benito & Reolid, 2012; Pérez-Huerta *et al*., 2013; Keul *et al*., 2013) have higher coordination number and substitute Ca via adsorption of cations within the lattice with an initial rapid surface uptake, followed by slower removal from solution (Comans & Middelburg, 1987; Stipp & Hochella, 1991). Live phytoplankton incorporate Ba by metabolic uptake or adsorption (Tribovillard *et al*., 2006) and many studies have examined the link between primary productivity and biogenic Ba abundance (e.g. McManus *et al*., 1999; Jeandel *et al*., 2000; Prakash Babu *et al*., 2002; Reolid *et al*., 2012).

Special attention is paid on the Mg concentrations (Fig. 7). This is a particularly important element in skeletal calcite because it varies with temperature, growth rate, and taxa (Buesing & Carison, 1992; see discussions on Pérez-Huerta *et al*., 2014; and Clark *et al*., 2016), as seen in the extant articulate brachiopods *Terebratulina unguicula* and *Terebratalia transversa*, where Mg increases as a response to higher growth rate and productivity. Experimental works have confirmed an increasing incorpora-

tion rate of other trace elements such as U into calcite with increasing growth rate of calcite crystals (Weremeichik *et al*., 2017). Moreover, the U abundance in sediments usually shows a good correlation with the organic matter rain rate in the water column (McManus *et al*., 2005). However, U content in the analyzed shells is very low (Figs. 7, 9). Cadmium presents a high affinity for adsorption onto calcite (Boyle, 1981; Papadopoulos & Rowell, 1989; Tesoriero & Pankow, 1996). Cd^{2+} and Ca^{2+} have similar chemical behavior and Cd^{2+} can replace Ca^{2+}, forming surface complexes of $CdCO_3$ (otavite) that co-precipitate with calcite (Papadopoulos & Rowell, 1989). The affinity series for divalent metals with respect to calcite incorporation is Cd>Zn>Co>Ni>Ba (Reeder, 1996; Smrzka *et al*., 2019), but this does not correspond to the abundance of these elements in the analyzed shells (Fig. 6) since the concentrations of these elements in seawater are variable.

Therefore, the increasing values of trace elements in brachiopod calcitic shells are related to their increased content in seawater as dissolved phase and/or high primary productivity, the last one also favoured by high content of the dissolved phase of some trace elements (Figs. 14, 15). The high phytoplankton productivity implicates increasing food resources for brachiopods that feed on phytoplankton such as diatoms and dinoflagellates (Fürsich & Hurst, 1974; Suchanek & Levinton, 1974; Stanton & Nelson, 1980; McCammon, 1981; James *et al*., 1992) and favored abundance of other trophic resources composing the seston as particulate organic matter, organic colloids and bacteria (Levinton & Suchanek, 1972; Suchanek & Levinton, 1974; Steele-Petrovic, 1979; James *et al*., 1992) and dissolved organic matter (dissolved carbohydrates and aminoacids; James *et al*., 1992) (Fig. 14). As well-known, brachiopods may be active/passive suspension feeders. There are experimental evidences on uptake of dissolved nutrients for brachiopods (McCammon & Reynolds, 1976; Doherty, 1981; Rosenberg *et al*., 1988; Tkachuck *et al*., 1989). The lophophore and mantle can directly assimilate dissolved nutrients (McCammon & Reynolds, 1976; Doherty, 1981; see discussion in McCammon, 1981; Rosenberg *et al*., 1988; Tkachuck *et al*., 1989) and surely related trace elements that work as micronutrients.

Sinemurian-Pliensbachian transition

From bottom to top, the first excursion in the geochemical signal recorded in the composite stratigraphical section occurred between the samples EFC2 and BOL1 in correspondence with the Sinemurian-Pliensbachian transition (Raricostatum-Aenigmaticum zones), where distribution of most of the trace elements (Mo, Ni, Cr, Ba, Pb, Ti, Al, Fe, Cd, and REE) marks a positive excursion in the *Calcirhynchia* shells (Figs. 8, 9). This excursion is mainly based in one data point corresponding to a well-preserved specimen of *Calcirhynchia*, but it is necessary to be cautious.

The diversity dynamics (burst in brachiopod species) and recent taphonomic assessment of these deposits (Baeza-Carratalá *et al*., 2014) provide a refined palaeoenvironmental setting, locating these shell beds in a shallow-water well-oxygenated bottom frequently affected by storms. In this context, the concentration values suddenly increase for most of the trace elements in this crucial timespan, decreasing upwards in most of the Pliensbachian samples to lower contents. The variations in content of trace elements in the shells are related to palaeotectonic events and climatic changes with incidence on the input of these elements to the sea from continental runoff and volcanic sources resulting on increased concentration in the seawater and primary productivity (Figs. 14, 15).

The geochemical perturbations in this timespan are concurrent with the initial tectonic pulses of rifting and drowning of the platform system developed in the South-Iberian Palaeomargin (Vera, 1988, 1998; Molina *et al*., 1999; Ruiz-Ortiz *et al*., 2004) (Fig. 15), which diversified the ecological niches leading to a renewal of brachiopod communities (Baeza-Carratalá, 2013). The abundance of the analysed trace elements in the calcite shells can be controlled by the transition to hemipelagic conditions and the change of current pattern favouring upwelling and increased productivity. The Cd content in brachiopod shells achieves the maximum values in a punctual excursion just concurring with the Sinemurian-Pliensbachian transition. Cadmium is a micronutrient and could favour an increase in productivity that may be in good accordance with the increasing in brachio-

pod diversity occurred in the Sinemurian-Pliensbachian transition (Figs. 6, 9).

The increased tectonic activity related to fragmentation of the South-Iberian Palaeomargin (García Hernández *et al*., 1989; Vera, 2001) and the opening of Hispanic Corridor (Aberhan, 2002; Korte *et al*., 2015; Schöllhorn *et al*., 2020; Storm *et al*., 2020) would have favoured the sediment runoff due to uplift of emerged reliefs (Figs. 14, 15). We cannot discard alternative sources for the trace elements analysed related to hydrothermal sources, submarine volcanic outgases or eruptions (e.g. Tribovillard *et al.,* 2006) for example in the case of Cd, Zn, Cu, and Pb (Chester & Jickells, 2012). Sinemurian alkaline submarine volcanism in the Subbetic area has been reported (Comas *et al*., 1986; García-Hernández *et al*., 1989; Portugal *et al*., 1995; Olóriz *et al*., 2002), which would be connected to the extensional palaeotectonic event of the first phase of the Atlantic Ocean opening that favoured the fragmentation of the western Tethys palaeomargins (Ruiz-Ortiz *et al*., 2004; Reolid *et al*., 2018) and the reactivation of the Central Atlantic Magmatic Province (Ruhl *et al*., 2016; Storm *et al*., 2020) (Fig. 15). Recent studies place the first clear evidences of volcanic activity and even the emplacement of the oceanic crust just in the late Sinemurian-earliest Pliensbachian, coinciding with the initial drifting stage (Sahabi *et al*., 2004; Klingelhoefer *et al*., 2009). Reolid *et al.* (2013) also linked volcanic activity with a higher tectonic activity episode in the Median Subbetic (Comas *et al*., 1986; Reolid & Abad, 2014). Increased values of Zn, Cd, Cu, and Pb in the seawater for this interval could be related with these mechanisms due to their hydrothermal/volcanic origin in seawater (Chester & Jickells, 2012).

In addition to the palaeotectonic event, the palaeoclimatic changes had an important relevance around the Sinemurian-Pliensbachian boundary. A global warming episode, mainly developed in the late Sinemurian, has been recorded in the westernmost Tethyan basins, followed by a decrease in palaeotemperature in the early Pliensbachian (e.g. Hesselbo *et al*., 2000; Korte & Hesselbo, 2011; Gómez *et al*., 2016). The increased values of Mg/Ca ratio is congruent with that global warming event that partly coincides with a perturbation in the oxygen and carbon cycles (excursions of the $\delta^{13}C$ and $\delta^{18}O$) and remarkably with the trace elements herein analysed. The increased temperature and humidity reported for the Sinemurian-Pliensbachian transition (Korte & Hesselbo, 2011; Schöllhorn *et al*., 2020) could facilitate the increase of continental weathering (Deconinck *et al*., 2003) and the subsequent input of trace elements to the sea, where the concentration of the dissolved phases and of those incorporated to the biological cycling increased.

This timespan is typified by enrichment in most of the trace elements, especially in those related to be proxies of continental influx (PC1, Fig. 9) as Ba, Ti, Al, Fe, Pb, and REEs (Fig. 8). Therefore, the global warming event in the latest Sinemurian could have been the responsible for an increase in trace elements content in brachiopod shells by adsorption on the shell surface or co-precipitation via incorporation of these elements to the metabolism after feeding of phytoplankton, bacteria, organic detritus, colloidal material, and dissolved nutrients (i.e. trophic resources according to Rosenberg *et al*., 1988; Tkachuck *et al*., 1989; James *et al*., 1992). Thus, weathering of the continental crust is the ultimate source of REE in the water reservoirs, whereas riverine discharge and aeolian deposition are the primary fluxes (Zaky *et al*., 2016, and references therein).

The brachiopod diversity peak and turnover episode, with the demise of endemic Sinemurian fauna (e.g. *Cincta peiroi, Praesphaeroidothyris cisnerosi*; Baeza-Carratalá, 2013) and their replacement by deeper Mediterranean Pliensbachian fauna, correlates with a regressive-transgressive cycle (Hallam, 1988; O'Dogherty *et al*., 2000; Sandoval *et al*., 2001, 2012; Schöllhorn *et al*., 2020).

This interpretation is congruent with the absence of black shales and oxygen depleted conditions in the studied area during the Sinemurian-Pliensbachian boundary that would limit the brachiopod survival as well as favour the co-precipitation of some trace elements with iron sulfides (Mo, Ni, and Cu) and fixation to buried organic matter (U, Cd, Zn, and V) but not an increase in their content in the brachiopod shells. Oxygen-depletion should be therefore reasonably excluded to explain trace elements variations in this timespan.

Variations around the Jenkyns Event

The return to the standard conditions in the Pliensbachian shows a very slight decreasing trend in the trace elements analyzed subsequently (CC1.1 to CC2.2 samples). After that, the next main perturbation imprints on the trace elements are located in the uppermost Pliensbachian-lowermost Toarcian (Emaciatum-Polymorphum zones), with several pulses showing positive excursions from CC2.2 to Z2B samples and a peak in Z2B, just prior to the extinction boundary. If we compare this interval with the $\delta^{13}C$ and $\delta^{18}O$ curves (Gómez & Goy, 2011; García Joral *et al*., 2011; Gómez *et al*., 2016; Ruebsam *et al*., 2020;) (Fig. 1), a high correlation between general trends of trace element perturbations and the C and O cycling oscillations can be deduced. Their occurrence in the pre-extinction interval of the Jenkyns Event really suggests a multi-phased stage in this biotic crisis (Figs. 4, 15), which started earlier in the latest Pliensbachian as deduced by several authors (cf. Little, 1996; Macchioni & Cecca, 2002; Wignall & Bond, 2008; Dera *et al*., 2010; Caruthers *et al*., 2013; Arias, 2013; Rita *et al*., 2016; Baeza-Carratalá *et al*., 2017). In the analyzed samples, the onset of these perturbations is coincident with the first record of koninckinid fauna in the Subbetic (CC 2.2 sample onwards) which was considered as precursor signal of the Jenkyns Event (Baeza-Carratalá *et al*., 2015, 2017).

The maximum positive excursion in trace elements is reached in the sample Z2B, just in the base of the marls of the Polymorphum Zone (lower Toarcian, Figs. 8, 9). An anoxic event is a recurrent factor used to explain the mass extinction occurring in the early Toarcian (e.g. Jenkyns, 1988; Bassoullet & Baudin, 1994; Harries & Little, 1999; Pálfy & Smith, 2000; Wignall *et al*., 2005; Mailliot *et al*., 2006; Ruebsam *et al*., 2020). However, in the Subbetic area, neither sedimentary evidence (black shales) nor TOC content points to the anoxia as the primary factor for the biotic crisis. Maximum TOC values from the Subbetic area in the basal Serpentinum Zone are around 0.4–0.9 wt.% (for the biotic crisis. Maximum TOC values from the Subbetic area in the basal Serpentinum Zone are around 0.4–0.9 wt.% (Reolid *et al*., 2013, 2014; Rodríguez-Tovar & Reolid, 2013; Rodrigues *et al*., 2019; Ruebsam *et al*., 2020) instead of the 5–15 wt.% present in the NW-European basins (e.g. Röhl *et al*., 2001; Bucefalo-Palliani *et al*., 2002; Mailliot *et al*., 2006; McArthur *et al*., 2008; Baroni *et al*., 2018; Thibault *et al*., 2018; Fantasia *et al*., 2019a). Moreover, under oxygen depleted conditions most of the trace elements would be incorporated to the bottom as sulfides (Fe, Mo, Ni, Cu, Pb) and complexed in the particulate organic matter (U, Mo, Cu, Cd, Zn, Co, Ni, V), instead in dissolved phase in the sea water. On the contrary, under oxic conditions, Zn, Ni, and Cu are strongly complexed by dissolved organic matter. Moreover, Zn, Mo, Cr, Cu, and Ni are related in the PC2 axis as redox sensitive elements, usually dissolved in the seawater under oxic conditions (Tribovillard *et al*., 2006).

Indeed, the maximum brachiopod diversity is reached just prior to the timing of this biotic crisis, dated in the westernmost Tethys in the lowermost Serpentinum Zone. Thus, in the Subbetic Domain, we can invoke from the biotic signals an alternative triggering mechanism as a primary responsible factor in this biotic crisis, such as an increasing temperature gradient. Firstly, koninckinid beds early appear in the basin just in the levels showing several trace elements perturbations (sample CC 2.2 upwards). This brachiopod clade (Athyridida) became extinct during the Jenkyns Event (Vörös, 2002; Baeza-Carratalá *et al*., 2015; Vörös *et al*., 2016) and their record in the Subbetic area (South-Iberian Palaeomargin), as results of their adaptive strategies, was considered as precursor signal of the Jenkyns Event (Baeza-Carratalá *et al*., 2015). On the other hand, the sudden occurrence in the basin of *Calyptoria vulgata* and *Lobothyris arcta* (Baeza-Carratalá, 2013; Baeza-Carratalá *et al*., 2018a), typical of warmer regions (García Joral *et al*., 2011; Baeza-Carratalá *et al*., 2018a), suggests a thermal maximum around the Z2B sample, in the Polymorphum Zone, just prior to their total extinction, not surpassing the hyperthermal event of the Serpentinum Zone.

Many authors have proposed a global warming related to the negative CIE of the Jenkyns Event and the correlative T-OAE (e.g. Suan *et al.,* 2010; Korte & Hesselbo, 2011; Korte *et al*., 2015; Them *et al*., 2017; Ruebsam *et al*., 2019; Baghli *et al*., 2020; Reolid *et al*., 2020) (Figs. 1, 15). The Mg/Ca values at

the beginning of the lower Toarcian increase respect to the Pliensbachian and confirm the global warming related with the Jenkyns Event. The enhanced weathering related to this climate change (Montero-Serrano *et al*., 2015; Fu *et al*., 2017; Them *et al*., 2017) drove to the subsequent detrital and nutrient input to the marine basin (Rodríguez-Tovar & Reolid, 2013; Danise *et al*., 2015; Fantasia *et al*., 2019b; Kemp *et al*., 2019) and the increase as dissolved phase where oxygen depleted conditions did not develop. This increased primary productivity also favoured the labile organic matter (particulate, colloidal and dissolved organic matter) for suspension-feeders such as brachiopods, with the subsequent increase of some trace metals in the shells (Fe, Cr, Zn, Ni, Mo, and Cu).

After reaching the maximum concentration values in the Jenkyns Event interval, the content of most trace elements slowly decreases progressively towards the top of the stratigraphical succession, although showing higher values than prior the Jenkyns Event. Thus, the repopulation interval just starts with the record of the opportunistic *Soaresirhynchia bouchardi* (Z2C1 sample) in the Serpentinum Zone (usually recorded in the Elegantulum Subzone) where the trace elements values start their decreasing trend. The reestablishment of the background conditions is reached from this sample upwards (Z2C1- Z2C2), in coincidence with the recovery of the brachiopod diversity led by the "Spanish Bioprovince" of brachiopods (García Joral & Goy, 1984, 2000; Alméras & Fauré, 1990; García Joral *et al*., 2011).

Some trace elements such as Ti, Fe, and REE, considered as reliable proxies of possible continental influx (Figs. 11, 14) (Zaky *et al*., 2016; Smrzka *et al*., 2019, and references therein), reach their highest values in the brachiopod shells during the Jenkyns Event interval and just in the onset of the repopulation interval (Z2C1 sample). Other typical elements such as Al, Ba, and Pb show a short increase delayed respect to the peak of Ti, Fe, and REE (Fig. 8).

Summarizing, in the South-Iberian Palaeomargin redox fluctuations in the seawater does not appear to have been a primary cause for oscillation of trace elements concentration in brachiopod shells. In fact, the record of benthic fauna is quite continuous, and this would not be the case in an anoxic environment. Other factors related to the global change induced by the Jenkyns Event (global warming, enhanced weathering, and subsequent changes in primary productivity) had impact on both assemblage structure and shell composition (with increasing content on some trace elements). In this sense, seawater temperature must be invoked to play a decisive role in this mass extinction event, as it is deduced by the biotic signals correlated with the palaeotemperatures deduced for the peri-Iberian platform system (García Joral *et al.*, 2011; Sandoval *et al.*, 2012, Gómez *et al.*, 2016; Rosales *et al.*, 2018; Ullmann *et al.*, 2020).

Conclusions

1. Trace element contents have been analysed on brachiopod shells derived from Lower Jurassic deposits from the South-Iberian Palaeomargin (Eastern Subbetic) revealing significant fluctuations throughout the late Sinemurian-early Toarcian (Raricostatum–Serpentinum zones).
2. The Sinemurian-Pliensbachian transition reveals the first main positive excursions of trace elements (Mo, Ni, Cr, Ba, Pb, Ti, Cd, Zn), REEs, and Fe content in brachiopod shells. This excursion is concurrent with a palaeotectonic event, the initial pulses of drowning of the South-Iberian platform system, a global warming episode, and a renewal and burst of brachiopod communities, which correlates with an enhanced weathering and submarine volcanism and delivered trace element to the marine basin. As a consequence, these trace elements were present as dissolved phases in the seawater, incorporated to phytoplankton, complexed in particulate organic matter, and subsequently incorporated to the shells through brachiopod metabolism. Facies analysis excludes major oxygen depletion and thus enrichment of brachiopod shells in these elements is not linked to pulses of oxygen depleted conditions in the South-Iberian Palaeomargin.
3. Several positive excursions of trace elements in brachiopod shells (Mo, Ni, Cr, Zn, Pb, REE) are recorded in the upper Pliensbachian-lower Toarcian (Emaciatum–Polymorphum zones), with a peak just in correspondence with the onset of the Jenkyns Event, prior to the extinction

boundary of this biotic crisis. These pulses show a high correlation with global trends in the C and O cycling oscillations, suggesting a multi-phased stage in this biotic crisis, and concurring with the first record of the koninckinid fauna, regarded as precursor of the Jenkyns Event. Sedimentary evidences, low TOC content, and the maximum brachiopod diversity reached just prior to the Jenkyns Event do not point to sea-bottom waters deoxygenation as the primary factor for this crisis in the South-Iberian Palaeomargin. Newly, global warming and correlative enhanced weathering and subsequent input of terrigenous and nutrients to the seawater can be reflected in the trophic resources of brachiopods and manifested in the shell composition.

4. The sudden occurrence of warmer brachiopod assemblages suggests a thermal maximum around the uppermost Emaciatum–Polymorphum zones, just prior to their total extinction, not surpassing the hyperthermal event of the Serpentinum Zone. On the other hand, increase on reliable proxies of higher primary productivity (e.g. Cd and Zn) in the pre-Jenkyns Event interval and just in the onset of the repopulation interval is in good accordance with the increasing brachiopod diversity.
5. Trace element contents gradually decrease during the post-Jenkyns Event interval, coinciding with the repopulation led by the opportunistic *Soaresirhynchia bouchardi* in the upper part of the Serpentinum Zone. The reestablishment of the background conditions in the Western Tethys (stabilization of redox values and temperature) are coincident with the brachiopod diversity recuperation led by the brachiopod "Spanish Fauna".
6. The correlation of the geochemical imprints with critical brachiopod bioevents and the episodes of evolution of the westernmost Tethyan basins allows increasing fidelity of the record of major environmental shifts around the Sinemurian-Pliensbachian boundary and the Jenkyns Event in the South-Iberian Palaeomargin and for a more detailed reconstruction of changes in the main palaeocological parameters.

ACKNOWLEDGMENTS

This research is a contribution to the IGCP-655 (Toarcian Oceanic Anoxic Event: Impact on marine carbon cycle and ecosystems), and was supported by projects CGL2015-66604-R, CGL2015-66835-P and PID2019-105537RB-100 (MINECO, Government of Spain) and P20_00111 (Junta de Andalucía), and the Research Groups VIGROB-167 (University of Alicante) and RNM-200 (University of Jaén). Authors expres gratitude to all who performed analytical research and technical and human support provided by the CICT of Universidad de Jaén. This contribution has benefited by the constructive comments by two reviewers (Dr. M. I. Benito and one anonymous).

References

Aberhan, M. (2002). Opening of the Hispanic Corridor and Early Jurassic bivalve biodiversity. Geological Society London Special Publications, 194: 127-139. https://doi.org/10.1144/GSL.SP.2002.194.01.10

Aberhan, M. & Fürsich, F.T. (1997). Diversity analysis of Lower Jurassic bivalves of the Andean Basin and the Pliensbachian-Toarcian mass extinction. Lethaia, 29: 181-195. https://doi.org/10.1111/j.1502-3931.1996.tb01874.x

Ager, D.V. (1987). Why the Rhynchonellid Brachiopods survived and the Spiriferids did not: a suggestion. Palaeontology, 30: 853-857.

Ait-Itto, F.Z.; Price, G.D.; Ait Addi, A.; Chafiki, D. & Mannani, I. (2017). Bulk-carbonate and belemnite carbon-isotope records across the Pliensbachian-Toarcian boundary on the northern margin of Gondwana (Issouka, Middle Atlas, Morocco). Palaeogeography, Palaeoclimatology, Palaeoecology, 466: 128-136. https://doi.org/10.1016/j.palaeo.2016.11.014

Akagi, T.; Hashimoto, Y.; Fu, F.F.; Tsuno, H.; Tao, H. & Nakano, T. (2004). Variation of the distribution coefficients of rare earth elements in modern coral-lattices: species and site dependencies. Geochimica and Cosmochimica Acta, 68: 2265-2273. https://doi.org/10.1016/j.gca.2003.12.014

Algeo, T.J. & Maynard, J.B. (2004). Trace-elements behaviour and redox facies in core shales of Upper Pensylvanian Kansas-type cyclothems. Chemical Geology, 206: 289-318. https://doi.org/10.1016/j.chemgeo.2003.12.009

Algeo, T.J. & Lyons, T.W. (2006). Mo-total organic carbon covariation in modern anoxic marine environments: implications for analysis of paleoredox and paleohydrographic conditions. Paleoceanography 21: PA1016. https://doi.org/10.1029/2004PA001112

Algeo, T.J. & Rowe, H. (2012). Paleoceanographic applications of trace metal concentrations data.

Chemical Geology, 324-325: 6-18. https://doi.org/10.1016/j.chemgeo.2011.09.002

Alméras, Y. & Fauré, P. (1990). Histoire des brachiopodes liasiques dans la Tethys occidentale: les crises et l'écologie. Cahiers de l'Université Catholique de Lyon Sciences, 4: 1-12.

Alméras, Y. & Elmi, S. (1993). Palaeogeography, physiography, palaeoenvironments and brachiopod communities. Example of the Liassic brachiopods in the Western Tethys. Palaeogeography, Palaeoclimatology, Palaeoecology, 100: 95-108. https://doi.org/10.1016/0031-0182(93)90035-H

Alméras, Y.; Elmi, S.; Mouterde, R.; Ruget, C. & Rocha, R. (1988). Evolution paléogéographique du Toarcien et influence sur les peuplements. 2nd International Symposium on Jurassic Stratigraphy, 2: 687-698, Lisbon.

Alméras, Y.; Mouterde, R.; Benest, M.; Elmi, S. & Bassoullet, J.-P. (1996). Les brachiopodes toarciens de la rampe carbonatée de Tomar (Portugal). Documents des Laboratoires de Géologie de Lyon, 138: 125-191. https://doi.org/10.1016/S0016-6995(97)80078-2

Anand, P., Elderfield, H. & Conte, M.H. (2003). Calibration of Mg/Ca thermometry in planktonic foraminifera from a sediment trap time series. Paleoceanography, 18: 1050. https://doi.org/10.1029/2002PA000846

Angiolini, L.; Stephenson, M.; Leng, M.J.; Jadoul, F.; Millward, D.; Aldridge, A.; Andrews, J.; Chenery, S. & Williams, G. (2012). Heterogeneity, cyclicity and diagenesis in a Mississippian brachiopod shell of palaeoequatorial Britain. Terra Nova, 24: 16-26. https://doi.org/10.1111/j.1365-3121.2011.01032.x

Arias, C. (2009). Extinction pattern of marine Ostracoda across the Pliensbachian Toarcian boundary in the Cordillera Ibérica, NE Spain: causes and consequences. Geobios, 42: 1-15. https://doi.org/10.1016/j.geobios.2008.09.004

Arias, C. (2013). The Early Toarcian (Early Jurassic) ostracod extinction events in the Iberian Range: The effect of temperature changes and prolonged exposure to low dissolved oxygen concentrations. Palaeogeography, Palaeoclimatology, Palaeoecology, 387: 40-55. https://doi.org/10.1016/j.palaeo.2013.07.004

Azéma, J.; Foucault, A.; Fourcade, E.; García-Hernández, M.; González-Donoso, J.M.; Linares, A.; Linares, D.; López-Garrido, A.C.; Rivas, P. & Vera, J.A. (1979). Las microfacies del Jurásico y Cretácico de las Zonas Externas de las Cordilleras Béticas. Publicaciones Universidad Granada, 83 pp.

Baeza-Carratalá, J.F. (2011). New Early Jurassic brachiopods from the Western Tethys (Eastern Subbetic, Spain) and their systematic and paleobiogeographic affinities. Geobios, 44: 345-360. https://doi.org/10.1016/j.geobios.2010.09.003

Baeza-Carratalá, J.F. (2013). Diversity patterns of Early Jurassic brachiopod assemblages from the westernmost Tethys (Eastern Subbetic). Palaeogeography, Palaeoclimatology, Palaeoecology, 381-382: 76-91. https://doi.org/10.1016/j.palaeo.2013.04.017

Baeza-Carratalá, J.F. & García Joral, F. (2012). Multicostate zeillerids (Brachiopoda, Terebratulida) from the Lower Jurassic of the Eastern Subbetic (SE Spain) and their use in correlation and paleobiogeography. Geologica Acta, 10: 1-12.

Baeza-Carratalá, J.F. & García Joral, F. (2020). Linking Western Tethyan Rhynchonellide morphogroups to the key post-Palaeozoic extinction and turnover events. Palaeogeography, Palaeoclimatology, Palaeoecology, 553: art. 09791. https://doi.org/10.1016/j.palaeo.2020.109791

Baeza-Carratalá, J.F.; García Joral, F. & Tent-Manclús, J.E. (2011). Biostratigraphy and palaeobiogeographic affinities of the Jurassic brachiopod assemblages from Sierra Espuña (Maláguide Complex, Internal Betic Zones, Spain). Journal of Iberian Geology, 37: 137-151. https://doi.org/10.5209/rev_JIGE.2011.v37.n2.3

Baeza-Carratalá, J.F.; Giannetti, A.; Tent-Manclús, J.E. & García Joral, F. (2014). Evaluating taphonomic bias in a storm-disturbed carbonate platform. Effects of compositional and environmental factors in Lower Jurassic brachiopod accumulations (Eastern Subbetic basin, Spain). Palaios, 29: 55-73. https://doi.org/10.2110/palo.2013.041

Baeza-Carratalá, J.F.; García Joral, F.; Giannetti, A. & Tent-Manclús, J.E. (2015). Evolution of the last koninckinids (Athyridida, Koninckinidae), a precursor signal of the Early Toarcian mass extinction event in the Western Tethys. Palaeogeography, Palaeoclimatology, Palaeoecology, 429: 41-56. https://doi.org/10.1016/j.palaeo.2015.04.004

Baeza-Carratalá, J.F.; García Joral, F. & Tent-Manclús, J.E. (2016a). Brachiopod faunal exchange through an epioceanic-epicontinental transitional area from the Early Jurassic South Iberian platform system. Geobios, 49: 243-255. https://doi.org/10.1016/j.geobios.2016.05.005

Baeza-Carratalá, J.F.; Manceñido, M.O. & García Joral, F. (2016b). *Cisnerospira* (Brachiopoda, Spiriferinida), an atypical Early Jurassic spire bearer from the Subbetic Zone (SE Spain) and its significance. Journal of Paleontology, 90: 1081-1099. https://doi.org/10.1017/jpa.2016.109

Baeza-Carratalá, J.F.; García Joral, F. & Tent-Manclús, J.E. (2016c). Lower Jurassic brachiopods from the Ibero-

Levantine sector (Iberian range): faunal turnovers and critical bioevents. Journal of Iberian Geology, 42: 355-369. https://doi.org/10.5209/JIGE.54666

Baeza-Carratalá, J.F.; Reolid, M. & García Joral, F. (2017). New deep-water brachiopod resilient assemblage from the South-Iberian Palaeomargin (Western Tethys) and its significance for the brachiopod adaptive strategies around the Early Toarcian Mass Extinction Event. Bulletin of Geosciences, 92: 233-256. https://doi.org/10.3140/bull.geosci.1631

Baeza-Carratalá, J.F.; García Joral, F.; Goy, A. & Tent-Manclús, J.E. (2018a). Arab-Madagascan brachiopod dispersal along the north-Gondwana paleomargin towards the western Tethys Ocean during the early Toarcian (Jurassic). Palaeogeography, Palaeoclimatology, Palaeoecology, 490: 256-268. https://doi.org/10.1016/j.palaeo.2017.11.004

Baeza-Carratalá, J.F.; Dulai, A. & Sandoval, J. (2018b). First evidence of brachiopod diversification after the end-Triassic extinction from the pre-Pliensbachian Internal Subbetic platform (South-Iberian Paleomargin). Geobios 51: 367-384. https://doi.org/10.1016/j.geobios.2018.08.010

Baghli, H.; Mattioli, E.; Spangenberg, J.E.; Bensalah, M.; Arnaud-Godet, F.; Pittet, B. & Suan, G. (2020). Early Jurassic climatic trends in the south-Tethyan margin. Gondwana Research, 77: 67-81. https://doi.org/10.1016/j.gr.2019.06.016

Baroni, I.R.; Pohl, A.; van Helmond, N.A.G.M.; Papadomanolaki, N.M.; Coe, A.L.; Cohen, A.S.; van de Schootbrugge, B.; Donnadieu, Y. & Slomp, C.P. (2018). Ocean circulation in the Toarcian (Early Jurassic): A key control on deoxygenation and carbon burial on the European Shelf. Paleoceanography and Paleoclimatology, doi:10.1029/2018PA003394. https://doi.org/10.1029/2018PA003394

Bassoullet, J.P. & Baudin, F. (1994). The Early Toarcian: a period of crisis in basins and carbonate platforms from Northwestern Europe and Tethys. Geobios, 27 (Sup. 3): 645-654. https://doi.org/10.1016/S0016-6995(94)80227-0

Bates, N.R. & Brand, U. (1991). Environmental and physiological influences on isotopic and elemental compositions of brachiopod shell calcite - Implications for the isotopic evolution of Paleozoic oceans. Chemical Geology, 94: 67-78. https://doi.org/10.1016/S0009-2541(10)80018-X

Benito, M.I. & Reolid, M. (2012). Belemnite taphonomy (Upper Jurassic, Western Tethys) part II: Fossil-diagenetic analysis including combined petrographic and geochemical techniques. Palaeogeography, Palaeoclimatology, Palaeoecology, 358-360: 89-108. https://doi.org/10.1016/j.palaeo.2012.06.035

Bernoulli, D. & Jenkyns, H.C. (1974). Alpine, Mediterranean, and Central Atlantic Mesozoic facies in relation to the early evolution of the Tethys. In: Modern and Ancient Geosynclinal Sedimentation (Dott, H.R. & Shaver, R.H., Eds.), SEPM Special Publications, 19: 129-160. https://doi.org/10.2110/pec.74.19.0129

Blanchard, R.L. & Oakes, D. (1965). Relationships between uranium and radium in coastal marine shells and their environments. Journal of Geophisical Research, 70: 2911-2921. https://doi.org/10.1029/JZ070i012p02911

Bodin, S.; Mattioli, E.; Frölich, S.; Marshall, J.D.; Boutib, L.; Lahsini, S. & Redfern, J. (2010). Toarcian carbon isotope shifts and nutrient changes from the Northern margin of Gondwana (High Atlas, Morocco, Jurassic): palaeoenvironmental implications. Palaeogeography, Palaeoclimatology, Palaeoecology, 297: 377-390. https://doi.org/10.1016/j.palaeo.2010.08.018

Böttcher, M.E. & Dietzel, M. (2010). Metal-ion partitioning during low-temperature precipitation and dissolution of anhydrous carbonates and sulphates. European Mineralogical Union Notes in Mineralogy, 10: 139-187. https://doi.org/10.1180/EMU-notes.10.4

Bougeault, C.; Pellenard, P.; Deconinck, J.F.; Hesselbo, S.P.; Dommergues, J.L.; Bruneau, L.; Cocquerez, T.; Laffont, R.; Huret, E. & Thibault, N. (2017). Climatic and palaeoceanographic changes during the Pliensbachian (Early Jurassic) inferred from clay mineralogy and stable isotope (C-O) geochemistry (NW Europe). Global and Planetary Change, 149: 139-152. https://doi.org/10.1016/j.gloplacha.2017.01.005

Boyle, E.A. (1981). Cadmium, zinc, copper, and barium in foraminifera tests. Earth Planetary Sciences Lettters, 53: 11-35. https://doi.org/10.1016/0012-821X(81)90022-4

Braga, J.C. (1983). Ammonites del Domerense de la zona Subbética (Cordilleras Béticas, S. de España). PhD Thesis Univ. Granada, 410 pp.

Braga, J.; Comas, M.C.; Delgado, F.; García-Hernández, M.; Jiménez, A.P,; Linares, A.; Rivas, P. & Vera, J.A. (1981). The Liassic Rosso Ammonitico facies in the Subbetic Zone (Spain). Genetic considerations. In: Rosso Ammonitico Symposium Proceedings (Farinacci, A. & Elmi, S., Eds., Tecnoscienza, Rome, pp. 61-76.

Brand, U.; Logan, L.; Hiller, N. & Richardson, J. (2003). Geochemistry of modern brachiopods: applications and implications for oceanography and paleoceanography. Chemical Geology, 198: 305-334. https://doi.org/10.1016/S0009-2541(03)00032-9

Brand, U.; Azmy, K.; Bitner, M.A.; Logan, A.; Zuschin, M.; Came, R. & Ruggiero, E. (2013). Oxygen

isotopes and $MgCO^3$ in brachiopod calcite and a new paleotemperature equation. Chemical Geology, 359: 23-31. https://doi.org/10.1016/j.chemgeo.2013.09.014

Brazier, J.M.; Suan, G.; Tacail, T.; Laurent, S.; Martin, J.E.; Mattioli, E. & Balter, V. (2015). Calcium isotope evidence for dramatic increase of continental weathering during the Toarcian oceanic anoxic event (Early Jurassic). Earth Planetary Sciences Lettters, 411: 164-176. https://doi.org/10.1016/j.epsl.2014.11.028

Bruland, K.W. (1980). Oceanographic distribution of cadmium, zinc, nickel, and copper in the North Pacific. Earth Planetary Sciences Lettters, 47: 176-198. https://doi.org/10.1016/0012-821X(80)90035-7

Bruland, K.W.; Donat, J.R. & Hutchins, D.A. (1991). Interactive influences of bioactive trace metals on biological production in oceanic waters. Limnology and Oceanography, 36: 1555-1577. https://doi.org/10.4319/lo.1991.36.8.1555

Bucefalo Palliani, R.; Mattioli, E. & Riding, J.B. (2002). The response of marine phytoplankton and sedimentary organic matter to the Early Toarcian (Lower Jurassic) oceanic anoxic event in northern England. Marine Micropaleontology, 46: 223-245. https://doi.org/10.1016/S0377-8398(02)00064-6

Buesing, N. & Carison, S.J. (1992). Geochemical investigation of growth in selected Recent articulate brachiopods. Lethaia, 25: 331-345. https://doi.org/10.1111/j.1502-3931.1992.tb01402.x

Calvert, S.E. (1990). Geochemistry and the origin of sapropel in the Black Sea. In: Facets of Modern Biogeochemistry (Ittekkot, V; Kempe, S., Michaelis, W. & Spitzy, A., Eds.), Berlin, Springer, 326-352. https://doi.org/10.1007/978-3-642-73978-1_26

Calvert, S.E. & Pedersen, T.F. (1993). Geochemistry of recent oxic and anoxic marine sediments: implications for the geological record. Marine Geology, 113: 67-88. https://doi.org/10.1016/0025-3227(93)90150-T

Caruthers, A.H.; Smith, P.L. & Gröcke, D.R. (2013). The Pliensbachian-Toarcian (Early Jurassic) extinction, a global multi-phased event. Palaeogeography, Palaeoclimatology, Palaeoecology, 386: 104-118. https://doi.org/10.1016/j.palaeo.2013.05.010

Cheng, L.; Fenter, P.; Sturchio, N.C.; Zhong, Z. & Bedzyk, M.J. (1999). X-ray standing wave study or arsenite incorporation at the calcite surface. Geochimica and Cosmochimica Acta, 63: 3153-3157.

Chester, R. & Jickells, T. (2012). Marine Geochemistry. John Wiley and Sons, 411 pp. https://doi.org/10.1002/9781118349083

Chester, R.; Baxter, G.B.; Behairy, A.K.A.; Connor, K.; Cross, D.; Elderfield, H. & Padgham, R.C. (1977). Soil-sized eolian dust from the lower troposphere of the eastern Mediterranean Sea. Marine Geology, 24: 201- 217. https://doi.org/10.1016/0025-3227(77)90028-7

Clark, J.V.; Pérez-Huerta, A.; Gillikin, D.P.; Aldridge, A.E.; Reolid, M. & Endo, K. (2016). Determination of paleoseasonality of fossil brachiopods using shell spiral deviations and chemical proxies. Palaeoworld, 25: 662-674. https://doi.org/10.1016/j.palwor.2016.05.010

Comans, R.N.J. & Middelburg, J.J. (1987). Sorption of trace metals on calcite: applicability of the surface precipitation model. Geochimica and Cosmochimica Acta, 51: 2587-2591. https://doi.org/10.1016/0016-7037(87)90309-7

Comas, M.C.; Puga, E.; Bargossi, G.M.; Morten, L. & Rossi, P.L. (1986). Paleogeography, sedimentation and volcanism of the Central Subbetic Zone, Betic Cordilleras, Southeastern Spain. Neues Jahrbuch für Geologie und Paläontologie-Abhandlungen, 7: 385-404. https://doi.org/10.1127/njgpm/1986/1986/385

Comas-Rengifo, M.J.; García Joral, F. & Goy, A. (2006). Spiriferinida (Brachiopoda) del Jurásico Inferior del NE y N de España: distribución y extinción durante el evento anóxico oceánico del Toarciense Inferior. Boletín Real Sociedad Española Historia Natural (Sec. Geológica), 101: 147-157.

Comas-Rengifo, M.J.; Duarte, L.V.; García Joral, F. & Goy, A. (2013). Los braquiópodos del Toarciense Inferior (Jurásico) en el área de Rabaçal-Condeixa (Portugal): distribución estratigráfica y paleobiogeografía. Comunicaçoes Geológicas, 100: 37-42.

Comas-Rengifo, M.J.; Duarte, L.V.; Félix, F.F.; García Joral, F., Goy, A. & Rocha, R.B. (2015). Latest Pliensbachian-Early Toarcian brachiopod assemblages from the Peniche section (Portugal) and their correlation. Episodes, 38: 2-8. https://doi.org/10.18814/epiiugs/2015/v38i1/001

Danise, S.; Twichett, R.J.; Little, C.T.S. & Clémence, M.E. (2013). The impact of global warming and anoxia on marine benthic community dynamics: an example from the Toarcian (Early Jurassic). PLoS ONE, 8: e56255. https://doi.org/10.1371/journal.pone.0056255

Danise, S.; Twichett, R.J. & Little, C.T.S. (2015). Environmental controls on Jurassic marine ecosystems during global warming. Geology, 43: 263-266. https://doi.org/10.1130/G36390.1

Deconinck, J.-F.; Hesselbo, S.P.; Debuisser, N.; Averbuch, O.; Baudin, F. & Bessa, J. (2003). Environmental controls on clay mineralogy of an Early Jurassic mudrock (Blue Lias Formation, southern England). International Journal of Earth Sciences, 92: 255-266. https://doi.org/10.1007/s00531-003-0318-y

De Lena, L.-F.; Taylor, D.; Guex, J.; Bartolini, A.; Adatte, T.; van Acken, D.; Spangenberg, J.E.; Samankassou, E.; Vernemann, T. & Schaltegger, U. (2019). The driving mechanisms of carbon cycle perturbation in the Pliensbachian (Early Jurassic). Scientific Reports, 9: art. 18430. https://doi.org/10.1038/s41598-019-54593-1

De Nooijer, L.J.; Reichart, G.J.; Dueñas Bohórquez, A.D.B.; Wolthers, M.; Ernst, S.R.; Mason, R.D. & Van der Zwaan, G.J. (2007). Copper incorporation in foraminiferal calcite: results from culturing experiments. Biogeosciences, 4: 9619-9991. https://doi.org/10.5194/bgd-4-961-2007

Delance, J.H. & Laurin, B, (1983). Contrôle de l'évolution des brachiopodes mésozoïques par les facteurs de l'environnement. Colloques internationaux du CNRS, 330: 91-99.

Delaney, M.L. & Boyle E.A. (1982). Uranium and thorium isotope concentrations in foraminiferal calcite. Earth and Planetary Science Letters, 62: 258-262. https://doi.org/10.1016/0012-821X(83)90088-2

Dera, G.; Neige, P.; Dommergues, J.L.; Fara, E.; Laffont, R. & Pellenard, P. (2010). High resolution dynamics of Early Jurassic marine extinctions: the case of Pliensbachian-Toarcian ammonites (Cephalopoda). Journal of the Geological Society London, 167: 21-33. https://doi.org/10.1144/0016-76492009-068

Doherty, P.J. (1981). The contribution of dissolved amino acids to the nutrition of articulate brachiopods. New Zealand Journal of Zoology, 8: 181-188. https://doi.org/10.1080/03014223.1981.10427960

Duarte, L.V. (2007). Lithostratigraphy, sequence stratigraphy and depositional setting of the Pliensbachian and Toarcian series in the Lusitanian Basin (Portugal). In: The Peniche section (Portugal), Contribution to the definition of the Toarcian GSSP (Rocha, R.B., Ed.), International Subcomission on Jurassic Stratigraphy, 17-23.

Dupont, C.L.; Buck, K.N.; Palenik, B. & Barbeau, K. (2010). Nickel utilization in phytoplankton assemblages from contrasting ocean regimes. Deep Sea Research I, 57: 533-566. https://doi.org/10.1016/j.dsr.2009.12.014

Fantasia, A.; Föllmi, K.B.; Adatte, T.; Spangenberg, J.E. & Mattioli, E. (2019a). Expression of the Toarcian Oceanic Anoxic Event: New insights from a Swiss transect. Sedimentology, 66: 262-284. https://doi.org/10.1111/sed.12527

Fantasia, A.; Thierry, A.; Spangenberg, J.E.; Font, E.; Duarte, L.V. & Follmi, K.B. (2019b). Global versus local processes during the Pliensbachian-Toarcian transition at the Peniche GSSP, Portugal: A multi-proxy record. Earth-Science Reviews, 198: art. 102932. https://doi.org/10.1016/j.earscirev.2019.102932

Fu, X.G.; Wang, M.; Zeng, S.Q.; Feng, X.L.; Wang, D. & Song, C.Y. (2017). Continental weathering and palaeoclimatic changes through the onset of the Early Toarcian oceanic anoxic event in the Qiangtang Basin, Eastern Tethys. Palaeogeography, Palaeoclimatology, Palaeoecology, 487: 241-250. https://doi.org/10.1016/j.palaeo.2017.09.005

Fürsich, F.T. & Hurst, J.M. (1974). Environmental factors determining the distribution of brachiopods. Paleontology, 17: 879-900.

Gahr, M. (2005). Response of Lower Toarcian (Lower Jurassic) macrobenthos of the Iberian Peninsula to sea level changes and mass extinction. Journal of Iberian Geology, 31: 197-215.

García-Hernández, M.; Rivas, P. & Vera, J.A. (1979). Distribución de las calizas de llanuras de mareas en el Jurásico del Subbético y Prebético. Cuadernos de Geología Universidad Granada 10: 557-569.

García-Hernández, M.; López-Garrido, A.C.; Martín-Algarra, A.; Molina, J.M.; Ruiz-Ortiz, P.A. & Vera, J.A. (1989). Las discontinuidades mayores del Jurásico de las Zonas Externas de las Cordilleras Béticas: Análisis e interpretación de los ciclos sedimentarios. Cuadernos de Geología Ibérica, 13: 35-52.

García Joral, F. & Goy, A. (1984). Características de la fauna de braquiópodos del Toarciense Superior en el Sector Central de la Cordillera Ibérica (Noreste de España). Estudios Geológicos, 40: 55-60. https://doi.org/10.3989/egeol.84401-2650

García Joral, F. & Goy, A. (2000). Stratigraphic distribution of Toarcian brachiopods from the Iberian Range and its relation to depositional sequences. Georesearch Forum, 6: 381-386.

García Joral, F.; Gómez, J.J. & Goy, A. (2011). Mass extinction and recovery of the Early Toarcian (Early Jurassic) brachiopods linked to climate change in northern and central Spain. Palaeogeography, Palaeoclimatology, Palaeoecology, 302: 367-380. https://doi.org/10.1016/j.palaeo.2011.01.023

Gendron, A.; Silverberg, N.; Sundby, B. & Lebel, J. (1996). Early diagenesis of cadmium and cobalt in sediments of the Laurentian Trough. Geochimica and Cosmochimica Acta, 50: 741-747. https://doi.org/10.1016/0016-7037(86)90350-9

Gómez, J.J. & Goy, A. (2011). Warming-driven mass extinction in the Early Toarcian (Early Jurassic) of northern and central Spain. Correlation with other time-equivalent European sections. Palaeogeography, Palaeoclimatology, Palaeoecology, 306: 176-195. https://doi.org/10.1016/j.palaeo.2011.04.018

Gómez, J.J.; Comas-Rengifo, M.J. & Goy, A. (2016). Palaeoclimatic oscillations in the Pliensbachian (Early Jurassic) of the Asturian Basin (Northern Spain). Climate of the Past, 12: 1199-1214. https://doi.org/10.5194/cp-12-1199-2016

Greaves, M.J.; Statham, P.J. & Elderfield, H. (1994). Rare earth element mobilization from marine atmospheric dust into seawater. Marine Chemistry, 46: 255-260. https://doi.org/10.1016/0304-4203(94)90081-7

Grossman, E.L.; Yancey, T.E.; Jones, T.E.; Bruckschen, P.; Chuvashov, B.; Mazzullo, S.J. & Mii, H.S. (2008). Glaciation, aridification, and carbon sequestration in the Permo-Carboniferous: the isotopic record from low latitude. Palaeogeography, Palaeoclimatology, Palaeoecology, 268: 222-233. https://doi.org/10.1016/j.palaeo.2008.03.053

Hallam, A. (1981). A revised sea-level curve for the Early Jurassic. Journal of Geological Society, 139: 735-743. https://doi.org/10.1144/gsjgs.138.6.0735

Hallam, A. (1986). The Pliensbachian and Tithonian extinction events. Nature, 319: 765-768. https://doi.org/10.1038/319765a0

Hallam, A. (1987). Radiations and extinctions in relation to environmental change in the marine Lower Jurassic of northwest Europe. Paleobiology, 13: 152-168. https://doi.org/10.1017/S0094837300008708

Hallam, A. (1988). A re-evaluation of Jurassic eustasy in the light of new data and the revised Exxon curve. In: Sea-level Changes: An integrated approach (Wilgus, C.K.; Hastings, B.S.; Posamentier, H.; Van Wagoner, J.; Ross, C.A. & Kendall, C.G.S., Eds.), Society of Economic Paleontologists and Mineralogists Special Publications 42, 261-273. https://doi.org/10.2110/pec.88.01.0261

Hallam, A. (1996). Recovery of the marine fauna in Europe after the end-Triassic and early Toarcian mass extinctions, In: Biotic Recovery from Mass Extinction Events (Hart, M.B., Ed.), Geological Society Special Publications, 102, 231-236. https://doi.org/10.1144/GSL.SP.1996.001.01.16

Hamroush, H.A. & Stanley, D.J. (1990) Paleoclimatic oscillations in East Africa interpreted by analysis of trace elements in Nile delta sediments. Episodes, 13: 264-269. https://doi.org/10.18814/epiiugs/1990/v13i4/006

Haq, B.U. (2018). Jurassic sea-level variations: a reappraisal. GSA Today, 28: 4-10. https://doi.org/10.1130/GSATG359A.1

Harlou, R.; Ullmann, C.V.; Korte, C.; Lauridsen, B.W.; Schovsbo, N.H.; Surlyk, F.; Thibault, N. & Stemmerik, L. (2016). Geochemistry of Campanian-Maastrichtian brachiopods from the Rørdal-1 core (Denmark): Differential responses to environmental change and diagenesis. Chemical Geology, 442: 35-46. https://doi.org/10.1016/j.chemgeo.2016.08.039

Harries, P.J. & Little, C.T.S. (1999). The Early Toarcian (Early Jurassic) and the Cenomanian-Turonian (Late Cretaceous) mass extinctions: similarities and contrasts. Palaeogeography, Palaeoclimatology, Palaeoecology, 154: 39-66. https://doi.org/10.1016/S0031-0182(99)00086-3

Hesselbo, S.P.; Gröcke, D.R.; Jenkyns, H.C.; Bjerrum, C.J.; Farrimond, P.; Morgans-Bell, H.S. & Green, O.R. (2000). Massive dissociation of gas hydrate during a Jurassic oceanic anoxic event. Nature, 406: 392-395. https://doi.org/10.1038/35019044

Hesselbo, S.P.; Jenkyns, H.C.; Duarte, L.V. & Oliveira L.C.V. (2007). Carbon-isotope record of the Early Jurassic (Toarcian) oceanic anoxic event from fossil wood and marine carbonate (Lusitanian Basin, Portugal). Earth and Planetary Science Letters, 253: 455-470. https://doi.org/10.1016/j.epsl.2006.11.009

Helz, G.R.; Bura-Nakic, E.; Mikac, N. & Ciglenecki, I. (2011). New model for molybdenum behavior in euxinic waters. Chemical Geology, 284: 323-332. https://doi.org/10.1016/j.chemgeo.2011.03.012

Holser, W.T. (1997). Evaluation of the application of rare-earth elements to paleoceanography. Palaeogeography, Palaeoclimatology, Palaeoecology, 132: 309-323. https://doi.org/10.1016/S0031-0182(97)00069-2

Immel, F.; Gaspard, D.; Guichard, N.; Cusack, M. & Marin, F. (2015). Shell proteome of rhynchonelliform brachiopods. Journal of Structural Biology, 190: 360-366. https://doi.org/10.1016/j.jsb.2015.04.001

Iñesta, M. (1988). Braquiópodos Liásicos del Cerro de La Cruz (La Romana, Prov. Alicante, España). Mediterránea Serie Geológica, 7: 45-64.

James, M.A.; Ansell, A.D.; Collins, M.J.; Curry, G.B.; Peck, L.S. & Rhodes, M.C. (1992). Biology of living brachiopods. Advances in Marine Biology, 28: 175-387. https://doi.org/10.1016/S0065-2881(08)60040-1

Jeandel, C.; Tachikawa, K.; Bory, A. & Dehairs, F. (2000). Biogenic barium in suspended and trapped material as a tracer of export production in tropical NE Atlantic (EUMELI sites). Marine Geochemistry, 71: 125-142. https://doi.org/10.1016/S0304-4203(00)00045-1

Jenkyns, H.C. (1988). The Early Toarcian (Jurassic) anoxic event: stratigraphy, sedimentary and geochemical evidence. American Journal of Science, 288: 101-151. https://doi.org/10.2475/ajs.288.2.101

Jenkyns, H.C. & Clayton, C.K. (1997). Lower Jurassic epicontinental carbonates and mudstones from England and Wales: chemostratigraphic signals and the early

Toarcian anoxic event. Sedimentology, 44: 687-706. https://doi.org/10.1046/j.1365-3091.1997.d01-43.x

Kemp, D.B.; Baranyi, V.; Izumi, K. & Burgess, R.D. (2019). Organic matter variations and links to climate across the early Toarcian oceanic anoxic event (T-OAE) in Toyora area, southwest Japan). Palaeogeography, Palaeoclimatology, Palaeoecology, 530: 90-102. https://doi.org/10.1016/j.palaeo.2019.05.040

Keul, N.; Langer, G.; de Nooijer, L.J.; Reichart, G.J. & Bijma, J. (2013). Incorporation of uranium in benthic foraminiferal calcite reflects seawater carbonate ion concentration. Geochemistry, Geophysics, Geosystems, 14: 102-111. https://doi.org/10.1029/2012GC004330

Klingelhoefer, F.; Labails, C.; Cosquer, E.; Rouzo, S.; Geli, L.; Aslanian, D.; Olivet, J.L.; Sahabi, M.; Nouze, H. & Unternehr, P. (2009). Crustal structure of the SW-Moroccan margin from wide-angle and reflection seismic data (the DAKHLA experiment) Part A: Wide-angle seismic models. Tectonophysics, 468: 63-82. https://doi.org/10.1016/j.tecto.2008.07.022

Korte, C. & Hesselbo, S.P. (2011). Shallow-marine carbon- and oxygen-isotope and elemental records indicate icehouse-greenhouse cycles during the Early Jurassic. Paleoceanography, 26: PA4219. https://doi.org/10.1029/2011PA002160

Korte, C.; Jasper, T.; Kozur, H.W. & Veizer, J. (2005). δ18O and $\delta^{13}C$ of Permian brachiopods: A record of seawater evolution and continental glaciation. Palaeogeography, Palaeoclimatology, Palaeoecology, 224: 333-351. https://doi.org/10.1016/j.palaeo.2005.03.015

Korte, C.; Jones, P.J.; Brand, U.; Mertmann, D. & Veizer, J. (2008). Oxygen isotope values from high-latitudes: Clues for Permian sea-surface temperature gradients and Late Palaeozoic deglaciation. Palaeogeography, Palaeoclimatology, Palaeoecology, 269: 1-16. https://doi.org/10.1016/j.palaeo.2008.06.012

Korte, C.; Hesselbo, S.P.; Ullmann, C.V.; Dietl, G.; Ruhl, M.; Schweigert, G. & Thibault, N. (2015). Jurassic climate mode governed by ocean gateway. Nature Communications, 6: 10015. https://doi.org/10.1038/ncomms10015

Korte, C.; Thibault, N.; Ullmann, C.V,; Clémence, M.E.; Mette, W.; Olsen, T.K.; Rizzi, M. & Ruhl, M. (2017). Brachiopod biogeochemistry and isotope stratigraphy from the Rhaetian Eiberg section in Austria: potentials and limitations. Neues Jahrbuch für Geologie und Paläontologie-Abhandlungen, 284: 117-138. https://doi.org/10.1127/njgpa/2017/0651

Lee, X.; Hu, R.; Brand, U.; Zhou, H.; Liu, X.; Yuan, H.; Yan, C. & Cheng, H. (2004). Ontogenetic trace element distribution in brachiopod shells: an indicator of original seawater chemistry. Chemical Geology, 209: 49-65. https://doi.org/10.1016/j.chemgeo.2004.04.029

Levinton, J. & Suchanek, T.H. (1972). The food of articulated brachiopod reconsidered. GSA Abstracts, 4: 575.

Little, C.T.S. (1996). The Pliensbachian-Toarcian (Lower Jurassic) extinction event. GSA Special Paper, 307: 505-512. https://doi.org/10.1130/0-8137-2307-8.505

Little, C.T.S. & Benton, M.J. (1995). Early Jurassic mass extinction: A global long-term event. Geology, 23: 495-498. https://doi.org/10.1130/0091-7613(1995)023<0495:EJMEAG>2.3.CO;2

Littler, K.; Hesselbo, S.P. & Jenkyns, H.C. (2010). A carbon-isotope perturbation at the Pliensbachian-Toarcian boundary: evidence from the Lias Group, NE England. Geological Magazine, 147: 181-192. https://doi.org/10.1017/S0016756809990458

Macchioni, F. & Cecca, F. (2002). Biodiversity and biogeography of middle-late liassic ammonoids: implications for the Early Toarcian mass extinction. Geobios, M.S. 24: 165-175. https://doi.org/10.1016/S0016-6995(02)00057-8

Machel, H.G. & Burton, E. (1991). Factors governing cathodoluminescence in calcite and dolomite and their implications for studies of carbonate diagenesis. SEPM Short Course, 25: 37-58. https://doi.org/10.2110/scn.91.25.0037

Machel, H.G.; Mason, R.A.; Mariano, A.N. & Mucci, A. (1991). Causes and measurements of luminescence in calcite and dolomite. SEPM Short Course, 25: 9-25. https://doi.org/10.2110/scn.91.25.0009

Mailliot, S.; Mattioli, E.; Guex, J. & Pittet, B. (2006). The early Toarcian anoxia; a synchronous event in the Western Tethys? An approach by quantitative biochronology (Unitary Associations), applied on calcareous nannofossils. Palaeogeography, Palaeoclimatology, Palaeoecology, 240: 562-586. https://doi.org/10.1016/j.palaeo.2006.02.016

McArthur, J.M.; Kennedy, W.J.; Chen, M.; Thirwall, M.F. & Gale, A.S. (1994). Strontium isotope stratigraphy for Late Cretaceous time: Direct numerical calibration of the Sr isotope curve based on the US Western Interior. Palaeogeography, Palaeoclimatology, Palaeoecology, 108: 95-119. https://doi.org/10.1016/0031-0182(94)90024-8

McArthur, J.M.; Algeo, T.J.; van de Schootbrugge, B.; Li, Q. & Howarth, R.J. (2008). Basinal restriction; black shales; Re-Os dating; and the Early Toarcian (Jurassic) oceanic anoxic event. Paleoceanography, 23: PA4217. https://doi.org/10.1029/2008PA001607

McCammon, H.M. (1981). Physiology of the brachiopod digestive system. In: Lophophorates, Notes for a

Short Course (Broadhead, T.W., Ed.), University of Tennessee, Dep. Geological Sciences. Studies in Geology, 5: 17G204. https://doi.org/10.1017/S0271164800000385

McCammon, H.M. & Reynolds, W.A. (1976). Experimental evidence for direct nutrient assimilation by the lophophore of articulate brachiopods. Marine Biology, 34: 41-51. https://doi.org/10.1007/BF00390786

McManus, J.; Berelson, W.M.; Hammond, D.E. & Klinkhammer, G.P. (1999). Barium cycling in the North Pacific: implication for the utility of Ba as a paleoproductivity and paleoalkalinity proxy. Paleoceanography, 14: 62-73. https://doi.org/10.1029/1998PA900007

McManus, J.; Berelson, W.M.; Klinkhammer, G.P.; Hammond, D.E. & Holm, C. (2005). Authigenic uranium: relationships to oxygen penetration depth and organic carbon rain. Geochimica and Cosmochimica Acta, 69: 95-108. https://doi.org/10.1016/j.gca.2004.06.023

Molina, J.M.; Ruiz-Ortiz, P.A. & Vera, J.A. (1999). A review of polyphase karstification in extensional tectonic regimes: Jurassic and Cretaceous examples, Betic Cordillera, southern Spain. Sedimentary Geology, 129: 71-84. https://doi.org/10.1016/S0037-0738(99)00089-5

Montero-Serrano, J.C.; Föllmi, K.B.; Adatte, T.; Spangenberg, J.E.; Tribovillard, N.; Fantasia, A. & Suan, G. (2015). Continental weathering and redox conditions during the early Toarcian Oceanic Anoxic Event in the northwestern Tethys: Insight from the Posidonia Shale section in the Swiss Jura Mountains. Palaeogeography, Palaeoclimatology, Palaeoecology, 429: 83-99. https://doi.org/10.1016/j.palaeo.2015.03.043

Moore, R.W.; Webb, R.; Tokarczyk, R. & Wever, R. (1996). Bromoperoxidase and iodoperoxidase enzymes and production of halogenated methanes in marine diatom cultures. Journal of Geophysical Research, 101: 20899-20908. https://doi.org/10.1029/96JC01248

Morel, F.M.M. & Price, N.M. (2003). The biogeochemical cycles of trace metals in the oceans. Science, 300: 944-947. https://doi.org/10.1126/science.1083545

Morse, J.W. & MacKenzie, F.T. (1990). Geochemistry of sedimentary carbonates. Developments in Sedimentology 48. Elsevier, Amsterdam. 707 pp.

Müller, T.; Price, G.D.; Bajnai, D.; Nyerges, A.; Kesjár, D.; Raucsik, B.; Varga, A.; Judik, K.; Fekete, J.; May, Z. & Pálfy, J. (2017). New multiproxy record of the Jenkyns Event (also known as the Toarcian Oceanic Anoxic Event) from the Mecsek Mountains (Hungary): Differences, duration and drivers. Sedimentology, 64: 66-86. https://doi.org/10.1111/sed.12332

Munsel, D.; Kramar, U.; Dissard, D.; Nehkre, G.; Berner, Z.; Bijma, J.; Reichart, G.J. & Neumann, T. (2010). Heavy metal incorporation in foraminifera calcite: results from multi-element enrichment culture experiments with *Ammonia tepida*. Biogeosciences, 7: 2339-2350. https://doi.org/10.5194/bg-7-2339-2010

Nalewajko, G.; Lee, K. & Jack, T.R. (1995). Effects of vanadium on freshwater phytoplankton photosynthesis. Water Air Soil Pollution, 81: 93-105. https://doi.org/10.1007/BF00477258

Nieto, L.; Ruiz-Ortiz, P.A.; Rey, J. & Benito, M.I. (2008). Strontium-isotope stratigraphy as a constraint on the age of condensed levels: examples from the Jurassic of the Subbetic Zone (southern Spain). Sedimentology, 55: 1-39.

O'Dogherty, L.; Sandoval, J. & Vera, J.A. (2000). Jurassic Ammonite faunal turnover tracing sea-level changes during the Jurassic (Betic Cordillera, southern Spain). Journal of the Geological Society London, 157: 723-736. https://doi.org/10.1144/jgs.157.4.723

Olóriz, F.; Linares, A.; Goy, A.; Sandoval, J.; Caracuel, J.E.; Rodríguez-Tovar, F.J. & Tavera, J.M. (2002). Jurassic. The Betic Cordillera and Balearic Islands. In: The Geology of Spain (Gibbons, W. & Moreno, M.T., Eds), Geological Society, London, 235-253.

Pálfy, J. & Smith, P.L. (2000). Synchrony between Early Jurassic extinction, oceanic anoxic event, and the Karoo-Ferrar flood basalt volcanism. Geology, 28: 747-750. https://doi.org/10.1130/0091-7613(2000)028<0747:SBEJEO>2.3.CO;2

Palmer, M.R. (1985). Rare earth elements in foraminifera tests. Earth and Planetary Science Letters, 73: 285-293. https://doi.org/10.1016/0012-821X(85)90077-9

Papadopoulo, P. & Rowell, D.L. (1989). The reactions of copper and zinc with calcium carbonate surfaces. Journal of Soil Science, 39: 23-36. https://doi.org/10.1111/j.1365-2389.1988.tb01191.x

Paquette, J. & Reeder, R.J. (1995). Relationships between surface structure, growth mechanism, and trace element incorporation in calcite. Geochimica and Cosmochimica Acta, 59: 735-749. https://doi.org/10.1016/0016-7037(95)00004-J

Pérez-Huerta, A.; Etayo-Cadavid, M.F.; Andrus, C.F.T.; Jeffries, T.E.; Watkins, C.; Street, S.C. & Sandweiss, D.H. (2013). El Niño Impact on mollusk biomineralization: Implications for trace element proxy reconstructions and the paleo-archeological record. Plos One, doi:10.1371/journal.pone.0054274. https://doi.org/10.1371/journal.pone.0054274

Pérez-Huerta, A.; Aldridge, A.E.; Endo, K. & Jeffries, T.E. (2014). Brachiopod shell spiral deviations (SSD):

Implications for trace element proxies. Chemical Geology, 374-375: 13-24. https://doi.org/10.1016/j.chemgeo.2014.03.002

Piazza, V.; Ullmann, C.V. & Aberahn, M. (2020). Ocean warming affected faunal dynamics of benthic invertebrate assemblages across the Toarcian Oceanic Anoxic Event in the Iberian Basin (Spain). Plos One, doi:10.1371/journal.pone.0242331 https://doi.org/10.1371/journal.pone.0242331

Piper, D.Z. & Dean, W.E. (2002). Trace-element deposition in the Cariaco Basin, Venezuela Shelf, under sulfate-reducing conditions: a history of the local hydrography and global climate, 20 ka to the present. USGS Professional Paper No. 1670. https://doi.org/10.3133/pp1670

Popp, B.; Anderson, T.F. & Sandberg, P.A. (1986). Brachiopods as indicators of original isotopic compositions in some Paleozoic limestones. GSA Bulletin, 97: 1262-1269. https://doi.org/10.1130/0016-7606(1986)97<1262:BAIOOI>2.0.CO;2

Portugal, M.; Morata, D.A.; Puga, E.; Demant, A. & Aguirre, L. (1995). Evolución geoquímica y temporal del magmatismo básico mesozoico en las Zonas Externas de las Cordilleras Béticas. Estudios Geológicos, 51: 109-118.

Prakash Babu, C.; Brumsack, H.J.; Schnetger, B. & Böttcher, M.E. (2002). Barium as a productivity proxy in continental margin sediments: a study from the eastern Arabian Sea. Marine Geology, 184: 189-206. https://doi.org/10.1016/S0025-3227(01)00286-9

Pye, K. (1987). Aeolian dust and dust deposits. 334 pp. Academic Press, San Diego.

Quillmann, U.; Marchitto, T.M.; Jennings, A.E.; Andrews, J.T. & Friestad, B.F. (2012). Cooling and freshening at 8.2 ka on the NW Iceland shelf recorded in paired $\delta^{18}O$ and Mg/Ca measurements of the benthic foraminifer *Cibicides lobatulus*. Quaternary Research, 78: 528-539. https://doi.org/10.1016/j.yqres.2012.08.003

Raddatz, J. & Rüggeberg, A. (2019). Constraining past environmental changes of cold-water coral mounds with geochemical proxies in corals and foraminifera. Depositional Record, doi: 10.1002/dep2.98. https://doi.org/10.1002/dep2.98

Rasmussen, C.M.Ø.; Ullmann, C.V.; Jakobsen, K.G.; Lindskog, A.; Hansen, J.; Hansen, T.; Eriksson, M.E.; Dronov, A.; Frei, R.; Korte, C.; Nielsen, A.T. & Harper, D.A.T. (2016). Onset of main Phanerozoic radiation sparked by emerging Mid Ordovician icehouse. Scientific Reports, 6: 18884. https://doi.org/10.1038/srep18884

Reeder, R.J. (1996). Interactions of divalent cobalt, zinc, cadmium, and barium with the calcite surface during layer growth. Geochimica and Cosmochimica Acta, 60: 1543-1552. https://doi.org/10.1016/0016-7037(96)00034-8

Reeder, R.J.; Lamble, G.M. & Northrup, P.A. (1999). XAFS study of the coordination and local relaxation around Co^{2+}, Zn^{2+}, Pb^{2+}, and Ba^{2+} trace elements in calcite. American Mineralogist, 84: 1049-1060. https://doi.org/10.2138/am-1999-7-807

Regenberg, M.; Steph, S.; Nurnberg, D.; Tiedemann, R. & Garbe-Schonberg, D. (2009). Calibrating Mg/Ca ratios of multiple planktonic foraminiferal species with $\delta^{18}O$-calcification temperatures: paleothermometry for the upper water column. Earth and Planetary Science Letters, 278: 324-336. https://doi.org/10.1016/j.epsl.2008.12.019

Reolid, M. (2014). Stable isotopes on foraminifera and ostracods for interpreting incidence of the Toarcian Oceanic Anoxic Event in Westernmost Tethys: role of water stagnation and productivity. Palaeogeography, Palaeoclimatology, Palaeoecology, 395: 77-91. https://doi.org/10.1016/j.palaeo.2013.12.012

Reolid, M. & Abad, I. (2014). Glauconitic laminated crusts as a consequence of hydrothermal alteration of Jurassic pillow-lavas from Mediam Subbetic (Betic Cordillera, S Spain): a microbial influence case. Journal of Iberian Geology, 40: 389-408. https://doi.org/10.5209/rev_JIGE.2014.v40.n3.43080

Reolid, M.; Rodríguez-Tovar, F.J.; Marok, A. & Sebane, A. (2012). The Toarcian oceanic anoxic event in the Western Saharan Atlas, Algeria (North African paleomargin): role of anoxia and productivity. GSA Bulletin, 124: 1646-1664. https://doi.org/10.1130/B30585.1

Reolid, M.; Nieto, L.M. & Sánchez-Almazo, I.M. (2013). Caracterización geoquímica de facies pobremente oxigenadas en el Toarciense inferior (Jurásico inferior) del Subbético Externo. Revista de la Sociedad Geológica de España, 26: 69-84.

Reolid, M.; Mattioli, E.; Nieto, L.M. & Rodríguez-Tovar, F.J. (2014). The Early Toarcian Oceanic Anoxic Event in the External Subbetic (Southiberian Palaeomargin, Westernmost Tethys): Geochemistry, nannofossils and ichnology. Palaeogeography, Palaeoclimatology, Palaeoecology, 411: 79-94. https://doi.org/10.1016/j.palaeo.2014.06.023

Reolid, M.; Rivas, P. & Rodríguez-Tovar, F.J. (2015). Toarcian ammonitico rosso facies from the South Iberian Paleomargin (Betic Cordillera, southern Spain): paleoenvironmental reconstruction. Facies, 61: 22. https://doi.org/10.1007/s10347-015-0447-3

Reolid, M.; Molina, J.M.; Nieto, L.M. & Rodríguez-Tovar, F.J. (2018). The Toarcian Oceanic Anoxic Event in the Southiberian Palaeomargin, SpringerBriefs in Earth

Sciences, 122 pp. https://doi.org/10.1007/978-3-319-67211-3

Reolid, M.; Copestake, P. & Johnson, B. (2019). Foraminiferal assemblages; extinctions and appearances associated with the Early Toarcian Oceanic Anoxic Event in the Llanbedr (Mochras Farm) Borehole, Cardigan Bay Basin, United Kingdom. Palaeogeography, Palaeoclimatology, Palaeoecology, 532: 109277. https://doi.org/10.1016/j.palaeo.2019.109277

Reolid, M.; Mattioli, E.; Duarte, L.V. & Marok, A. (2020). The Toarcian Oceanic Anoxic Event and the Jenkyns Event (IGCP-655 final report). Episodes, 43: 833-844. https://doi.org/10.18814/epiiugs/2020/020051

Reolid, M.; Mattioli, E.; Duarte, L.V. & Ruebsam, W. (2021). The Toarcian Oceanic Anoxic Event: where do we stand? Geological Society, London, Special Publications, 514, 1-12. doi:10.1144/SP514-2021-74 https://doi.org/10.1144/SP514-2021-74

Rey, J. (1998) Extensional Jurassic tectonism of an eastern Subbetic section (southern Spain). Geological Magazine 135: 685-697. https://doi.org/10.1017/S0016756898001277

Rita, P.; Reolid, M. & Duarte, L.V. (2016). The incidence of the Late Pliensbachian-Early Toarcian biotic crisis from ecostratigraphy of benthic foraminiferal assemblages: new insights from the Peniche reference section, Portugal. Palaeogeography, Palaeoclimatology, Palaeoecology, 454: 267-281. https://doi.org/10.1016/j.palaeo.2016.04.039

Rodrigues, B.; Silva, R.L.; Reolid, M.; Mendonça Filho, J.G. & Duarte, L.V. (2019). Sedimentary organic matter and δ^{13}Ckerogen variation on the southern Iberian palaeomargin (Betic Cordillera, SE Spain) during the latest Pliensbachian-Early Toarcian. Palaeogeography, Palaeoclimatology, Palaeoecology, 534: 109342. https://doi.org/10.1016/j.palaeo.2019.109342

Rodríguez-Tovar, F.J. & Reolid, M. (2013). Environmental conditions during the Toarcian Oceanic Anoxic Event (T-OAE) in the westernmost Tethys: influence of the regional context on a global phenomenon. Bulletin of Geosciences, 88: 697-712. https://doi.org/10.3140/bull.geosci.1397

Rodríguez-Tovar, F.J & Uchman, A. (2011). Ichnofabric evidence for the lack of bottom anoxia during the lower Toarcian Oceanic Anoxic Event (T-OAE) in the Fuente de la Vidriera section, Betic Cordillera, Spain. Palaios, 25: 576-587. https://doi.org/10.2110/palo.2009.p09-153r

Röhl, H.J.; Schmid-Röhl, A.; Oschmann, W.; Frimmel, A. & Scwark, L. (2001). The Posidonian Shale (Lower Toarcian) of SW-Germany: an oxygen-depleted ecosystem controlled by sea level and paleoclimate. Palaeogeography, Palaeoclimatology, Palaeoecology, 165: 27-52. https://doi.org/10.1016/S0031-0182(00)00152-8

Rosales, I.; Barnolas, A.; Goy, A.; Sevillano, A.; Armendáriz, M. & López-García, J.M. (2018). Isotope records (C-O-Sr) of late Pliensbachian-early Toarcian environmental perturbations in the westernmost Tethys (Majorca Island, Spain). Palaeogeography, Palaeoclimatology, Palaeoecology, 497: 168-185. https://doi.org/10.1016/j.palaeo.2018.02.016

Rosenberg, G.D.; Hughes, W.W. & Tkachuck, R.D. (1988). Intermediatory metabolism and shell growth in the brachiopod *Terebratalia transversa*. Lethaia, 21: 219-230. https://doi.org/10.1111/j.1502-3931.1988.tb02074.x

Ruban, D.A. (2004). Diversity dynamics of Early-Middle Jurassic brachiopods of Caucasus, and the Pliensbachian-Toarcian mass extinction. Acta Palaeontologica Polonica, 49: 275-282.

Ruban, D.A. (2009). Brachiopod decline preceded the Early Toarcian mass extinction in the Northern Caucasus (northern Neo-Tethys Ocean): A palaeogeographical context. Revue de Paléobiologie, 28: 85-92.

Ruebsam, W.; Mayer, B. & Schwark, L. (2019). Cryosphere carbon dynamics control early Toarcian global warming and sea level evolution. Global and Planetary Change, 172: 440-453. https://doi.org/10.1016/j.gloplacha.2018.11.003

Ruebsam, W.; Reolid, M. & Schwark, L. (2020). δ^{13}C of terrestrial vegetation records Toarcian CO_2 and climate gradients. Scientific Reports, 10: art. 117. https://doi.org/10.1038/s41598-019-56710-6

Ruhl, M,; Hesselbo, S.P.; Hinnov, L.; Jenkyns, H.C.; Xu, W.; Riding, J.; Srom, M.; Minisini, D.; Ullmann, C.V. & Leng, M.J. (2016). Earth and Planetary Science Letters, 455: 149-165. https://doi.org/10.1016/j.epsl.2016.08.038

Ruiz-Ortiz, P.A.; Bosence, D.W.J.; Rey, J.; Nieto, L.M.; Castro, J.M. & Molina, J.M. (2004). Tectonic control of facies architecture, sequence stratigraphy and drowning of a Liassic carbonate platform (Betic Cordillera, Southern Spain). Basin Research, 16: 235-257. https://doi.org/10.1111/j.1365-2117.2004.00231.x

Russell, A.D.; Emerson, S.; Nelson, B.K.; Erez, J. & Lea, D.W. (1994). Uranium in foraminiferal calcite as a recorder of seawater uranium concentrations. Geochimica and Cosmochimica Acta, 58: 671-681 https://doi.org/10.1016/0016-7037(94)90497-9

Sahabi, M.; Aslanian, D. & Oliver, J.L. (2004). Un nouveau point de départ pour l'histoire de l'Atlantique central. Comptes Rendus Geoscience, 336: 1041-1052. https://doi.org/10.1016/j.crte.2004.03.017

Sandoval, J.; O'Dogherty, L. & Guex, J. (2001). Evolutionary rates of Jurassic ammonites in relation to Sea-level fluctuations. Palaios, 16: 311-335. https://doi.org/10.1669/0883-1351(2001)016<0311:EROJAI>2.0.CO;2

Sandoval, J.; Bill, M.; Aguado, R.; O'Dogherty, L.; Rivas, P.; Morard, A. & Guex, J. (2012). The Toarcian in the Subbetic basin (southern Spain): Bioevents (ammonite and calcareous nannofossils) and carbon-isotope stratigraphy. Palaeogeography, Palaeoclimatology, Palaeoecology, 342-343: 40-63. https://doi.org/10.1016/j.palaeo.2012.04.028

Scherer, M. & Seitz, H. (1980). Rare-earth element distribution in Holocene and Pleistocene corals and their redistribution during diagenesis. Chemical Geology, 28: 279-289. https://doi.org/10.1016/0009-2541(80)90049-2

Schöllhorn, I.; Adatte, T.; Van de Schootbrugge, B.; Houben, A.; Charbonnier, G.; Janssen, N. & Follmi, K.B. (2020). Climate and environmental response to the break-up of Pangea during the Early Jurassic (Hettangian-Pliensbachian), the Dorset coast (UK) revisited. Global and Planetary Change, 185: 103096. https://doi.org/10.1016/j.gloplacha.2019.103096

Shen, G.T. & Dunbar, R.B. (1995). Environmental controls on uranium in reef corals. Geochimica and Cosmochimica Acta, 59: 2009-2024. https://doi.org/10.1016/0016-7037(95)00123-9

Sholkovitz, E. & Shen, G.T. (1995). The incorporation of rare elements in modern coral. Geochimica and Cosmochimica Acta, 59: 2749-2756. https://doi.org/10.1016/0016-7037(95)00170-5

Simon, E.; Motchurova-Dekova, N. & Mottequin B. (2018). A reappraisal of the genus *Tethyrhynchia* Logan, 1994 (Rhynchonellida, Brachiopoda): a conflict between phylogenies obtained from morphological characters and molecular data. Zootaxa, 4471: 535-555. https://doi.org/10.11646/zootaxa.4471.3.6

Simonet Roda, M.; Zieglerb, A.; Griesshabera, E.; Yina, X.; Ruppb, U.; Greinera, M.; Henkelc, D.; Häussermannd, V.; Eisenhauerc, A.; Laudienf, J. & Schmahla, W.W. (2019). Terebratulide brachiopod shell biomineralization by mantle epithelial cells. Journal of Structural Biology, 207: 136-157. https://doi.org/10.1016/j.jsb.2019.05.002

Smrzka, D.; Zwicker, J.; Bach, W.; Himmler, T.; Chen, D. & Peckmann, J. (2019). The behaviour of trace elements in seawater, sedimentary pore water, and their incorporation into carbonate minerals: a review. Facies, 65: 41. https://doi.org/10.1007/s10347-019-0581-4

Stanton Jr., R.J. & Nelson, P.C. (1980). Reconstruction of the trophic web in paleontology: Community structure in the Stone City Formation (Middle Eocene, Texas). Journal of Paleontology, 54: 118-135.

Steele-Petrovic, H.M. (1979). The physiological differences between articulate brachiopods and filter feeding bivalves as a factor in the evolution of marine level bottom communities. Palaeontology, 22: 101-134.

Stipp, S.L. & Hochella, M.F.J. (1991). Structure and bionding envinronments at the calcite surface observed with X-ray photoelectron spectroscopy (XPS) and low energy diffraction (LEED). Geochimica and Cosmochimica Acta, 55: 1723-1736. https://doi.org/10.1016/0016-7037(91)90142-R

Storm, M.S.; Hesselbo, S.P.; Jenkyns, H.C.; Ruhl, M.; Ullmann, C.V.; Xu, W.; Leng, M.; Riding, J. & Gorbanenko, O. (2020). Orbital pacing and secular evolution of the Early Jurassic carbon cycle. PNAS, doi:10.1073/pnas.1912094117. https://doi.org/10.1073/pnas.1912094117

Suan, G.; Pittet, B.; Bour, I.; Mattioli, E.; Duarte, L.V. & Mailliot, S. (2008). Duration of the Early Toarcian carbon isotope excursion deduced from spectral analysis: consequence for its possible causes. Earth and Planetary Science Letters, 267: 666-679. https://doi.org/10.1016/j.epsl.2007.12.017

Suan, G.; Mattioli, E.; Pittet, B.; Lécuyer, C.; Suchéras-Marx, B.; Duarte, L.V.; Philippe, M.; Reggiani, L. & Martineau, F. (2010). Secular environmental precursors to Early Toarcian (Jurassic) extreme climate changes. Earth and Planetary Science Letters, 290: 448-458. https://doi.org/10.1016/j.epsl.2009.12.047

Suchanek, T.H. & Levinton, J. (1974). Articulate brachiopod food. Journal of Paleontology, 48: 1-5.

Swart, P.K. & Hubbard, J.A.E.B. (1982). Uranium in scleractinian corals. Coral Reefs 1: 13-19. https://doi.org/10.1007/BF00286535

Tent-Manclús, J.E. (2006). Estructura y estratigrafía de las sierras de Crevillente, Abanilla y Algayat: su relación con la Falla de Crevillente. PhD Thesis, Universidad de Alicante, 970 pp., http://hdl.handle.net/10045/10414.

Tesoriero, A.J. & Pankow, J.F. (1996). Solid solution partitioning of Sr^{2+}, Ba^{2+}, and Cd^{2+} to calcite. Geochimica and Cosmochimica Acta, 60: 1053-1063. https://doi.org/10.1016/0016-7037(95)00449-1

Thébault, J.; Chauvaud, L.; L'Helguen, S.; Clavier, J.; Barats, A.; Jacquet, S.; Pécheyran, C. & Amoroux, D. (2009). Barium and molydenum records in bivalve shells: Geochemical proxies for phytoplankton dynamics in coastal environments? Limnology and Oceanography, 54: 1002-1014. https://doi.org/10.4319/lo.2009.54.3.1002

Them, T.R.; Gill, B.C.; Selby, D.; Grocke, D.R.; Friedman, R.M. & Owens, J.D. (2017). Evidence for rapid weathering response to climatic warming during the Toarcian Oceanic Anoxic Event. Scientific Reports, 7: 5003. https://doi.org/10.1038/s41598-017-05307-y

Thibault, N.; Ruhl, M.; Ullmann, C.V.; Korte, C.; Kemp, D.; Gröcke, D.R. & Hesselbo, S.P. (2018). The wider context of the Lower Jurassic Toarcian oceanic anoxic event in Yorkshire coastal outcrops, UK. Proceedings of the Geologists' Association, 129: 372-391. https://doi.org/10.1016/j.pgeola.2017.10.007

Tkachuck, R.D.; Rosenberg, G.D.; Hughes, W.W. (1989). Utilization of free amino acids by mantle tissue in the brachiopod *Terebratalia transversa* and the bivalve mollusc *Chlamys hastata*. Comparative Biochemistry and Physiology, 92B: 747-750. https://doi.org/10.1016/0305-0491(89)90261-7

Tribovillard, N.; Algeo, T.; Lyons, T. & Riboulleau, A. (2006). Trace metals as palaeoredox and palaeoproductivity proxies: an update. Chemical Geology, 232: 12-32. https://doi.org/10.1016/j.chemgeo.2006.02.012

Ullmann, C.V.; Campbell, H.C.; Frei, R. & Korte, C. (2014). Geochemical signatures in Late Triassic brachiopods from New Caledonia. New Zealand Journal of Geology and Geophysics, 57: 420-431. https://doi.org/10.1080/00288306.2014.958175

Ullmann, C.V.; Campbell, H.C.; Frei, R. & Korte, C. (2016). Oxygen and carbon isotope and Sr/Ca signatures of high-latitude Permian to Jurassic calcite fossils from New Zealand and New Caledonia. Gondwana Research, 38: 60-73. https://doi.org/10.1016/j.gr.2015.10.010

Ullmann, C.V.; Boyles, R.; Duarte, L.V.; Hesselbo, S.P.; Kasemanns, S.A.; Kleins, T.; Lenton, T.M.; Piazza, V. & Aberhan, M. (2020). Warm afterglow from the Toarcian Oceanic Anoxic Event drives the success of deep-adapted brachiopods. Scientific Reports, 10: 6549. https://doi.org/10.1038/s41598-020-63487-6

Van Geldern, R.; Joachimnki, M.M.; Day, J.; Jansen, U.; Alvarez, F.; Yolkin, E.A. & Ma, X.P. (2006). Carbon, oxygen and strontium isotope records of Devonian brachiopod shell calcite. Palaeogeography, Palaeoclimatology, Palaeoecology, 240: 47-67. https://doi.org/10.1016/j.palaeo.2006.03.045

Veizer, J. (1983). Chemical diagenesis of carbonates: theory and application of trace element technique. Sedimentary Geology, 10: 3-100.

Veizer, J.; Ala, D.; Azmy, K.; Bruckschen, P.; Buhl, D.; Bruhn, F.; Carden, G.A.F.; Diener, A.; Ebneth, S.; Godderis, Y.; Jasper, T.; Korte, G.; Pawellek, F.; Podlaha, O.G. & Strauss, H. (1999). Sr^{87}/Sr^{86}, δC^{13} and δO^{18} evolution of Phanerozoic seawater. Chemical Geology, 161: 59-88. https://doi.org/10.1016/S0009-2541(99)00081-9

Vera, J.A. (1988). Evolución de los sistemas de depósito en el margen ibérico de la Cordillera Bética. Revista de la Sociedad Geológica de España, 1: 373-391.

Vera, J.A. (1998). El Jurásico de la Cordillera Bética: Estado actual de conocimientos y problemas pendientes. Cuadernos de Geología Ibérica, 24: 17-42.

Vera, J.A. (2001). Evolution of the Iberian Continental Margin. Mémoires du Musée National d'Histoire Naturelle Paris, 186: 109-143.

Vera, J.A.; Martín-Algarra, A.; Sánchez-Gómez, M.; Fornós, J.J. & Gelabert, B. (2004). Cordillera Bética y Baleares, In: Geología de España (Vera, J.A., Ed.), SGE-IGME, 345-464.

Vörös, A. (1993). Jurassic microplate movements and brachiopod migrations in the western part of the Tethys. Palaeogeography, Palaeoclimatology, Palaeoecology, 100: 125-145. https://doi.org/10.1016/0031-0182(93)90037-J

Vörös, A. (2002). Victims of the Early Toarcian anoxic event: the radiation and extinction of Jurassic Koninckinidae (Brachiopoda). Lethaia, 35: 345-357. https://doi.org/10.1080/002411602320790652

Vörös, A.; Kocsis, Á.T. & Pálfy, J. (2016). Demise of the last two spire-bearing brachiopod orders (Spiriferinida and Athyridida) at the Toarcian (Early Jurassic) extinction event. Palaeogeography, Palaeoclimatology, Palaeoecology, 457: 233-241. https://doi.org/10.1016/j.palaeo.2016.06.022

Vörös, A.; Kocsis, Á.T. & Pálfy, J. (2019). Mass extinctions and clade extinctions in the history of brachiopods: brief review and a post-Paleozoic case study. Rivista Italiana di Paleontologia e Stratigrafia, 125(3): 711-724.

Wang, X.L.; Plnavsky, N.J.; Hull, P.M.; Tripati, A.E.; Zou, H.J.; Elder, L. & Henehan, M. (2016). Chromium isotopic composition of core-top planktonic foraminifera. Geobiology, 15: 51-64. https://doi.org/10.1111/gbi.12198

Weremeichnik, J.M.; Gabitov, R.I.; Thien, B.M. & Sadekov. A. (2017) The effect of growth rate on uranium partitioning between individual calcite crystals and fluid. Chemical Geology, 450: 145-153. https://doi.org/10.1016/j.chemgeo.2016.12.026

Wignall, P.B. & Bond, D.P.G. (2008) The end-Triassic and Early Jurassic mass extinction records in the British Isles. Proceedings of the Geologists' Association, 119: 73-84. https://doi.org/10.1016/S0016-7878(08)80259-3

Wignall, P.B.; Newton, R.J. & Little, C.T.S. (2005). The timing of paleoenvironmental change and cause-and-effect relationships during the Early Jurassic mass extinction in Europe. American Journal of Science, 305: 1014-1032. https://doi.org/10.2475/ajs.305.10.1014

Winterer E.L. & Bosselini, A. (1981) Subsidence and sedimentation on Jurassic passive continental margin, Southern Alps, Italy. AAPG Bulletin, 65: 394-421. https://doi.org/10.1306/2F9197E2-16CE-11D7-8645000102C1865D

Wyndham, T.; McCulloch, M.; Fallon, S. & Alibert, C. (2004). High-resolution coral records of the earth elements in coastal seawater: biogeochemical cycling and a new environmental proxy. Geochimica and Cosmochimica Acta, 68: 2067-2080. https://doi.org/10.1016/j.gca.2003.11.004

Zachara, J.M.; Kittrixk, J.A. & Harsh, J.B. (1988). The mechanism of Zn^{2+} adsorption on calcite. Geochimica and Cosmochimica Acta, 52: 2281-2291. https://doi.org/10.1016/0016-7037(88)90130-5

Zachara, J.M.; Cowan, C.E. & Resch, C.T. (1991). Sorption of divalent metal son calcite. Geochimica and Cosmochimica Acta, 55: 1549-1562. https://doi.org/10.1016/0016-7037(91)90127-Q

Zaky, A.H.; Brand, U.; Azmy, K.; Logan, A.; Hooper, R.G. & Svavarsson, J. (2016). Rare earth elements of shallow-water articulated brachiopods: A bathymetric sensor. Palaeogeography, Palaeoclimatology, Palaeoecology, 461: 178-194. https://doi.org/10.1016/j.palaeo.2016.08.021

Zhao, Y.; Vance, D.; Abouchami, W. & de Baar, H.J.W. (2014). Biogeochemical cycling of zinc and its isotopes in the Southern Ocean. Geochimica and Cosmochimica Acta, 125: 653-672. https://doi.org/10.1016/j.gca.2013.07.045